
Survey of Period Variations of Superhumps in SU UMa-Type Dwarf Novae. IX: The Ninth Year (2016–2017)

Taichi KATO,^{1*} Keisuke ISOGAI,¹ Franz-Josef HAMBSCH,^{2,3,4}
Tonny VANMUNSTER,⁵ Hiroshi ITOH,⁶ Berto MONARD,^{7,8} Tamás TORDAI,⁹
Mariko KIMURA,¹ Yasuyuki WAKAMATSU,¹ Seiichiro KIYOTA,¹⁰
Peter STARR,¹¹ Kiyoshi KASAI,¹² Sergey Yu. SHUGAROV,^{13,14}
Drahomir CHOCHOL,¹⁴ Natalia KATYSHEVA,¹³ Anna M. ZAOSTROJNYKH,¹⁵
Matej SEKERÁŠ,¹⁴ Yuliana G. KUZNYETSOVA,¹⁶ Eugenia S. KALINICHEVA,¹⁷
Polina GOLYSHEVA,¹³ Viktoriia KRUSHEVSKA,¹⁶ Yutaka MAEDA,¹⁸
Pavol A. DUBOVSKY,¹⁹ Igor KUDZEJ,¹⁹ Elena P. PAVLENKO,^{20,21}
Kirill A. ANTONYUK,²⁰ Nikolaj V. PIT,²⁰ Aleksei A. SOSNOVSKIJ,²⁰
Oksana I. ANTONYUK,²⁰ Aleksei V. BAKLANOV,²⁰ Roger D. PICKARD,^{22,23}
Naoto KOJIGUCHI,²⁴ Yuki SUGIURA,²⁴ Shihei TEI,²⁴ Kenta YAMAMURA,²⁴
Katsura MATSUMOTO,²⁴ Javier RUIZ,^{25,26,27} Geoff STONE,²⁸
Lewis M. COOK,²⁹ Enrique de MIGUEL,^{30,31} Hidehiko AKAZAWA,³²
William N. GOFF,³³ Etienne MORELLE,³⁴ Stella KAFKA,²⁸
Colin LITTLEFIELD,³⁵ Greg BOLT,³⁶ Franky DUBOIS,³⁷
Stephen M. BRINCAT,³⁸ Hiroyuki MAEHARA,³⁹ Takeshi SAKANOI,⁴⁰
Masato KAGITANI,⁴⁰ Akira IMADA,^{41,42} Irina B. VOLOSHINA,¹³
Maksim V. ANDREEV,^{43,44} Richard SABO,⁴⁵ Michael RICHMOND,⁴⁶
Tony RODDA,⁴⁷ Peter NELSON,⁴⁸ Sergey NAZAROV,²⁰
Nikolay MISHEVSKIY,²⁸ Gordon MYERS,⁴⁹ Denis DENISENKO,¹³
Krzysztof Z. STANEK,⁵⁰ Joseph V. SHIELDS,⁵⁰

Christopher S. KOCHANEK,⁵⁰ Thomas W.-S. HOLOIEN,⁵⁰
Benjamin SHAPPEE,⁵¹ José L. PRIETO,^{52,53} Koh-ichi ITAGAKI,⁵⁴
Koichi NISHIYAMA,⁵⁵ Fujio KABASHIMA,⁵⁵ Rod STUBBINGS,⁵⁶
Patrick SCHMEER,⁵⁷ Eddy MUYLLAERT,⁵⁸ Tsuneo HORIE,⁵⁹
Jeremy SHEARS,^{60,22} Gary POYNER,⁶¹ Masayuki MORIYAMA,⁶²

¹ Department of Astronomy, Kyoto University, Kyoto 606-8502, Japan

² Groupe Européen d'Observations Stellaires (GEOS), 23 Parc de Levesville, 28300 Bailleau l'Evêque, France

³ Bundesdeutsche Arbeitsgemeinschaft für Veränderliche Sterne (BAV), Munsterdamm 90, 12169 Berlin, Germany

⁴ Vereniging Voor Sterrenkunde (VVS), Oude Bleken 12, 2400 Mol, Belgium

⁵ Center for Backyard Astrophysics Belgium, Walhostraat 1A, B-3401 Landen, Belgium

⁶ Variable Star Observers League in Japan (VSOLJ), 1001-105 Nishiterakata, Hachioji, Tokyo 192-0153, Japan

⁷ Bronberg Observatory, Center for Backyard Astrophysics Pretoria, PO Box 11426, Tiegerpoort 0056, South Africa

⁸ Kleinkaroo Observatory, Center for Backyard Astrophysics Kleinkaroo, Sint Helena 1B, PO Box 281, Calitzdorp 6660, South Africa

⁹ Polaris Observatory, Hungarian Astronomical Association, Laborc utca 2/c, 1037 Budapest, Hungary

¹⁰ VSOLJ, 7-1 Kitahatsutomi, Kamagaya, Chiba 273-0126, Japan

¹¹ Warrumbungle Observatory, Tenby, 841 Timor Rd, Coonabarabran NSW 2357, Australia

¹² Baselstrasse 133D, CH-4132 MuttENZ, Switzerland

¹³ Sternberg Astronomical Institute, Lomonosov Moscow State University, Universitetsky Ave., 13, Moscow 119992, Russia

¹⁴ Astronomical Institute of the Slovak Academy of Sciences, 05960 Tatranska Lomnica, Slovakia

¹⁵ Institute of Physics, Kazan Federal University, Ulitsa Kremlevskaya 16a, Kazan 420008, Russia

¹⁶ Main Astronomical Observatory of National Academy of Sciences of Ukraine, 27 Akademika Zabolotnoho St., Kyiv 03143, Ukraine

¹⁷ Faculty of Physics, Lomonosov Moscow State University, Leninskie gory, Moscow 119991, Russia

- ¹⁸ Kaminishiyamamachi 12-14, Nagasaki, Nagasaki 850-0006, Japan
- ¹⁹ Vihorlat Observatory, Mierova 4, 06601 Humenne, Slovakia
- ²⁰ Federal State Budget Scientific Institution “Crimean Astrophysical Observatory of RAS”, Nauchny, 298409, Republic of Crimea
- ²¹ V. I. Vernadsky Crimean Federal University, 4 Vernadskogo Prospekt, Simferopol, 295007, Republic of Crimea
- ²² The British Astronomical Association, Variable Star Section (BAA VSS), Burlington House, Piccadilly, London, W1J 0DU, UK
- ²³ 3 The Birches, Shobdon, Leominster, Herefordshire, HR6 9NG, UK
- ²⁴ Osaka Kyoiku University, 4-698-1 Asahigaoka, Osaka 582-8582, Japan
- ²⁵ Observatorio de Cántabria, Ctra. de Rocamundo s/n, Valderredible, 39220 Cantabria, Spain
- ²⁶ Instituto de Física de Cantabria (CSIC-UC), Avenida Los Castros s/n, E-39005 Santander, Cantabria, Spain
- ²⁷ Agrupación Astronómica Cántabria, Apartado 573, 39080, Santander, Spain
- ²⁸ American Association of Variable Star Observers, 49 Bay State Rd., Cambridge, MA 02138, USA
- ²⁹ Center for Backyard Astrophysics Concord, 1730 Helix Ct. Concord, California 94518, USA
- ³⁰ Departamento de Ciencias Integradas, Facultad de Ciencias Experimentales, Universidad de Huelva, 21071 Huelva, Spain
- ³¹ Center for Backyard Astrophysics, Observatorio del CIECEM, Parque Dunar, Matalascañas, 21760 Almonte, Huelva, Spain
- ³² Department of Biosphere-Geosphere System Science, Faculty of Informatics, Okayama University of Science, 1-1 Ridai-cho, Okayama, Okayama 700-0005, Japan
- ³³ 13508 Monitor Ln., Sutter Creek, California 95685, USA
- ³⁴ 9 rue Vasco de GAMA, 59553 Lauwin Planque, France
- ³⁵ Department of Physics, University of Notre Dame, 225 Nieuwland Science Hall, Notre Dame, Indiana 46556, USA
- ³⁶ Camberwarra Drive, Craigie, Western Australia 6025, Australia
- ³⁷ Public observatory Astrolab Iris, Verbrandemolenstraat 5, B 8901 Zillebeke, Belgium
- ³⁸ Flarestar Observatory, San Gwann SGN 3160, Malta
- ³⁹ Okayama Astrophysical Observatory, National Astronomical Observatory of Japan, Asakuchi, Okayama 719-0232, Japan
- ⁴⁰ Planetary Plasma and Atmospheric Research Center, Graduate School of Science,

Tohoku University, Sendai 980-8578, Japan

⁴¹ Hamburger Sternwarte, Universität Hamburg, Gojenbergsweg 112, D-21029 Hamburg, Germany

⁴² Kwasan and Hida Observatories, Kyoto University, Yamashina, Kyoto 607-8471, Japan

⁴³ Terskol Branch of Institute of Astronomy, Russian Academy of Sciences, 361605, Peak Terskol, Kabardino-Balkaria Republic, Russia

⁴⁴ International Center for Astronomical, Medical and Ecological Research of NASU, Ukraine
27 Akademika Zabolotnoho Str. 03680 Kyiv, Ukraine

⁴⁵ 2336 Trailcrest Dr., Bozeman, Montana 59718, USA

⁴⁶ Physics Department, Rochester Institute of Technology, Rochester, New York 14623, USA

⁴⁷ 1, Rivermede, Ponteland, Newcastle upon Tyne, NE20 9XA, UK

⁴⁸ 1105 Hazeldean Rd, Ellinbank 3820, Australia

⁴⁹ Center for Backyard Astrophysics San Mateo, 5 Inverness Way, Hillsborough, CA 94010, USA

⁵⁰ Department of Astronomy, the Ohio State University, Columbia, OH 43210, USA

⁵¹ Carnegie Observatories, 813 Santa Barbara Street, Pasadena, CA 91101, USA

⁵² Núcleo de Astronomía de la Facultad de Ingeniería, Universidad Diego Portales, Av. Ejército 441, Santiago, Chile

⁵³ Department of Astrophysical Sciences, Princeton University, NJ 08544, USA

⁵⁴ Itagaki Astronomical Observatory, Teppo-cho, Yamagata 990-2492

⁵⁵ Miyaki-Argenteus Observatory, Miyaki, Saga 840-1102, Japan

⁵⁶ Tetoora Observatory, 2643 Warragul-Korumburra Road, Tetoora Road, Victoria 3821, Australia

⁵⁷ Bischmisheim, Am Probstbaum 10, 66132 Saarbrücken, Germany

⁵⁸ Vereniging Voor Sterrenkunde (VVS), Moffelstraat 13 3370 Boutersem, Belgium

⁵⁹ 759-10 Tokawa, Hadano-shi, Kanagawa 259-1306, Japan

⁶⁰ "Pemberton", School Lane, Bunbury, Tarporley, Cheshire, CW6 9NR, UK

⁶¹ BAA Variable Star Section, 67 Ellerton Road, Kingstanding, Birmingham B44 0QE, UK

⁶² 290-383, Ogata-cho, Sasebo, Nagasaki 858-0926, Japan

*E-mail: *tkato@kusastro.kyoto-u.ac.jp

Received 201 0; Accepted 201 0

Abstract

Continuing the project described by Kato et al. (2009, PASJ, 61, S395), we collected times of

superhump maxima for 127 SU UMa-type dwarf novae observed mainly during the 2016–2017 season and characterized these objects. We provide updated statistics of relation between the orbital period and the variation of superhumps, the relation between period variations and the rebrightening type in WZ Sge-type objects. We obtained the period minimum of 0.05290(2) d and confirmed the presence of the period gap above the orbital period ~ 0.09 d. We note that four objects (NY Her, 1RXS J161659.5+620014, CRTS J033349.8–282244 and SDSS J153015.04+094946.3) have supercycles shorter than 100 d but show infrequent normal outbursts. We consider that these objects are similar to V503 Cyg, whose normal outbursts are likely suppressed by a disk tilt. These four objects are excellent candidates to search for negative superhumps. DDE 48 appears to be a member of ER UMa-type dwarf novae. We identified a new eclipsing SU UMa-type object MASTER OT J220559.40–341434.9. We observed 21 WZ Sge-type dwarf novae during this interval and reported 18 out of them in this paper. Among them, ASASSN-16js is a good candidate for a period bouncer. ASASSN-16ia showed a precursor outburst for the first time in a WZ Sge-type superoutburst. ASASSN-16kg, CRTS J000130.5+050624 and SDSS J113551.09+532246.2 are located in the period gap. We have newly obtained 15 orbital periods, including periods from early superhumps.

Key words: accretion, accretion disks — stars: novae, cataclysmic variables — stars: dwarf novae

1 Introduction

This is a continuation of series of papers Kato et al. (2009), Kato et al. (2010), Kato et al. (2012a), Kato et al. (2013), Kato et al. (2014b), Kato et al. (2014a), Kato et al. (2015a) and Kato et al. (2016a) reporting new observations of superhumps in SU UMa-type dwarf novae. SU UMa-type dwarf novae are a class of cataclysmic variables (CVs) which are close binary systems transferring matter from a low-mass dwarf secondary to a white dwarf, forming an accretion disk [see e.g. Warner (1995) for CVs in general].

In SU UMa-type dwarf novae, there are two types of outbursts (normal outbursts and superoutbursts). Outbursts and superoutbursts in SU UMa-type dwarf novae are considered to be a result of the combination of thermal and tidal instabilities [thermal-tidal instability (TTI) model by Osaki (1989); Osaki (1996)].

During superoutbursts, semi-periodic variations called superhumps are observed

whose period (superhump period, P_{SH}) is a few percent longer than the orbital period (P_{orb}). Superhumps are considered to originate from a precessing eccentric (or flexing) disk in the gravity field of the rotating binary, and the eccentricity in the disk is believed to be a consequence of the 3:1 resonance in the accretion disk [see e.g. Whitehurst (1988); Hirose, Osaki (1990); Lubow (1991); Wood et al. (2011)].

It has become evident since Kato et al. (2009) that the superhump periods systematically vary in a way common to many objects. Kato et al. (2009) introduced superhump stages (stages A, B and C): initial growing stage with a long period (stage A) and fully developed stage with a systematically varying period (stage B) and later stage C with a shorter, almost constant period (see figure 1).

It has recently been proposed by Osaki, Kato (2013b) that stage A superhumps reflect the dynamical precession rate at the 3:1 resonance radius and that the rapid decrease of the period (stage B) reflects the pressure effect which has an effect of retrograde precession (Lubow 1992; Hirose, Osaki 1993; Murray 1998; Montgomery 2001; Pearson 2006). As proposed by Kato, Osaki (2013) stage A superhumps can be then used to “dynamically” determine the mass ratio (q), which had been difficult to measure except for eclipsing systems and systems with bright secondaries to detect radial-velocity variations. It has been confirmed that this stage A method gives q values as precise as in eclipsing systems. There have been more than 50 objects whose q values are determined by this method and it has been proven to be an especially valuable tool in depicting the terminal stage of CV evolution (cf. Kato et al. 2015a; Kato 2015).

In this paper, we present new observations of SU UMa-type dwarf novae mainly obtained in 2016–2017. We present basic observational materials and discussions in relation to individual objects. Starting from Kato et al. (2014a), we have been intending these series of papers to be also a source of compiled information, including historical, of individual dwarf novae.

The material and methods of analysis are given in section 2, observations and analysis of individual objects are given in section 3, including discussions particular to the objects. General discussions are given in section 4 and the summary is given in section 5. Some tables and figures are available online only.

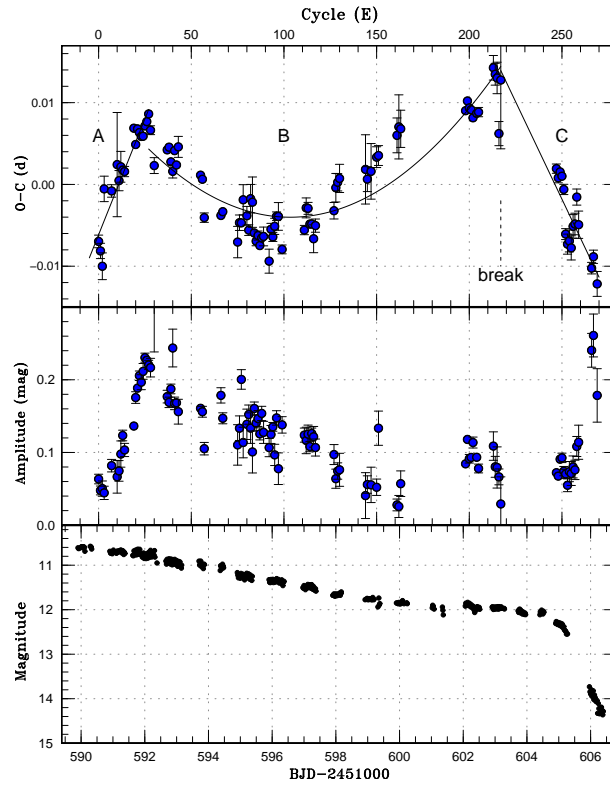


Fig. 1. Representative $O - C$ diagram showing three stages (A–C) of $O - C$ variation. The data were taken from the 2000 superoutburst of SW UMa. (Upper:) $O - C$ diagram. Three distinct stages (A – evolutionary stage with a longer superhump period, B – middle stage, and C – stage after transition to a shorter period) and the location of the period break between stages B and C are shown. (Middle): Amplitude of superhumps. During stage A, the amplitude of the superhumps grew. (Lower:) Light curve. (Reproduction of figure 1 in Kato, Osaki 2013)

2 Observation and Analysis

2.1 Data Source

The data were obtained under campaigns led by the VSNET Collaboration (Kato et al. 2004). We also used the public data from the AAVSO International Database¹. Outburst detections of many new and known objects relied on the ASAS-SN CV patrol (Davis et al. 2015)², the MASTER network (Gorbovskoy et al. 2013), and Catalina Real-time Transient Survey (CRTS; Drake et al. 2009)³ in addition to outburst detections reported to VSNET, AAVSO⁴, BAAVSS alert⁵ and cvnet-outburst.⁶

¹ <<http://www.aavso.org/data-download>>.

² <<http://cv.asassn.astronomy.ohio-state.edu/>>.

³ <<http://nesssi.cacr.caltech.edu/catalina/>>. For the information of the individual Catalina CVs, see <<http://nesssi.cacr.caltech.edu/catalina/AllCV.html>>.

⁴ <<https://www.aavso.org/>>.

⁵ <<https://groups.yahoo.com/neo/groups/baavss-alert/>>.

⁶ <<https://groups.yahoo.com/neo/groups/cvnet-outburst/>>.

For objects detected in CRTS, we preferably used the names provided in Drake et al. (2014) and Coppejans et al. (2016). If these names are not yet available, we used the International Astronomical Union (IAU)-format names provided by the CRTS team in the public data release⁷ Since Kato et al. (2009), we have used coordinate-based optical transient (OT) designations for some objects, such as apparent dwarf nova candidates reported in the Transient Objects Confirmation Page of the Central Bureau for Astronomical Telegrams⁸ and CRTS objects without registered designations in Drake et al. (2014) or in the CRTS public data release and listed the original identifiers in table 1.

We provided coordinates from astrometric catalogs for ASAS-SN (Shappee et al. 2014) CVs and two objects without precise coordinate-based names other than listed in the General Catalog of Variable Stars (Kholopov et al. 1985) in table 2. We mainly used Gaia DR1 (Gaia Collaboration 2016), Sloan Digital Sky Survey (SDSS, Ahn et al. 2012), the Initial Gaia Source List (IGSL, Smart 2013) and Guide Star Catalog 2.3.2 (GSC 2.3.2, Lasker et al. 2007). Some objects were detected as transients by Gaia⁹ and CRTS and we used their coordinates. The coordinates used in this paper are J2000.0. We also supplied SDSS *g*, Gaia *G* and GALEX NUV magnitudes when counterparts are present.

2.2 Observations and Basic Reduction

The majority of the data were acquired by time-resolved CCD photometry by using 20–60cm telescopes located world-wide. The list of outbursts and observers is summarized in table 1. The data analysis was performed in the same way described in Kato et al. (2009) and Kato et al. (2014a) and we mainly used R software¹⁰ for data analysis.

In de-trending the data, we mainly used locally-weighted polynomial regression (LOWESS: Cleveland 1979) and sometimes lower (1–3rd order) polynomial fitting when the observation baseline was short. The times of superhumps maxima were determined by the template fitting method as described in Kato et al. (2009). The times of all observations are expressed in barycentric Julian days (BJD).

In figures, the points are accompanied by 1σ error bars whenever available, which are omitted when the error is smaller than the plot mark or the errors were not available (as in

⁷ <<http://nessi.cacr.caltech.edu/DataRelease/>>.

⁸ <<http://www.cbat.eps.harvard.edu/unconf/tocp.html>>.

⁹ <<http://gsaweb.ast.cam.ac.uk/alerts/alertsindex>> and Gaia identifications supplied by the AAVSO VSX.

¹⁰The R Foundation for Statistical Computing:

<<http://cran.r-project.org/>>.

some raw light curves of superhumps).

2.3 Abbreviations and Terminology

The abbreviations used in this paper are the same as in Kato et al. (2014a): we used $\epsilon \equiv P_{\text{SH}}/P_{\text{orb}} - 1$ for the fractional superhump excess. We have used since Osaki, Kato (2013a) the alternative fractional superhump excess in the frequency unit $\epsilon^* \equiv 1 - P_{\text{orb}}/P_{\text{SH}} = \epsilon/(1 + \epsilon)$ because this fractional superhump excess is a direct measure of the precession rate. We therefore used ϵ^* in discussing the precession rate.

The P_{SH} , P_{dot} and other parameters are listed in table 3 in same format as in Kato et al. (2009). The definitions of parameters P_1, P_2, E_1, E_2 and P_{dot} are the same as in Kato et al. (2009): P_1 and P_2 represent periods in stage B and C, respectively (P_1 is averaged during the entire course of the observed segment of stage B), and E_1 and E_2 represent intervals (in cycle numbers) to determine P_1 and P_2 , respectively.¹¹ Some superoutbursts are not listed in table 3 due to the lack of observations (e.g. single-night observations with less than two superhump maxima or poor observations for the object with already well measured P_{SH}).

We used the same terminology of superhumps summarized in Kato et al. (2012a). We especially call attention to the term “late superhumps”. We only used the concept of “traditional” late superhumps when there is an ~ 0.5 phase shift [Vogt (1983); see also table 1 in Kato et al. (2012a) for various types of superhumps], since we suspect that many of the past claims of detections of “late superhumps” were likely stage C superhumps before it became evident that there are complex structures in the $O - C$ diagrams of superhumps (see discussion in Kato et al. 2009).

2.4 Period Analysis

We used phase dispersion minimization (PDM; Stellingwerf 1978) for period analysis and 1σ errors for the PDM analysis was estimated by the methods of Fernie (1989) and Kato et al. (2010). We have used a variety of bootstrapping in estimating the robustness of the result of the PDM analysis since Kato et al. (2012a). We analyzed 100 samples which randomly contain 50% of observations, and performed PDM analysis for these samples. The bootstrap result is shown as a form of 90% confidence intervals in the resultant PDM θ statistics. If this paper provides the first solid presentation of a new SU UMa-type classification, we provide

¹¹The intervals (E_1 and E_2) for the stages B and C given in the table sometimes overlap because there is sometimes observational ambiguity (usually due to the lack of observations and errors in determining the times of maxima) in determining the stages.

the result of PDM period analysis and averaged superhump profile.

2.5 $O - C$ Diagrams

Comparisons of $O - C$ diagrams between different superoutbursts are also presented whenever available. This figure not only provides information about the difference of $O - C$ diagrams between different superoutbursts but also helps identifying superhump stages especially when observations were insufficient or the start of the outburst was missed. In drawing combined $O - C$ diagrams, we usually used $E = 0$ for the start of the superoutburst, which usually refers to the first positive detection of the outburst. This epoch usually has an accuracy of ~ 1 d for well-observed objects, and if the outburst was not sufficiently observed, we mentioned in the figure caption how to estimate E in such an outburst. In some cases, this $E = 0$ is defined as the appearance of superhumps. This treatment is necessary since some objects have a long waiting time before appearance of superhumps. We also note that there is sometimes an ambiguity in selecting the true period among aliases. In some cases, this can be resolved by the help of the $O - C$ analysis. The procedure and example are shown in subsection 2.2 in Kato et al. (2015a).

3 Individual Objects

3.1 V1047 Aquilae

V1047 Aql was discovered as a dwarf nova (S 8191) by Hoffmeister (1964). Hoffmeister (1964) reported a blue color in contrast to the nearby stars. Mason, Howell (2003) obtained a spectrum typical for a quiescent dwarf nova. According to R. Stubbings, the observation by Greg Bolt during the 2005 August outburst detected superhumps, and the superhump period was about 0.074 d (see Kato et al. 2012b). The object shows rather frequent outbursts (approximately once in 50 d), and a number of outbursts have been detected mainly by R. Stubbings visually since 2004.

The 2016 superoutburst was detected by R. Stubbings at a visual magnitude of 15.0 on July 8. Subsequent observations detected superhumps (vsnet-alert 19974; e-figure 1). Using the 2005 period, we could identify two maxima on two nights: $E=0$, BJD 2457581.3853(7) ($N=74$) and $E=14$, BJD 2457582.4190(11) ($N=72$). The period given in table 3 is determined by the PDM method.

Although observations are not sufficient, visual observations by R. Stubbings suggest a supercycle of ~ 90 d, which would make V1047 Aql one of ordinary SU UMa-type dwarf

Table 1. List of Superoutbursts.

Subsection	Object	Year	Observers or references*	ID [†]
3.1	V1047 Aql	2016	Trt	
3.2	BB Ari	2016	Kis, AAVSO, SRI, RPc, Ioh, Shu, RAE	
3.3	V391 Cam	2017	Trt, DPV	
3.4	OY Car	2016	SPE, HaC, MGW	
–	HT Cas	2016	Y. Wakamatsu et al. in preparation	
3.5	GS Cet	2016	Kis, OKU, HaC, Shu, CRI, KU, Ioh, Trt	
3.6	GZ Cet	2016	OKU	
3.7	AK Cnc	2016	Aka	
3.8	GZ Cnc	2017	KU, Mdy, HaC	
3.9	GP CVn	2016	RPc, Kai, Trt, IMi, Kis, CRI, deM, AAVSO	
3.10	V337 Cyg	2016	Kai	
3.11	V1113 Cyg	2016	OKU, Ioh, Kis	
3.12	IX Dra	2016	Kis, SGE, COO	

*Key to observers: Aka (H. Akazawa, OUS), BSM[‡](S. Brincat), COO (L. Cook), CRI (Crimean Astrophys. Obs.), DDe (D. Denisenko), deM (E. de Miguel), DPV (P. Dubovsky), Dub (F. Dubois team), GBo (G. Bolt), GFB[‡](W. Goff), HaC (F.-J. Hamsch, remote obs. in Chile), IMi[‡](I. Miller), Ioh (H. Itoh), KU (Kyoto U., campus obs.), Kai (K. Kasai), Kis (S. Kiyota), LCO (C. Littlefield), MEV[‡](E. Morelle), NGW (G. Myers), MLF (B. Monard), MNI (N. Mishevskiy), Mdy (Y. Maeda), Mhh (H. Maehara), NKa (N. Katysheva and S. Shugarov), Naz (S. Nazarov), Nel (P. Nelson), OKU (Osaya Kyoiku U.), RAE (T. Rodda), RIT (M. Richmond), RPc[‡](R. Pickard), Rui (J. Ruiz), SGE[‡](G. Stone), SPE[‡](P. Starr), SRI[‡](R. Sabo), Shu (S. Shugarov team), T60 (Haleakala Obs. T60 telescope), Trt (T. Tordai), Van (T. Vanmunster), Vol (I. Voloshina), AAVSO (AAVSO database)

[†]Original identifications, discoverers or data source.

[‡]Inclusive of observations from the AAVSO database.

Table 1. List of Superoutbursts (continued).

Subsection	Object	Year	Observers or references*	ID [†]
3.13	IR Gem	2016	Kai, Aka, CRI, BSM, AAVSO, Trt	
		2017	Kai, Trt	
3.14	NY Her	2016	GFB, Ioh, DPV, Trt, COO, IMi, SGE	
3.15	MN Lac	2016	Van	
3.16	V699 Oph	2016	Kis, Ioh	
3.17	V344 Pav	2016	HaC	
3.18	V368 Peg	2016	Trt	
3.19	V893 Sco	2016	GBo, HaC, Kis, Aka	
3.20	V493 Ser	2016	Shu	
3.21	AW Sge	2016	DPV	
3.22	V1389 Tau	2016	HaC, KU, Ioh	
3.23	SU UMa	2017	Trt	
3.24	HV Vir	2016	HaC, DPV, AAVSO, deM, Mdy, KU, RPc, GBo, Aka, IMi, BSM, Kis	
3.25	NSV 2026	2016b	Trt, Dub	
3.26	NSV 14681	2016	Van	
3.27	1RXS J161659	2016	deM, MEV, IMi, Van, Trt	1RXS J161659.5+620014
		2016b	MEV, DPV, IMi	
3.28	ASASSN-13ak	2016	Trt, Kis	
3.29	ASASSN-13al	2016	Van	
3.30	ASASSN-13bc	2015	LCO, Rui, Trt	
		2016	SGE, Shu, NKa, Ioh, Rui	
3.31	ASASSN-13bj	2016	Kai, OKU, Trt, SGE, DPV, IMi, KU	
3.32	ASASSN-13bo	2016	IMi, Shu	
3.33	ASASSN-13cs	2016	SGE, KU, COO	
3.34	ASASSN-13cz	2016	Kai, Trt, Rui, DPV	
3.35	ASASSN-14gg	2016	Van, GFB	

Table 1. List of Superoutbursts (continued).

Subsection	Object	Year	Observers or references*	ID [†]
3.36	ASASSN-15cr	2017	DPV, Ioh, Shu, CRI	
3.37	ASASSN-16da	2016	deM, Van, GFB, SGE, Kai	
3.38	ASASSN-16dk	2016	HaC	
3.39	ASASSN-16ds	2016	MLF, HaC, SPE	
–	ASASSN-16dt	2016	Kimura et al. (2017)	
3.40	ASASSN-16dz	2016	Van	
–	ASASSN-16eg	2016	Wakamatsu et al. (2017)	
3.41	ASASSN-16ez	2016	DPV, Ioh, Kis, MEV, IMi, Van, KU	
3.42	ASASSN-16fr	2016	KU, Ioh, HaC	
3.43	ASASSN-16fu	2016	HaC, MLF	
–	ASASSN-16fy	2016	K. Isogai et al. in preparation	
3.44	ASASSN-16gh	2016	MLF	
3.45	ASASSN-16gj	2016	MLF, HaC	
3.46	ASASSN-16gl	2016	MLF, HaC, DDe	
–	ASASSN-16hg	2016	Kimura et al. (2017)	
3.47	ASASSN-16hi	2016	HaC	
3.48	ASASSN-16hj	2016	HaC, KU	
3.49	ASASSN-16ia	2016	GFB, Ioh, Ter, Van, SGE, CRI, COO, Trt	
3.50	ASASSN-16ib	2016	MLF, HaC	
3.51	ASASSN-16ik	2016	MLF, HaC	
3.52	ASASSN-16is	2016	Shu, IMi, Van, Ioh, Rui	
3.53	ASASSN-16iu	2016	HaC, MLF	
3.54	ASASSN-16iw	2016	HaC, SPE, NKa, Kis, Van, Ioh	
3.55	ASASSN-16jb	2016	MLF, HaC, SPE	
3.56	ASASSN-16jd	2016	HaC, Ioh	
3.57	ASASSN-16jk	2016	CRI, Van	
3.58	ASASSN-16js	2016	HaC, MLF, SPE	
3.59	ASASSN-16jz	2016	Van	

Table 1. List of Superoutbursts (continued).

Subsection	Object	Year	Observers or references*	ID [†]
3.60	ASASSN-16kg	2016	MLF, HaC	
3.61	ASASSN-16kx	2016	HaC, MLF	
3.62	ASASSN-16le	2016	KU, Ioh	
3.63	ASASSN-16lj	2016	Van	
3.64	ASASSN-16lo	2016	KU, IMi, OKU, Ioh	
3.65	ASASSN-16mo	2016	OKU, KU, Trt, Dub, Van	
3.66	ASASSN-16my	2016	HaC, Ioh	
3.67	ASASSN-16ni	2016	KU, Ioh, Trt	
3.68	ASASSN-16nq	2016	Kis, Ioh, RPe, Van, Trt	
3.69	ASASSN-16nr	2016	MLF, HaC	
3.70	ASASSN-16nw	2016	Kai	
3.71	ASASSN-16ob	2016	MLF, HaC, SPE	
3.72	ASASSN-16oi	2016	MLF, HaC, SPE	
3.73	ASASSN-16os	2016	MLF, HaC, SPE	
3.74	ASASSN-16ow	2016	Ioh, Van, NKa, Mdy, MEV, Kis, Kai	
3.75	ASASSN-17aa	2017	MLF, SPE, HaC	
3.76	ASASSN-17ab	2017	HaC	
3.77	ASASSN-17az	2017	MLF	
3.78	ASASSN-17bl	2017	HaC, SPE	
3.79	ASASSN-17bm	2017	MLF, HaC	
3.80	ASASSN-17bv	2017	MLF, SPE, HaC	
3.81	ASASSN-17ce	2017	SPE, MLF, HaC	
3.82	ASASSN-17ck	2017	HaC	
3.83	ASASSN-17cn	2017	MLF, SPE, HaC, Ioh	
3.84	ASASSN-17cx	2017	Mdy	
3.85	ASASSN-17dg	2017	HaC, MLF, SPE	
3.86	ASASSN-17dq	2017	HaC, MLF	
3.87	CRTS J000130	2016	Van, Shu	CRTS J000130.5+050624
3.88	CRTS J015321	2016	Kai	CRTS J015321.5+340857
3.90	CRTS J033349	2016	MLF, HaC, KU	CRTS J033349.8–282244

Table 1. List of Superoutbursts (continued).

Subsection	Object	Year	Observers or references*	ID [†]
3.89	CRTS J023638	2016	CRI, Trt, Shu, Rui	CRTS J023638.0+111157
3.91	CRTS J044637	2017	Ioh, KU	CRTS J044636.9+083033
3.92	CRTS J082603	2017	Van	CRTS J082603.7+113821
3.93	CRTS J085113	2008	Mhh	CRTS J085113.4+344449
		2016	KU, Trt	
3.94	CRTS J085603	2016	Van, Ioh	CRTS J085603.8+322109
3.95	CRTS J164950	2015	RIT, Van	CRTS J164950.4+035835
		2016	CRI, Rui	
3.96	CSS J062450	2017	Trt, Van	CSS131223:062450+503111
3.97	DDE 26	2016	Ioh, IMi, Shu, RPc	
3.98	DDE 48	2016	MNI, IMi	
3.99	MASTER J021315	2016	Van	MASTER OT J021315.37+533822.7
3.100	MASTER J030205	2016	OKU, deM, Van, COO, Ioh, Mdy, T60, NKa, RPc, Trt, Naz	MASTER OT J030205.67+254834.3
3.101	MASTER J042609	2016	Kis, Ioh, Kai, Shu, Trt	MASTER OT J042609.34+354144.8
3.102	MASTER J043220	2017	Van	MASTER OT J043220.15+784913.8
3.103	MASTER J043915	2016	Ioh, CRI	MASTER OT J043915.60+424232.3
3.104	MASTER J054746	2016	Van	MASTER OT J054746.81+762018.9
3.105	MASTER J055348	2017	Van, Mdy	MASTER OT J055348.98+482209.0
3.106	MASTER J055845	2016	Shu	MASTER OT J055845.55+391533.4
3.107	MASTER J064725	2016	Ioh, RPc, CRI	MASTER OT J064725.70+491543.9
3.108	MASTER J065330	2017	Van, Ioh	MASTER OT J065330.46+251150.9
3.109	MASTER J075450	2017	Van	MASTER OT J075450.18+091020.2
3.110	MASTER J150518	2017	HaC	MASTER OT J150518.03–143933.6
3.111	MASTER J151126	2016	HaC, MLF	MASTER OT J151126.74–400751.9
3.112	MASTER J162323	2015	Van	MASTER OT J162323.48+782603.3
		2016	COO, Trt, IMi	
3.113	MASTER J165153	2017	Van	MASTER OT J165153.86+702525.7
3.114	MASTER J174816	2016	Van, Mdy	MASTER OT J174816.22+501723.3
–	MASTER J191841	2016	K. Isogai et al. in preparation	MASTER OT J191841.98+444914.5

Table 1. List of Superoutbursts (continued).

Subsection	Object	Year	Observers or references*	ID [†]
3.115	MASTER J211322	2016	Van	MASTER OT J211322.92+260647.4
3.116	MASTER J220559	2016	MLF, HaC	MASTER OT J220559.40−341434.9
–	OT J002656	2016	Kato et al. (2017)	CSS101212:002657+284933
3.117	SBS 1108	2016	Ioh, COO, Vol, Kai, KU	SBS 1108+574
3.118	SDSS J032015	2016	Van, IMi	SDSS J032015.29+441059.3
3.119	SDSS J032015	2016	Van	SDSS J091001.63+164820.0
3.120	SDSS J113551	2017	Van, Mdy	SDSS J113551.09+532246.2
3.121	SDSS J115207	2009	Kato et al. (2010)	SDSS J115207.00+404947.8
		2017	Mdy, KU, LCO, Ioh, DPV, Kis	
3.122	SDSS J131432	2017	Mdy, Van	SDSS J131432.10+444138.7
3.123	SDSS J153015	2017	Van	SDSS J153015.04+094946.3
3.124	SDSS J155720	2016	HaC, Kis	SDSS J155720.75+180720.2
–	SDSS J173047	2016	K. Isogai et al. in preparation	SDSS J173047.59+554518.5
3.125	SSS J134850	2016	MLF, HaC	SSS J134850.1−310835
3.126	TCP J013758	2016	Kis, IMi, Ioh, RPc, Shu, CRI, Rui, Trt	TCP J01375892+4951055
3.127	TCP J180018	2016	HaC, Nel, SPE	TCP J18001854−3533149

novae with shortest supercycles.

3.2 BB Arietis

This object was discovered as a variable star (Ross 182, NSV 907) on a plate on 1926 November 26 (Ross 1927). The dwarf nova-type nature was suspected by the association with an ROSAT source (Kato, vsnet-chat 3317). The SU UMa-type nature was confirmed during the 2004 superoutburst. For more information, see Kato et al. (2014a).

The 2016 superoutburst was detected by P. Schmeer at a visual magnitude of 13.2 on October 30 (vsnet-alert 20273). Thanks to the early detection (this visual detection was 1 d earlier than the ASAS-SN detection), stage A growing superhumps were detected (vsnet-alert 20292). At the time of the initial observation, the object was fading from a precursor outburst. Further observations recorded development of superhumps clearly (vsnet-alert

Table 2. Coordinates of objects without coordinate-based names.

Object	Right Ascension	Declination	Source*	SDSS <i>g</i>	Gaia <i>G</i>	GALEX NUV
ASASSN-13ak	17 ^h 48 ^m 27 ^s .87	+50°50'39".8	Gaia	19.89(2)	19.06	–
ASASSN-13al	19 ^h 32 ^m 06 ^s .39	+67°27'40".4	GSC2.3.2	–	–	21.5(4)
ASASSN-13bc	18 ^h 02 ^m 22 ^s .44	+45°52'44".6	Gaia	19.53(2)	18.40	19.4(1)
ASASSN-13bj	16 ^h 00 ^m 20 ^s .52	+70°50'07".2	Gaia	–	18.43	–
ASASSN-13bo	01 ^h 43 ^m 54 ^s .23	+29°01'03".8	SDSS	20.94(4)	–	21.8(2)
ASASSN-13cs	17 ^h 11 ^m 38 ^s .40	+05°39'51".0	Gaia	–	19.80	20.9(2)
ASASSN-13cz	15 ^h 27 ^m 55 ^s .11	+63°27'54".2	Gaia	18.94(1)	18.74	–
ASASSN-14gg	18 ^h 21 ^m 38 ^s .61	+61°59'04".0	Gaia	–	19.74	19.4(1)
ASASSN-15cr	07 ^h 34 ^m 42 ^s .71	+50°42'29".0	Gaia	–	19.33	20.2(1)
ASASSN-16da	12 ^h 56 ^m 09 ^s .83	+62°37'04".4	SDSS	21.55(5)	–	21.6(4)
ASASSN-16dk	10 ^h 20 ^m 53 ^s .48	–86°17'29".77	Gaia	–	20.41	19.31(7)
ASASSN-16ds	18 ^h 25 ^m 09 ^s .96	–46°20'17".9	ASAS-SN	–	–	–
ASASSN-16dz	06 ^h 42 ^m 25 ^s .58	+08°25'46".6	Gaia	–	19.10	–
ASASSN-16ez	15 ^h 31 ^m 29 ^s .87	+21°38'30".2	SDSS	21.28(4)	–	–
ASASSN-16fr	16 ^h 42 ^m 51 ^s .80	–08°52'41".0	SDSS	20.97(4)	–	–
ASASSN-16fu	22 ^h 14 ^m 05 ^s .03	–09°04'19".4	SDSS	21.64(7)	–	–
ASASSN-16gh	18 ^h 15 ^m 57 ^s .62	–72°40'38".1	ASAS-SN	–	–	–
ASASSN-16gj	09 ^h 59 ^m 58 ^s .97	–19°01'00".0	GSC2.3.2	–	–	21.3(3)
ASASSN-16gl	18 ^h 27 ^m 16 ^s .25	–52°47'44".1	ASAS-SN	–	–	–
ASASSN-16hi	21 ^h 38 ^m 58 ^s .01	–73°19'17".5	Gaia	–	18.86	20.9(2)
ASASSN-16ia	20 ^h 51 ^m 59 ^s .24	+34°49'46".1	Gaia	–	–	–
ASASSN-16ib	14 ^h 32 ^m 03 ^s .74	–33°08'13".9	IGSL	–	–	21.5(4)
ASASSN-16ik	19 ^h 27 ^m 45 ^s .88	–67°15'16".7	IGSL	–	–	21.8(5)
ASASSN-16is	18 ^h 31 ^m 03 ^s .63	+11°32'02".9	Gaia	–	20.36	–
ASASSN-16iu	01 ^h 43 ^m 47 ^s .87	–70°17'01".1	Gaia	–	19.99	20.39(9)
ASASSN-16iw	00 ^h 58 ^m 11 ^s .10	–01°07'50".9	SDSS	21.9(1)	–	–

*source of the coordinates: 2MASS (2MASS All-Sky Catalog of Point Sources; Cutri et al. 2003), ASAS-SN (ASAS-SN measurements), CRTS (CRTS measurements), Gaia (Gaia DR1, Gaia Collaboration 2016 and outburst detections), GSC2.3.2 (The Guide Star Catalog, Version 2.3.2, Lasker et al. 2007), IGSL (The Initial Gaia Source List 3, Smart 2013), IPHAS DR2 (INT/WFC Photometric H α Survey, Witham et al. 2008), SDSS (The SDSS Photometric Catalog, Release 9, Ahn et al. 2012).

Table 2. Coordinates of objects without coordinate-based names (continued).

Object	Right Ascension	Declination	Source*	SDSS <i>g</i>	Gaia G	GALEX NUV
ASASSN-16jb	17 ^h 50 ^m 44 ^s .99	−25°58′37″.1	ASAS-SN	–	–	–
ASASSN-16jd	18 ^h 50 ^m 33 ^s .33	−26°50′40″.8	ASAS-SN	–	–	–
ASASSN-16jk	15 ^h 40 ^m 24 ^s .84	+23°07′50″.8	Gaia	20.73(3)	20.68	21.7(3)
ASASSN-16js	00 ^h 51 ^m 19 ^s .17	−65°57′17″.0	Gaia	–	20.08	22.1(2)
ASASSN-16jz	19 ^h 18 ^m 53 ^s .39	+79°32′16″.0	IGSL	–	–	–
ASASSN-16kg	21 ^h 36 ^m 29 ^s .86	−25°13′48″.3	CRTS	–	–	–
ASASSN-16kx	06 ^h 17 ^m 18 ^s .72	−49°38′57″.3	ASAS-SN	–	–	–
ASASSN-16le	23 ^h 34 ^m 35 ^s .56	+54°33′25″.5	Gaia	–	18.83	–
ASASSN-16lj	20 ^h 15 ^m 46 ^s .04	+75°47′41″.7	Gaia	20.99(5)	20.17	21.5(2)
ASASSN-16lo	18 ^h 08 ^m 41 ^s .02	+46°19′34″.9	IGSL	–	–	–
ASASSN-16mo	02 ^h 56 ^m 56 ^s .67	+49°27′47″.1	Gaia	–	20.19	–
ASASSN-16my	07 ^h 41 ^m 08 ^s .46	−30°03′17″.9	Gaia	–	18.52	–
ASASSN-16ni	05 ^h 05 ^m 00 ^s .32	+60°45′53″.7	ASAS-SN	–	–	–
ASASSN-16nq	23 ^h 22 ^m 09 ^s .25	+39°50′07″.8	Gaia	–	19.10	21.1(3)
ASASSN-16nr	07 ^h 09 ^m 49 ^s .33	−49°09′03″.6	GSC2.3.2	–	–	–
ASASSN-16nw	01 ^h 53 ^m 49 ^s .09	+52°52′05″.1	IGSL	–	–	–
ASASSN-16ob	06 ^h 47 ^m 18 ^s .89	−64°37′07″.3	Gaia	–	–	–
ASASSN-16oi	06 ^h 21 ^m 32 ^s .38	−62°58′15″.6	GSC2.3.2	–	–	22.0(5)
ASASSN-16os	08 ^h 43 ^m 05 ^s .59	−84°53′45″.6	GSC2.3.2	–	–	–
ASASSN-16ow	06 ^h 30 ^m 47 ^s .05	+02°39′31″.4	IPHAS	–	–	–
ASASSN-17aa	04 ^h 23 ^m 56 ^s .40	−74°05′27″.5	ASAS-SN	–	–	–
ASASSN-17ab	10 ^h 40 ^m 51 ^s .25	−37°03′30″.2	Gaia	–	–	–
ASASSN-17az	00 ^h 15 ^m 09 ^s .31	−69°45′49″.2	ASAS-SN	–	–	–
ASASSN-17bl	12 ^h 31 ^m 50 ^s .86	−50°25′07″.4	ASAS-SN	–	–	–
ASASSN-17bm	10 ^h 55 ^m 27 ^s .84	−48°04′27″.4	GSC2.3.2	–	–	–
ASASSN-17bv	09 ^h 08 ^m 45 ^s .65	−62°37′11″.0	IGSL	–	–	–
ASASSN-17ce	13 ^h 24 ^m 24 ^s .46	−54°09′21″.7	Gaia	–	18.52	–
ASASSN-17ck	08 ^h 30 ^m 46 ^s .29	−28°58′13″.5	GSC2.3.2	–	–	–
ASASSN-17cn	09 ^h 31 ^m 22 ^s .60	−35°20′54″.3	Gaia	–	–	–
ASASSN-17cx	10 ^h 59 ^m 57 ^s .97	−11°57′56″.8	GSC2.3.2	–	–	20.8(2)
ASASSN-17dg	16 ^h 02 ^m 33 ^s .49	−60°32′50″.3	2MASS	–	–	–
ASASSN-17dq	09 ^h 01 ^m 25 ^s .26	−59°31′40″.1	ASAS-SN	–	–	–
DDE 26	22 ^h 03 ^m 28 ^s .21	+30°56′36″.18	Gaia	19.61(1)	19.32	–
SBS 1108+574	11 ^h 11 ^m 26 ^s .83	+57°12′38″.6	Gaia	19.22(1)	19.26	19.5(1)

Table 3. Superhump Periods and Period Derivatives

Object	Year	P_1 (d)	err	E_1^*	$P_{\dot{\text{d}}\text{ot}}^\dagger$	err [†]	P_2 (d)	err	E_2^*	P_{orb} (d) [‡]	Q [§]		
V1047 Aql	2016	0.073666	0.000054	0	14	–	–	–	–	–	C		
BB Ari	2016	0.072491	0.000026	27	70	19.7	4.2	0.072179	0.000019	70	115	–	A
OY Car	2016	0.064653	0.000028	0	104	9.9	1.7	0.064440	0.000049	103	159	0.063121	B
HT Cas	2016	0.076333	0.000005	19	62	–	–	0.075886	0.000005	72	145	0.073647	A
GS Cet	2016	0.056645	0.000014	14	156	6.3	0.6	–	–	–	–	0.05597	AE
GZ Cet	2016	0.056702	0.000028	0	54	11.4	2.8	0.056409	0.000006	141	425	0.055343	B
AK Cnc	2016	0.067454	0.000030	0	76	–	–	–	–	–	–	0.0651	C
GZ Cnc	2017	0.092881	0.000022	32	91	–0.9	4.9	0.092216	0.000291	91	113	0.08825	C
GP CVn	2016	0.064796	0.000027	17	96	9.5	2.5	–	–	–	–	0.062950	B
V1113 Cyg	2016	0.078848	0.000028	52	141	–2.4	2.9	–	–	–	–	–	B
IX Dra	2016	0.066895	0.000045	0	92	4.7	4.6	–	–	–	–	–	C
IR Gem	2016	0.071090	0.000047	0	33	–	–	0.070633	0.000047	56	104	0.0684	C
IR Gem	2017	0.071098	0.000020	25	56	–	–	–	–	–	–	0.0684	C
NY Her	2016	0.075832	0.000043	0	42	–	–	0.075525	0.000051	49	114	–	B
V699 Oph	2016	0.070212	0.000096	0	28	–	–	–	–	–	–	–	C
V344 Pav	2016	0.079878	0.000031	0	76	–8.8	2.7	–	–	–	–	–	CG
V893 Sco	2016	0.074666	0.000326	0	26	–	–	–	–	–	–	0.075961	C2
V493 Ser	2016	–	–	–	–	–	–	0.082730	0.000129	0	13	0.08001	C
V1389 Tau	2016	0.080456	0.000081	0	35	–	–	0.079992	0.000025	34	121	–	C

*Interval used for calculating the period (corresponding to E in section 3).

[†]Unit 10^{-5} .

[‡]References:

GZ Cet (Pretorius et al. 2004), AK Cnc (Arenas, Mennickent 1998), GZ Cnc (Tappert, Bianchini 2003), IR Gem (Feinswog et al. 1988), V493 Ser (Thorstensen et al. 2015), HV Vir (Patterson et al. 2003), SBS 1108 (Kato et al. 2013), OY Car, GS Cet, GP CVn, V893 Sco, ASASSN-16da, ASASSN-16fu, ASASSN-16ia, ASASSN-16is, ASASSN-16jb, ASASSN-16js, ASASSN-16lo, ASASSN-16oi, ASASSN-16os, ASASSN-17bl, ASASSN-17cn, MASTER J042609, MASTER J220559, SDSS J115207 (this work)

[§]Data quality and comments. A: excellent, B: partial coverage or slightly low quality, C: insufficient coverage or observations with large scatter, G: $P_{\dot{\text{d}}\text{ot}}$ denotes global $P_{\dot{\text{d}}\text{ot}}$, M: observational gap in middle stage, U: uncertainty in alias selection, 2: late-stage coverage, the listed period may refer to P_2 , a: early-stage coverage, the listed period may be contaminated by stage A superhumps, E: P_{orb} refers to the period of early superhumps, P: P_{orb} refers to a shorter stable periodicity recorded in outburst.

Table 3. Superhump Periods and Period Derivatives (continued)

Object	Year	P_1	err	E_1	$P_{\dot{}}$	err	P_2	err	E_2	P_{orb}	Q		
HV Vir	2016	0.058244	0.000009	31	227	3.1	0.4	-	-	-	0.057069	A	
NSV 2026	2016b	0.069906	0.000022	0	13	-	-	-	-	-	-	C	
NSV 14681	2016	0.090063	0.000008	0	77	-0.5	0.8	-	-	-	-	C	
1RXS J161659	2016	0.071370	0.000063	0	43	-	-	0.071063	0.000054	56	74	-	C
1RXS J161659	2016b	0.071229	0.000056	0	58	-	-	-	-	-	-	-	C
ASASSN-13al	2016	0.0783	0.0002	0	3	-	-	-	-	-	-	-	C
ASASSN-13bc	2015	0.070393	0.000118	0	16	-	-	-	-	-	-	-	C
ASASSN-13bc	2016	0.070624	0.000100	0	39	-	-	0.070101	0.000046	39	85	-	C
ASASSN-13bj	2016	0.072553	0.000047	0	21	-	-	0.071918	0.000053	23	44	-	C
ASASSN-13bo	2016	0.071860	0.000025	0	41	-	-	-	-	-	-	-	CU
ASASSN-13cs	2016	0.077105	0.000098	0	20	-	-	-	-	-	-	-	C
ASASSN-13cz	2016	0.080135	0.000044	0	13	-	-	0.079496	0.000368	62	76	-	C
ASASSN-14gg	2016	0.059311	0.000035	0	89	13.1	2.9	-	-	-	-	-	B
ASASSN-15cr	2017	0.061554	0.000021	16	149	7.8	1.5	0.061260	0.000005	146	217	-	B
ASASSN-16da	2016	0.057344	0.000024	10	175	7.5	0.9	0.056994	0.000062	203	239	0.05610	BE
ASASSN-16dk	2016	-	-	-	-	-	-	0.075923	0.000047	0	67	-	C
ASASSN-16ds	2016	0.067791	0.000027	33	195	7.1	0.6	0.067228	0.000051	-	-	-	B
ASASSN-16dt	2016	0.064507	0.000005	62	214	-1.6	0.5	-	-	-	-	0.064197	AE
ASASSN-16dz	2016	0.066260	0.000170	0	16	-	-	-	-	-	-	-	CU
ASASSN-16eg	2016	0.077880	0.000003	15	106	10.4	0.8	0.077589	0.000007	120	181	0.075478	AE
ASASSN-16ez	2016	0.057621	0.000017	0	77	2.1	2.9	-	-	-	-	-	C
ASASSN-16fr	2016	0.071394	0.000144	0	35	-	-	-	-	-	-	-	C
ASASSN-16fu	2016	0.056936	0.000013	35	195	4.6	0.6	-	-	-	-	0.05623	BE
ASASSN-16gh	2016	0.061844	0.000017	16	100	6.7	2.7	-	-	-	-	-	B
ASASSN-16gj	2016	0.057997	0.000022	74	208	7.0	1.0	-	-	-	-	-	B
ASASSN-16gl	2016	0.055834	0.000010	0	118	1.6	1.2	-	-	-	-	-	B
ASASSN-16hg	2016	0.062371	0.000014	15	115	0.6	1.7	-	-	-	-	-	B
ASASSN-16hi	2016	0.059040	0.000024	0	121	8.6	1.5	0.058674	0.000023	118	188	-	B
ASASSN-16hj	2016	0.055644	0.000041	20	145	11.3	1.3	0.055465	0.000036	144	324	0.05499	BE

Table 3. Superhump Periods and Period Derivatives (continued)

Object	Year	P_1	err	E_1	P_{dot}	err	P_2	err	E_2	P_{orb}	Q		
ASASSN-16ib	2016	0.058855	0.000015	47	144	2.2	2.0	–	–	–	–	C	
ASASSN-16ik	2016	0.064150	0.000018	33	126	1.0	2.1	–	–	–	–	B	
ASASSN-16is	2016	0.058484	0.000015	0	105	4.2	1.7	–	–	–	0.05762	CE	
ASASSN-16iu	2016	0.058720	0.000062	0	104	26.7	3.3	0.058661	0.000300	34	53	–	C
ASASSN-16iw	2016	0.065462	0.000039	42	153	10.0	3.2	–	–	–	–	0.06495	BE
ASASSN-16jb	2016	0.064397	0.000021	30	193	5.9	0.7	0.064170	0.000075	193	232	0.06305	AE
ASASSN-16jd	2016	0.058163	0.000039	34	223	7.9	0.6	0.057743	0.000159	223	258	–	B
ASASSN-16jk	2016	0.061391	0.000028	16	146	8.6	1.3	–	–	–	–	–	C
ASASSN-16js	2016	0.060934	0.000015	48	173	4.9	1.0	–	–	–	–	0.06034	AE
ASASSN-16jz	2016	0.060936	0.000014	0	51	–	–	–	–	–	–	–	C
ASASSN-16kg	2016	0.100324	0.000189	0	30	–	–	–	–	–	–	–	CU
ASASSN-16kx	2016	0.080760	0.000036	0	54	–6.4	6.5	0.080536	0.000041	79	153	–	C
ASASSN-16le	2016	0.0808	0.0013	0	2	–	–	–	–	–	–	–	C
ASASSN-16lj	2016	0.0857	0.0004	0	2	–	–	–	–	–	–	–	C
ASASSN-16lo	2016	0.054608	0.000036	38	86	–	–	–	–	–	–	0.05416	CE
ASASSN-16mo	2016	0.066477	0.000016	0	84	3.9	2.3	–	–	–	–	–	C
ASASSN-16my	2016	0.087683	0.000049	23	92	3.0	5.7	–	–	–	–	–	C
ASASSN-16ni	2016	0.115242	0.000442	0	11	–	–	–	–	–	–	–	CU
ASASSN-16nq	2016	0.079557	0.000045	0	39	0.0	9.3	0.079069	0.000035	59	161	–	B
ASASSN-16nr	2016	0.082709	0.000080	0	59	–19.8	10.1	–	–	–	–	–	CG
ASASSN-16nw	2016	0.072813	0.000045	0	43	–	–	–	–	–	–	–	C
ASASSN-16ob	2016	0.057087	0.000014	52	249	1.8	0.5	–	–	–	–	–	B
ASASSN-16oi	2016	0.056241	0.000017	12	122	5.0	1.7	–	–	–	–	0.05548	BE
ASASSN-16os	2016	0.054992	0.000013	39	168	0.3	1.4	–	–	–	–	0.05494	BE
ASASSN-16ow	2016	0.089311	0.000052	0	40	–	–	0.088866	0.000022	55	102	–	B
ASASSN-17aa	2017	0.054591	0.000013	0	182	2.8	0.3	–	–	–	–	0.05393	BE
ASASSN-17ab	2017	0.070393	0.000016	15	88	3.6	2.5	–	–	–	–	–	C
ASASSN-17az	2017	0.056492	0.000038	0	36	–	–	–	–	–	–	–	CU
ASASSN-17bl	2017	0.055367	0.000010	53	237	3.6	0.6	–	–	–	–	0.05467	CE

Table 3. Superhump Periods and Period Derivatives (continued)

Object	Year	P_1	err	E_1	$P_{\dot{}}$	err	P_2	err	E_2	P_{orb}	Q	
ASASSN-17bm	2017	0.082943	0.000056	0	53	-	-	-	-	-	C	
ASASSN-17bv	2017	0.082690	0.000021	12	52	-6.3	3.9	0.082489	0.000048	58 103	B	
ASASSN-17ce	2017	0.081293	0.000111	0	22	-	-	0.080796	0.000042	21 139	C	
ASASSN-17ck	2017	0.083	0.001	0	1	-	-	-	-	-	C	
ASASSN-17cn	2017	0.053991	0.000014	0	137	5.6	0.8	-	-	-	0.05303	BE
ASASSN-17cx	2017	0.0761	0.0007	0	2	-	-	-	-	-	-	C
ASASSN-17dg	2017	-	-	-	-	-	-	0.066482	0.000046	0 36	-	C
ASASSN-17dq	2017	0.058052	0.000034	0	93	9.3	3.5	0.057660	0.000076	90 142	-	C
CRTS J000130	2016	0.094749	0.000066	0	63	-	-	-	-	-	-	C
CRTS J023638	2016	0.073703	0.000057	0	42	-	-	0.073504	0.000053	40 80	-	C
CRTS J033349	2016	-	-	-	-	-	-	0.076159	0.000049	0 60	-	C
CRTS J082603	2017	0.0719	0.0004	0	1	-	-	-	-	-	-	C
CRTS J085113	2016	0.08750	0.00009	0	1	-	-	-	-	-	-	C
CRTS J085603	2016	0.060043	0.000193	0	18	-	-	-	-	-	-	C
CRTS J164950	2016	0.064905	0.000091	0	61	-	-	-	-	-	-	C
CSS J044637	2017	0.093	0.001	0	1	-	-	-	-	-	-	C
CSS J062450	2017	0.077577	0.000094	0	14	-	-	-	-	-	-	C
DDE 26	2016	0.088804	0.000067	0	44	-	-	-	-	-	-	C
MASTER J021315	2016	0.105124	0.000252	10	21	-	-	-	-	-	-	C
MASTER J030205	2016	0.061553	0.000022	1	96	8.4	2.5	-	-	-	-	B
MASTER J042609	2016	0.067624	0.000016	0	64	6.4	2.7	0.067221	0.000051	64 122	0.065502	B
MASTER J043220	2017	0.0640	0.0006	0	1	-	-	-	-	-	-	C
MASTER J043915	2016	0.062428	0.000045	0	112	-	-	-	-	-	-	C
MASTER J054746	2016	0.0555	0.0004	0	3	-	-	-	-	-	-	C
MASTER J055348	2017	0.0750	0.0001	0	24	-	-	-	-	-	-	CU
MASTER J064725	2016	0.067584	0.000020	0	108	1.2	3.5	-	-	-	-	CG
MASTER J065330	2017	0.064012	0.000167	0	13	-	-	-	-	-	-	C
MASTER J075450	2017	0.0664	0.0050	0	1	-	-	-	-	-	-	C
MASTER J150518	2017	0.071145	0.000125	0	56	-29.5	1.0	-	-	-	-	CGU

Table 3. Superhump Periods and Period Derivatives (continued)

Object	Year	P_1	err	E_1	P_{dot}	err	P_2	err	E_2	P_{orb}	Q		
MASTER J151126	2016	0.058182	0.000016	16	171	4.5	0.6	–	–	–	–	C	
MASTER J055845	2016	0.058070	0.000081	0	19	–	–	–	–	–	–	C2	
MASTER J162323	2016	0.09013	0.00007	0	4	–	–	–	–	–	–	Ca	
MASTER J165153	2017	0.071951	0.000079	0	31	–	–	–	–	–	–	C	
MASTER J174816	2016	0.083328	0.000120	0	21	–	–	–	–	–	–	CU	
MASTER J191841	2016	0.022076	0.000007	0	51	–	–	–	–	–	–	B	
MASTER J220559	2016	0.061999	0.000067	0	83	28.4	6.5	0.061434	0.000078	81	116	0.061286	C
OT J002656	2016	0.132240	0.000054	30	112	16.4	1.6	–	–	–	–	–	B
SBS 1108	2016	0.039051	0.000008	0	72	–	–	–	–	–	0.038449	–	CP
SDSS J032015	2016	0.073757	0.000028	0	137	2.5	4.2	–	–	–	–	–	CG
SDSS J091001	2017	0.0734	0.0002	0	2	–	–	–	–	–	–	–	C
SDSS J113551	2017	0.0966	0.0001	0	18	–	–	–	–	–	–	–	CU
SDSS J115207	2009	0.070028	0.000088	0	68	–	–	–	–	–	0.067750	–	CG
SDSS J115207	2017	0.070362	0.000044	0	52	–	–	0.069914	0.000019	52	131	0.067750	B
SDSS J131432	2017	0.065620	0.000034	0	55	18.3	8.6	–	–	–	–	–	C
SDSS J153015	2017	0.075241	0.000039	0	41	–	–	–	–	–	–	–	C
SDSS J155720	2016	0.085565	0.000131	0	29	–	–	–	–	–	–	–	C
SDSS J173047	2016	0.024597	0.000007	0	329	0.8	0.3	–	–	–	–	–	B
SSS J134850	2016	0.084534	0.000017	0	80	–3.0	1.6	–	–	–	–	–	CG
TCP J013758	2016	0.061692	0.000024	31	142	12.6	0.8	0.061408	0.000032	140	208	–	B
TCP J180018	2016	0.058449	0.000024	26	233	5.7	0.7	–	–	–	–	–	B

20312, 20321). The times of superhump maxima are listed in e-table 1. There were clear stages A–C (figure 2). The 2013 superoutburst had a separate precursor outburst and a comparison of the $O - C$ diagrams suggests a difference of 44 cycle count from that used in Kato et al. (2014a). The value suggests that superhumps during the 2013 superoutburst evolved 3 d after the precursor outburst.

3.3 V391 Camelopardalis

This object (=1RXS J053234.9+624755) was discovered as a dwarf nova by Bernhard et al. (2005). Kapusta, Thorstensen (2006) provided a radial-velocity study and yielded an orbital

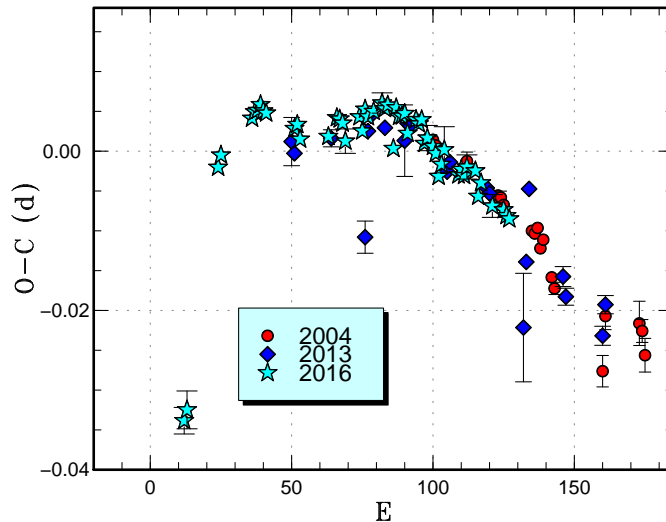


Fig. 2. Comparison of $O - C$ diagrams of BB Ari between different superoutbursts. A period of 0.07249 d was used to draw this figure. Approximate cycle counts (E) after the starts of outbursts were used. The definition is different from the corresponding figure in Kato et al. (2014a). The 2013 superoutburst had a separate precursor outburst and the cycle count is different by 44 from that used in Kato et al. (2014a). The value suggests that superhumps during the 2013 superoutburst evolved 3 d after the precursor outburst. Since the start of the 2004 superoutburst was not well constrained, we shifted the $O - C$ diagram to best fit the 2016 one.

period of 0.05620(4) d. The SU UMa-type nature was established during the 2005 superoutburst (Imada et al. 2009). See Kato et al. (2009) for more history. The 2009 superoutburst was also studied in Kato et al. (2010).

The 2017 superoutburst was detected by P. Schmeer at a visual magnitude of 11.4 and also by the ASAS-SN team at $V=11.82$ on March 15. Single superhump was recorded at BJD 2457829.3171(2) ($N=236$). Although there were observations on three nights immediately after the superoutburst, we could neither detect superhump nor orbital periods.

3.4 OY Carinae

See Kato et al. (2015a) for the history of this well-known eclipsing SU UMa-type dwarf nova. The 2016 superoutburst was detected by R. Stubbings at a visual magnitude of 11.6 on April 2 (vsnet-alert 19676). Due to an accidental delay in the start of observations, the earliest time-resolved CCD observations were obtained on April 3 (vsnet-alert 19706). On that night, superhumps (likely in the growing phase) unfortunately overlapped with eclipses (figure 3, upper panel). Distinct superhumps were recorded on April 4 (vsnet-alert 19692; figure 3, middle panel). A further analysis suggested that stage A superhumps escaped detection before April 4 (due to the lack of observations and overlapping eclipses). At the time of April 4, the superhumps were already likely stage B (e-table 2, maxima outside eclipses).

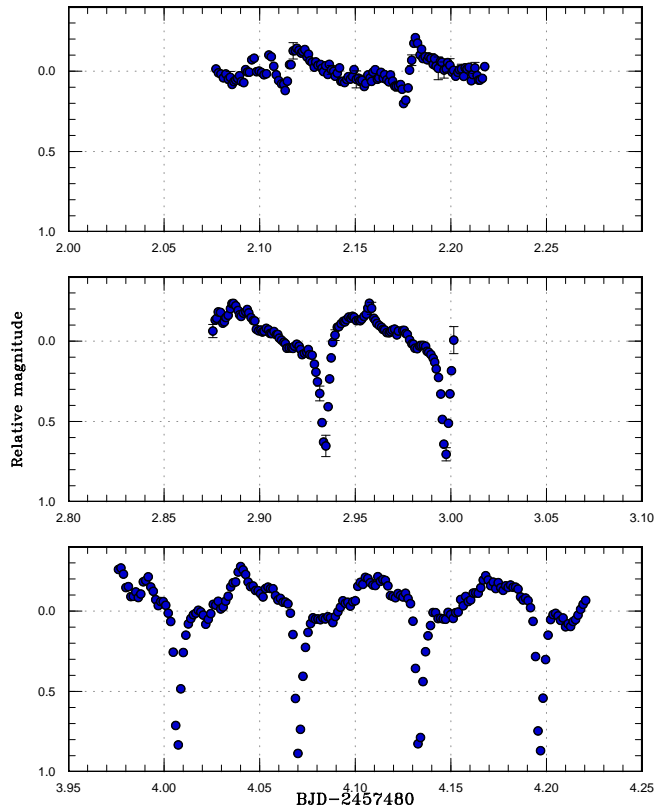


Fig. 3. Eclipses and superhumps in OY Car in the earliest phase (2016). The data were binned to 0.001 d. During the first run (upper panel), eclipses were very shallow since they overlapped with superhumps.

We could, however, confirm a positive P_{dot} for stage B superhumps (cf. figure 4), whose confirmation had been still awaited (cf. Kato et al. 2015a).

The combined data used in Kato et al. (2015a) and new observations, we have obtained the eclipse ephemeris for the use of defining the orbital phases in this paper using the MCMC analysis (Kato et al. 2013):

$$\text{Min(BJD)} = 2457120.49413(2) + 0.0631209131(5)E. \quad (1)$$

The epoch corresponds to the center of the entire observation. The mean period, however, did not show a secular decrease (e.g. Han et al. 2015; Kato et al. 2015a). It may be that period changes in this system are sporadic and do not reflect the secular CV evolution.

3.5 GS Ceti

This object (SDSS J005050.88+000912.6) was selected as a CV during the course of the SDSS (Szkody et al. 2005). The spectrum was that of a quiescent dwarf nova. Southworth et al. (2007) obtained 8 hr of photometry giving a suspected orbital period of ~ 76 min.

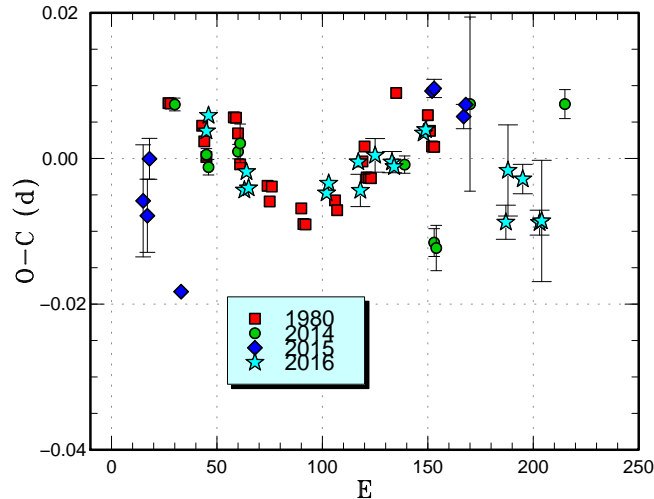


Fig. 4. Comparison of $O - C$ diagrams of OY Car between different superoutbursts. A period of 0.06465 d was used to draw this figure. Approximate cycle counts (E) after the starts of outbursts were used. The 2015 superoutburst with a separate precursor outburst was shifted by 15 cycles to best match the others. Since the start of the 2016 superoutburst was not well constrained, the values were shifted by 45 cycles to best match the others. This shift suggests that the actual start of the 2016 superoutburst occurred 2 d before the initial detection.

Although there were no secure outburst record in the past, the object was detected in bright outburst on 2016 November 9 at $V=13.0$ by the ASAS-SN team (vsnet-alert 20328). Subsequent observations detected early superhumps (vsnet-alert 20334, 20342). Although the profile was not doubly peaked as in many WZ Sge-type dwarf novae (cf. Kato 2015), we consider the signal to be that of early superhumps since it was seen before the appearance of ordinary superhumps and the period was close to the suggested orbital period by quiescent photometry (e-figure 2). The object started to show ordinary superhumps on November 17 (vsnet-alert 20368, 20381, 20395, 20404; e-figure 3). The times of superhump maxima are listed in e-table 3. There were clear stages A and B.

The best period of early superhumps by the PDM method was 0.05597(3) d. Combined with the period of stage A superhumps, the ϵ^* of 0.0288(8) corresponds to $q=0.078(2)$. Although the object is a WZ Sge-type dwarf nova, it is not a very extreme one as judged from the relatively large P_{dot} of stage B superhumps and the lack of the feature of an underlying white dwarf in the optical spectra in quiescence (Szkody et al. 2005; Southworth et al. 2007). Although there were some post-superoutburst observations, the quality of the data was not sufficient to detect superhumps.

3.6 GZ Ceti

This object was originally selected as a CV (SDSS J013701.06–091234.9) during the course of the SDSS (Szkody et al. 2003). Szkody et al. (2003) obtained spectra showing broad absorption surrounding the emission lines of $H\beta$ and higher members of the Balmer series. The object showed the TiO bandheads of an M dwarf secondary. A radial-velocity study by Szkody et al. (2003) suggested an orbital period of 80–86 min. There was a superoutburst in 2003 December and Pretorius et al. (2004) reported the orbital and superhump periods of 79.71(1) min and 81.702(7) min, respectively. Pretorius et al. (2004) reported the period variation of superhumps, which can be now interpreted as stages B and C. Pretorius et al. (2004) suggested that this object has a low mass-transfer rate. The same superoutburst was studied by Imada et al. (2006), who reported the superhump period of 0.056686(12) d. Imada et al. (2006) noticed the unusual presence of the TiO bands for this short- P_{SH} object and discussed that the secondary should be luminous. Ishioka et al. (2007) obtained an infrared spectrum dominated by the secondary component. Ishioka et al. (2007) suggested that the evolutionary path of GZ Cet is different from that of ordinary CVs, and that it is a candidate of a member of EI Psc-like systems. EI Psc-like systems are CVs below the period minimum showing hydrogen (likely somewhat reduced in abundance) in their spectra (cf. Thorstensen et al. 2002; Uemura et al. 2002; Littlefield et al. 2013) and are considered to be evolving towards AM CVn-type objects. Superhump observations during the superoutbursts in 2009 and 2011 were also reported in Kato et al. (2009) and Kato et al. (2013), respectively.

The 2016 superoutburst was detected by R. Stubbings at a visual magnitude of 12.6 on December 18 (vsnet-alert 20493). The ASAS-SN team also recorded the outburst at $V=12.66$ on December 17. This superoutburst was observed in its relatively late phase to the post-superoutburst phase (vsnet-alert 20594). There was also a post-superoutburst rebrightening on 2017 January 15 (vsnet-alert 20569). The times of superhump maxima are listed in e-table 4. The times after $E=266$ represent post-superoutburst superhumps. The maxima for $E \leq 54$ were stage B superhumps and “textbook” stage C superhumps continued even during the post-superoutburst phase without a phase jump as in traditional late superhumps (figure 5).

3.7 AK Cancr

AK Cnc was discovered as a short-period variable star (AN 77.1933) with a photographic range of 14 to fainter than 15.5 (Morgenroth 1933). Morgenroth (1933) detected two maxima

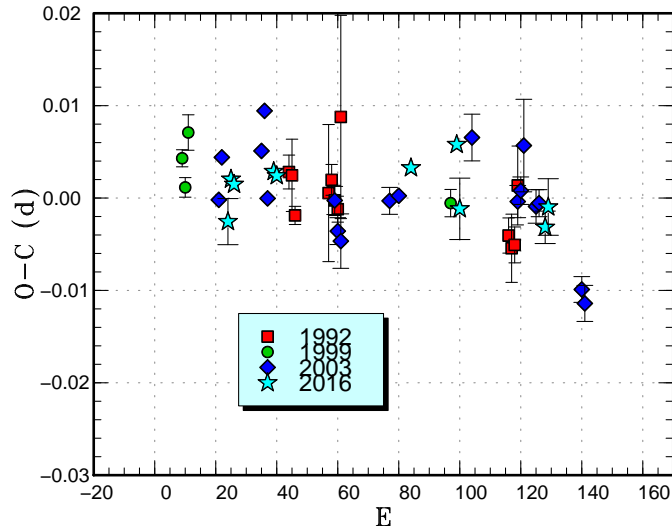


Fig. 5. Comparison of $O - C$ diagrams of GZ Cet between different superoutbursts. A period of 0.05672 d was used to draw this figure. Approximate cycle counts (E) after the start of the superoutburst were used.

on 48 plates between JD 2425323 and 2426763. Tsevech (1967) classified this object to be a U Gem-type variable without a particular remark. Williams (1983) reported a G-type spectrum unlike for a CV. The identification was later found to be incorrect (Howell et al. 1990; Wenzel 1993b). The identification chart by Vogt, Bateson (1982) was correct. Amateur observers, particularly AAVSO and VSOLJ observers, made regular monitoring since 1986 and detected several outbursts. Time-resolved CCD observation by Howell et al. (1990) recorded a declining part of an outburst. Szkody, Howell (1992) obtained a spectrum in quiescence, which was characteristic to a dwarf nova. Wenzel (1993b) and Wenzel (1993a) reported observations using photographic archival materials and discussed outburst properties. Wenzel (1993b) also gave a summary of confusing history of the identification of this object.

Kato (1994) was the first to identify this object to be an SU UMa-type dwarf nova by observing the 1992 superoutburst. Mennickent et al. (1996) reported another superoutburst in 1995. The orbital period was spectroscopically measured to be 0.0651(2) d (Arenas, Mennickent 1998). Kato et al. (2009) provided analyses of the 1999 and 2003 superoutbursts. Kato et al. (2013) further reported observations of the 2012 superoutburst.

The 2016 superoutburst was detected at a visual magnitude of 13.5 by G. Poyner on April 5. The times of superhump maxima are listed in e-table 5. Due to the rather poor coverage, we could not determine P_{dot} for stage B although the distinction between stages B and C was clear. Although positive P_{dot} for stage B is expected for this P_{orb} , it still awaits better observations (figure 6).

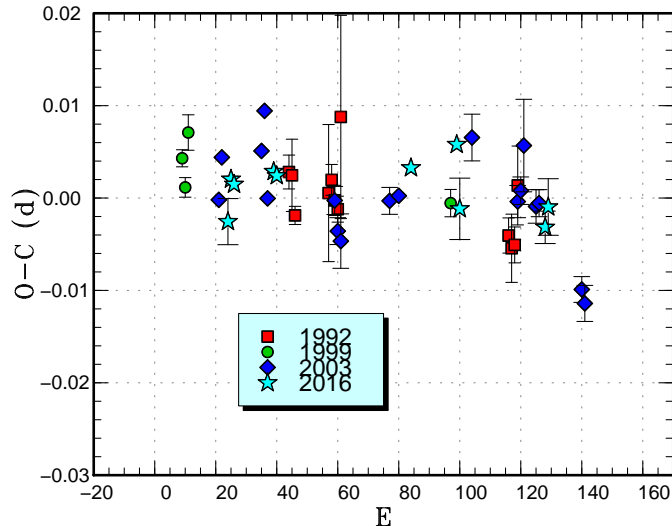


Fig. 6. Comparison of $O - C$ diagrams of AK Cnc between different superoutbursts. A period of 0.06743 d was used to draw this figure. Approximate cycle counts (E) after the start of the superoutburst were used.

3.8 GZ Cancri

GZ Cnc was discovered by K. Takamizawa as a variable star (=TmzV34). The object was confirmed as a dwarf nova (Kato et al. 2001b; Kato et al. 2002a). Tappert, Bianchini (2003) obtained the orbital period of 0.08825(28) d by radial-velocity observations. The SU UMa-type nature was established during the 2010 (Kato et al. 2010). See Kato et al. (2014a) for more information.

The 2017 superoutburst was detected by R. Stubbings at a visual magnitude of 13.0 on February 2 and on the same night at 12.5 mag by T. Horie. Subsequent observations detected growing superhumps on February 3 and 4. Superhumps grew further on February 6 (vsnet-alert 20642). The times of superhump maxima are listed in e-table 6. Thanks to the early detection of the outburst, stage A superhumps were clearly detected (figure 7). The ϵ^* for stage A superhumps [0.081(3)] corresponds to $q=0.27(2)$.

3.9 GP Canum Venaticorum

This object was originally selected as a CV (SDSS J122740.83+513925.0) during the course of the SDSS (Szkody et al. 2006). Szkody et al. (2006) obtained a spectrum showing an underlying white dwarf. Littlefair et al. (2008) clarified that this object is an eclipsing dwarf nova with a short orbital period. The object underwent the first-recorded superoutburst in 2007 June. This 2007 superoutburst was analyzed by Shears et al. (2008) and Kato et al. (2009). Kato et al. (2012a) reported on the 2011 superoutburst and provided a corrected

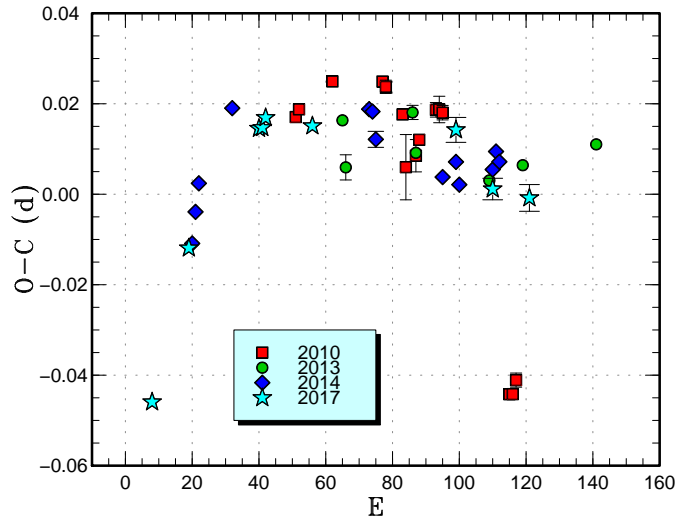


Fig. 7. Comparison of $O - C$ diagrams of GZ Cnc between different superoutbursts. A period of 0.09290 d was used to draw this figure. Approximate cycle counts (E) after the start of the superoutburst were used.

eclipse ephemeris. Savoury et al. (2011) reported the orbital parameters (including q) by modeling the eclipse profile. Although Zengin Çamurdan et al. (2010) suspected cyclic $O - C$ variation of eclipses, their result was doubtful due to the very low time-resolution of observations and very few points on the $O - C$ diagram.

The 2016 superoutburst was detected by the ASAS-SN team at $V=15.29$ on April 25. Both superhumps and eclipses were recorded (vsnet-alert 19778). Using the combined data of 2007, 2011 and 2016 observations, we have refined the eclipse ephemeris by the MCMC modeling (Kato et al. 2013):

$$\text{Min(BJD)} = 2455395.37115(4) + 0.0629503676(9)E. \quad (2)$$

The epoch in Littlefair et al. (2008) corresponds to an $O - C$ value of 0.00168 d against this ephemeris. The ephemeris in Littlefair et al. (2008) predicts eclipses to occur 0.0096 d later than our actual observations in 2016.

The times of superhump maxima during the 2016 superoutburst are listed in e-table 7. Stage B with a positive P_{dot} and a transition to stage C superhumps were recorded (see also figure 8).

3.10 V337 Cygni

V337 Cyg was discovered as a long-period variable (AN 101.1928). The dwarf nova-type nature was confirmed in 1996. The SU UMa-type nature was established during the 2006 superoutburst (cf. Boyd et al. 2007). See Kato et al. (2015a) for more history.

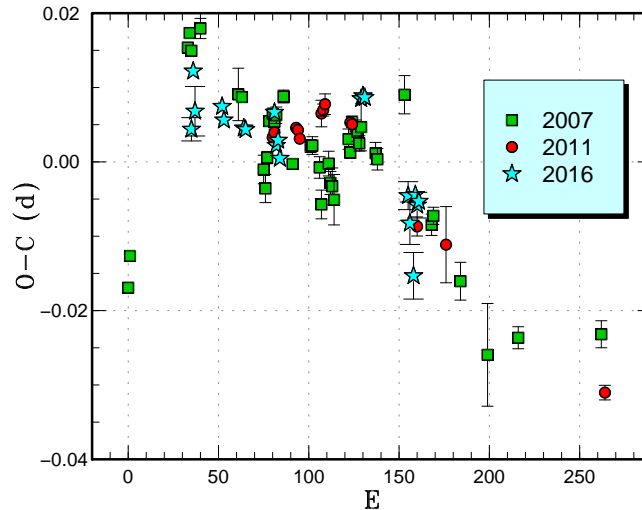


Fig. 8. Comparison of $O - C$ diagrams of GP CVn between different superoutbursts. A period of 0.05828 d was used to draw this figure. Approximate cycle counts (E) after the appearance of superhumps were used. Note that this treatment is different from the corresponding figure in Kato et al. (2012a). Since the 2007 observation apparently caught the early part of stage A, we set the initial superhump of 2007 to be $E=0$ in this figure. Other superoutbursts have been shifted to best match the 2007 one. The shift value suggests that the ASAS-SN detection of the 2016 superoutburst occurred ~ 13 cycles after the appearance of superhumps.

The 2016 superoutburst was detected by M. Moriyama at an unfiltered CCD magnitude of 15.5 on November 17. Observations on a single night yielded three superhumps (e-table 8). The maximum $E=2$ suffered from large atmospheric extinction and the quality of this measurement was poor. The P_{SH} is omitted from table 3 since there were observations with much more accurate values in the past.

3.11 V1113 Cygni

V1113 Cyg was discovered as a dwarf nova by Hoffmeister (1966). The SU UMa-type nature was identified by Kato et al. (1996b). See Kato et al. (2016a) for more history.

The 2016 superoutburst was detected by H. Maehara at a visual magnitude of 14.3 on July 27 (vsnet-alert 20003). A visual observation by P. Dubovsky on the same night and ASAS-SN detection on the next night indicated further brightening (vsnet-alert 20011, 20015). Thanks to the early detection and notification, growing superhumps were detected (vsnet-alert 20022). The times of superhump maxima are listed in e-table 9, which clearly indicate the presence of stage A superhumps (figure 9). It may be noteworthy that stage A lasted nearly 40 cycles (figure 9), which may be analogous to long- P_{orb} SU UMa-type dwarf novae with slowly evolving superhumps (such as V1006 Cyg: Kato et al. 2016b; V452 Cas: Kato et al. 2016a). Since stage A superhumps were observed, a spectroscopic radial-velocity

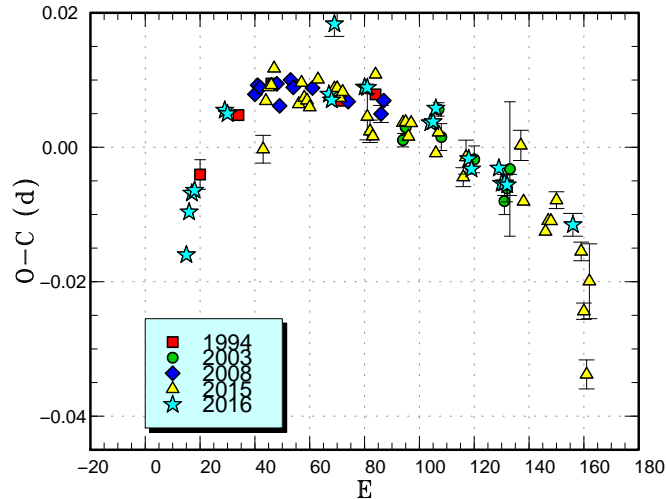


Fig. 9. Comparison of $O - C$ diagrams of V1113 Cyg between different superoutbursts. A period of 0.07911 d was used to draw this figure. Approximate cycle counts (E) after the peak of the superoutburst were used. Since the start of the 2016 superoutburst was very well defined, we used the peak of the superoutburst and redefined the cycle counts. The other outbursts were shifted to best match the 2016 one.

study is desired to determine q using the stage A superhump method.

3.12 IX Draconis

IX Dra is one of ER UMa-type dwarf novae (Ishioaka et al. 2001). See Kato et al. (2014a) and Olech et al. (2004) for the history.

The 2016 May superoutburst was detected by P. Dubovsky at a visual magnitude of 15.2 on May 29. Subsequent observations detected superhumps (vsnet-alert 19868). The times of superhump maxima are listed in e-table 10. A combined $O - C$ diagram (figure 10) did not show a strong sign of a stage transition.

In order to determine the change in the supercycle (cf. Otulakowska-Hypka et al. 2013), we have extracted nine maxima of superoutbursts since 2015 April, when the ASAS-SN team started a good coverage of this field. The mean supercycle between JD 2457142 and 2457305 (2015 April to October) was 54.4(3) d, while it increased to 58.9(3) d between JD 2457420 and 2457657 (2016 February to September). These values are much shorter than what is predicted (should be longer than 62 d by 2015) by a claimed secular trend in Otulakowska-Hypka et al. (2013). The rapid variation suggests that snapshot values as in Otulakowska-Hypka et al. (2013) probably did not reflect the long-term trend well.

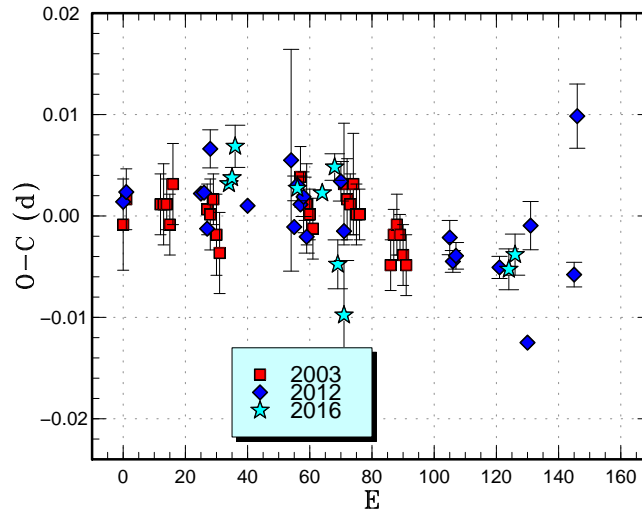


Fig. 10. Comparison of $O - C$ diagrams of IX Dra between different superoutbursts. A period of 0.06700 d was used to draw this figure. Approximate cycle counts (E) after the start of the superoutburst were used.

3.13 IR Geminorum

IR Gem was discovered as a U Gem-type variable star (AN S5423) by Popowa (1961). Although little was known other than outbursts with an interval of ~ 75 d and amplitudes of ~ 2.5 mag (Popova 1960; Meinunger 1976),¹² this object has been well monitored by AAVSO observers since its discovery. Several outbursts were already recorded in the 1960s (Mayall 1968). Bond (1978) obtained a spectrum typical for an outbursting dwarf nova. Burenkov, Voikhanskaia (1979) reported a dwarf nova-type spectrum in quiescence. Shafter et al. (1984) identified this object to be an SU UMa-type dwarf nova by detecting superhumps. Shafter et al. (1984) suggested a small mass ratio (either a massive white dwarf or an undermassive secondary) based on a radial-velocity study. Although Feinswog et al. (1988), Lázaro et al. (1990) and Lazaro et al. (1991) reported more detailed spectroscopic studies, the orbital period was not well measured. Observations of superhumps during the 1991 superoutburst were reported in Kato (2001). Kato et al. (2009) reanalyzed this superoutburst and reported another one in 2009. Another superoutburst in 2010 was reported in Kato et al. (2010).

The 2016 superoutburst was detected by the ASAS-SN team at $V=12.95$ on March 22 and $V=12.00$ on March 24. Subsequent observations detected superhumps (vsnet-alert 19645). The times of superhump maxima are listed in e-table 11. The observation started two days later than the announcement and stage A superhumps were not recorded.

The 2017 superoutburst was detected by K. Kasai on March 12 (vsnet-alert 20763) while observing KaiV36, an ellipsoidal variable star in the field of IR Gem. The outburst

¹²There is a close companion star and old literature often referred to combined magnitudes.

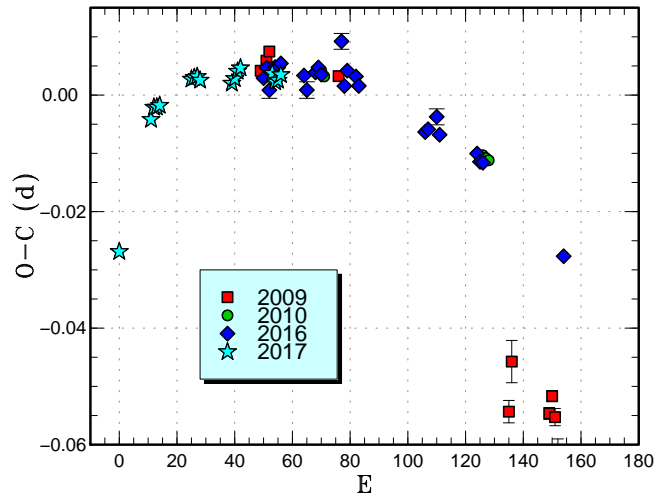


Fig. 11. Comparison of $O - C$ diagrams of IR Gem between different superoutbursts. A period of 0.07109 d was used to draw this figure. Approximate cycle counts (E) after the start of the superoutburst were used. The 2010 superoutburst was preceded by a separate precursor. We shifted the $O - C$ values to best fit the 2016 ones. The result suggests that superhumps started to evolve 20 cycles after the peak of the precursor outburst. The final points in the 2009 superoutbursts probably correspond to traditional late superhumps.

was detected early enough and stage A superhumps were observed (figure 11). The object was still in quiescence on March 10. The times of superhump maxima are listed in e-table 12. The observations were not long enough and P_{dot} was not determined. The ϵ^* for stage A superhumps is 0.068(11), whose errors mainly comes from the uncertainty in the orbital period [0.0684(6) d] (Feinswog et al. 1988). This ϵ^* corresponds to $q=0.22(4)$. Accurate determination of the orbital period is desired since the object is bright enough and its behavior during superoutbursts has been well documented.

3.14 NY Herculis

NY Her was originally discovered by Hoffmeister (1949) as a Mira-type variable. Based on photographic observations by Pastukhova (1988) and the CRTS detection on 2011 June 10, the object was identified as an SU UMa-type dwarf nova with a short supercycle (Kato et al. 2013). For more history, see Kato et al. (2013).

The 2016 June superoutburst was detected by the ASAS-SN team at $V=16.19$ on June 28. Subsequent observations detected superhumps (vsnet-alert 19938, 19939, 19948). The times of superhump maxima are listed in e-table 13. There was a rather smooth transition from stage B to C. Since the 2016 observations was much better than the 2011 one, we provide an updated superhump profile in e-figure 4. It is noteworthy that the mean superhump amplitude (0.10 mag) is much smaller than most of SU UMa-type dwarf novae with similar

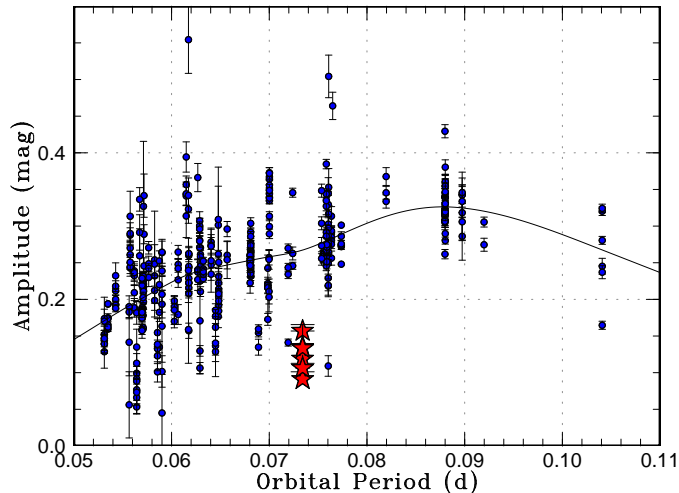


Fig. 12. Dependence of superhump amplitudes on orbital period. The superoutburst samples are described in subsection 4.7.1 in Kato et al. (2012a). We selected the range of $-5 < E < 10$ respect to the peak superhump amplitude to illustrate the maximum superhump amplitudes. The curve indicates a spline-smoothed interpolation of the sample in Kato et al. (2012a). The location of NY Her (reflecting the first night of observation; we consider that these observations were early enough to make a comparison in this figure) is shown by stars. The single point right to NY Her is a superhump of QY Per in 1999. The other superhumps of the same superoutburst had amplitudes larger than 0.2 mag and this measurement does not reflect the characteristic amplitude of superhumps in QY Per.

P_{SH} (or P_{orb}) (see figure 12). Such an unusual low superhump amplitude is commonly seen in period bouncers and it may be a signature that NY Her is in a different evolutionary location from the standard one with this P_{orb} .

ASAS-SN light curve suggest that bright outbursts (likely superoutbursts) tend to occur in every $\sim 60\text{--}70$ d (figure 13). We selected long outbursts (presumable superoutbursts) from the ASAS-SN and Poyner’s observations and listed in table 4. Note that we selected the brightest points of outbursts and they do not necessarily reflect the starts of the outbursts. These maxima can be well expressed by a period of 63.5(2) d with residuals less than 5 d. We consider that this period is the supercycle of this system. The entire durations of superoutbursts were less than 10 d, which are much shorter than those in ER UMa-type dwarf nova (cf. Kato, Kunjaya 1995; Robertson et al. 1995) but are similar to that of V503 Cyg with a supercycle of 89 d (Harvey et al. 1995). Although the supercycle is between ER UMa-type dwarf novae and ordinary SU UMa-type dwarf novae, it is not clear whether NY Her fills a gap between them since NY Her does not have intermediate properties between them. NY Her may be classified as an unique object with a short supercycle and a small superhump amplitude despite the relatively long P_{SH} .

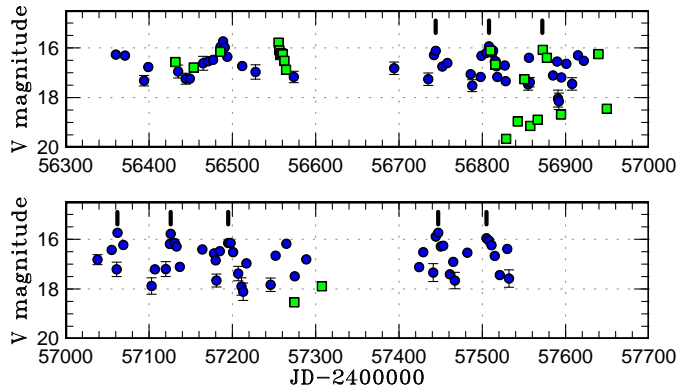


Fig. 13. ASAS-SN and unfiltered CCD light curve of NY Her. Filled circles and squares represent ASAS-SN and Poyner's measurements, respectively. Although details of each outburst are not very clear, bright outbursts (likely superoutbursts) tend to occur in every $\sim 60\text{--}70$ d. The maxima of bright outbursts listed in table 4 and covered by observations in this figure are shown by ticks.

Table 4. List of recent superoutbursts of NY Her

Cycle	JD-2400000	magnitude
0	56744	16.12
1	56808	15.94
2	56872	16.08
5	57062	15.74
6	57126	15.78
7	57195	16.15
8	57258	15.94
11	57447	15.74
12	57505	15.96
13	57568	16.19

3.15 MN Lacertae

This object (=VV 381) was discovered by Miller (1971). Relatively frequent outbursts were recorded in Miller (1971) and the object was originally considered to be a Z Cam-type dwarf nova. T. Kato, however, noted a very faint quiescence during a systematic survey of *I*-band photometry of dwarf novae (1990, unpublished) and he suggested that the outburst amplitude should be comparable to those of SU UMa-type dwarf novae.

Since this object was initially cataloged as a Z Cam-type dwarf nova, Simonsen (2011) included it as a target for “Z CamPaign” project. As a result, the outburst behavior was relatively well recorded in the AAVSO database, particularly in 2010–2012. The possibility of an SU UMa-type dwarf nova was particularly noted after a long outburst in 2011 June (vsnet-

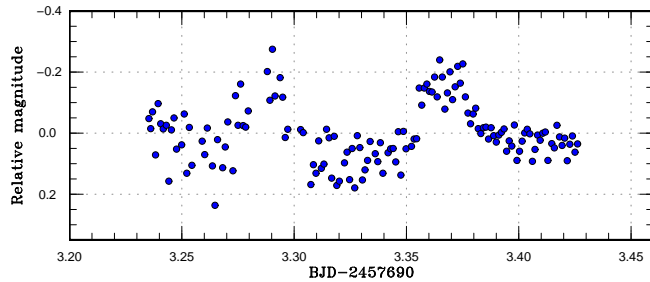


Fig. 14. Superhumps in MN Lac (2016).

Table 5. List of likely superoutbursts of MN Lac in 2010–2012

Year	Month	Day	max*	V-mag
2010	11	6	55506	15.93
2011	5	31	55713	15.74
2011	11	24	55890	16.12
2012	4	30	56048	15.94

*JD–2400000.

alert 13420, 13424). During this outburst, accurate astrometry was obtained confirming that the true quiescent magnitude is indeed faint (22nd mag or even fainter). There was another outburst in 2012 October, during which a call for observations of superhumps was issued (vsnet-alert 15063). Following this outburst, the object was withdrawn from the Z CamPaign project and it has not been observed as frequently as before.

The 2016 bright outburst was detected by the ASAS-SN team at $V=15.32$ on October 30. Single-night observations on October 31 indeed detected superhumps (vsnet-alert 20283; figure 14). The times of superhump maxima were BJD 2457693.2873(15) ($N=37$) and 2457693.3684(8) ($N=53$). The best superhump period by the PDM method is 0.080(1) d. Although the SU UMa-type nature was confirmed, more observations are needed to establish a more accurate superhump period.

Thanks to the excellent coverage in 2010–2012, we could determine the supercycle. The maxima of superoutbursts (table 5) can be expressed by a supercycle of 180(8) d with the maximum $|O - C|$ of 14 d. The result is consistent with the high outburst frequency reported in Miller (1971).

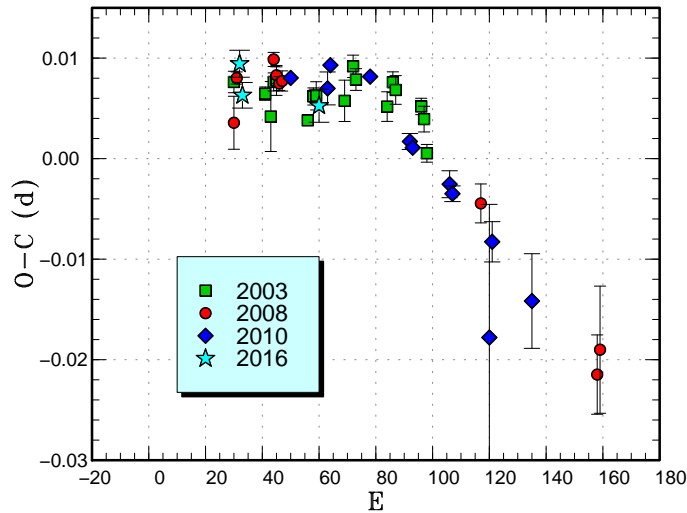


Fig. 15. Comparison of $O - C$ diagrams of V699 Oph between different superoutbursts. A period of 0.07031 d was used to draw this figure. Approximate cycle counts (E) after the start of the superoutburst were used.

3.16 V699 Ophiuchi

This object was discovered as a dwarf nova (HV 10577) with a photographic range of 13.8 to fainter than 16.0 (Boyce 1942). Boyce (1942) recorded five outbursts between 1937 June 5 and 1940 July 5. The intervals of the first four outbursts were in the range of 320–390 d. Although Walker, Olmsted (1958) presented a finding chart, later spectroscopic studies have shown that the marked object is a normal star (Zwitter, Munari 1996; Liu et al. 1999).

On 1999 April 16, A. Pearce detected an outburst (vsnet-alert 2877). Accurate astrometry and photometry of the outbursting object indicated that the true V699 Oph is an unresolved companion to a 16-th magnitude star (vsnet-alert 2878, vsnet-chat 1810, 1868). The first confirmed superoutburst was recorded in 2003. This outburst was preceded by a separate precursor and followed by a rebrightening, forming a “triple outburst”. (Kato et al. 2009). The 2008 and 2010 superoutbursts were also reported in Kato et al. (2009) and Kato et al. (2010), respectively.

The 2016 superoutburst was detected by the ASAS-SN team at $V=14.56$ on May 15 and by R. Stubbings at a visual magnitude of 14.4 on the same night. Time-resolved photometric observations were obtained on two nights and the times of superhump maxima are listed in e-table 14. The 2016 observation probably recorded the early part of stage B superhumps (figure 15).

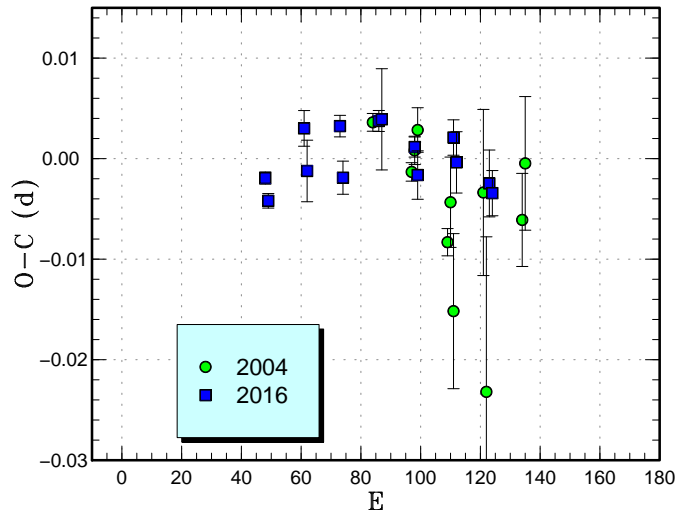


Fig. 16. Comparison of $O - C$ diagrams of V344 Pav between different superoutbursts. A period of 0.07988 d was used to draw this figure. Approximate cycle counts (E) after the start of the superoutburst were used. Since the start of the 2004 outburst was not well constrained, we shifted the $O - C$ diagram so that the rapid fading of the two superoutbursts match each other.

3.17 V344 Pavonis

This dwarf nova was discovered in outburst on 1990 July 21. The object was spectroscopically confirmed as a dwarf nova. There were two outbursts recorded in archival plates between 1979 May and 1984 September (Maza et al. 1990). Mason, Howell (2003) obtained a typical spectrum of a dwarf nova in quiescence. Uemura et al. (2004) studied the 2004 outburst and identified the SU UMa-type nature. The analysis was refined in Kato et al. (2009).

The 2016 superoutburst was detected by R. Stubbings at a visual magnitude of 14.4 on April 25. Subsequent observations detected superhumps (vsnet-alert 19796). The times of superhump maxima are listed in e-table 15. Time-resolved photometry was obtained only in the later phase of the superoutbursts both in 2004 and 2016. The superhump stage has been therefore unclear (figure 16). We listed a global P_{dot} in table 3. Observations in the earlier phase of the superoutburst are needed to characterize superhumps of this object better.

3.18 V368 Pegasi

V368 Peg is a dwarf nova (Antipin Var 63) discovered by Antipin (1999). See Kato et al. (2016a) for the summary of the history. The 2016 superoutburst was detected by P. Schmeer at a visual magnitude of 13.0 on September 28. Time-resolved photometry was performed only on a single night. The resultant superhump maxima were BJD 2457661.4175(5) ($N=66$) and 2457661.4883(4) ($N=76$).

3.19 V893 Sco

V893 Sco was discovered as a variable star by Satyvoldiev (1972). The variable had been lost for a long time, and was rediscovered by K. Haseda (Kato et al. 1998). For more historical information, see Kato et al. (2014a). This object is an eclipsing SU UMa-type dwarf nova (cf. Bruch et al. 2000; Matsumoto et al. 2000).

The 2016 superoutburst was detected by R. Stubbings at a visual magnitude of 12.8 on March 21. It once faded to $V=13.64$ on the same night and brightened to $V=12.37$ on March 25 (vsnet-alert 19652). The outburst on March 21 should have been a precursor. Our time-resolved photometry started on March 28 and detected superhumps (vsnet-alert 19661; figure 17). Since our observation started relatively late, we could record only the final part of the superoutburst. Later observations were dominated by the orbital humps and we could only extract a small number of superhump maxima outside the eclipses (e-table 16). We obtained the eclipse ephemeris for the use of defining the orbital phases in this paper

$$\text{Min(BJD)} = 2454173.3030(3) + 0.0759614600(16)E \quad (3)$$

using the MCMC modeling (Kato et al. 2013) using the data up to Kato et al. (2014a) and current set of observation.

3.20 V493 Serpentis

This object (=SDSS J155644.24–000950.2) was selected as a dwarf nova by SDSS (Szkody et al. 2002). The SU UMa-type nature was identified by observations of the 2006 and 2007 superoutbursts (Kato et al. 2009). See Kato et al. (2014b) for more history.

The 2016 superoutburst was detected by T. Horie at a visual magnitude of 12.5 on June 5. It was pointed out by H. Maehara the outburst already started on June 1 (vsnet-alert 19872). Time-resolved photometry was carried out on two nights, yielding superhump maxima in e-table 17. A comparison of $O - C$ diagrams (figure 18) suggest that these observations recorded the early phase of stage C.

3.21 AW Sagittae

AW Sge was discovered as a dwarf nova by Wolf, Wolf (1906). The object was identified as an SU UMa-type dwarf nova during the 2000 outburst (Kato et al. 2009). See Kato et al. (2014a) for more history.

The 2016 superoutburst was detected by R. Stubbings at a visual magnitude of 14.6

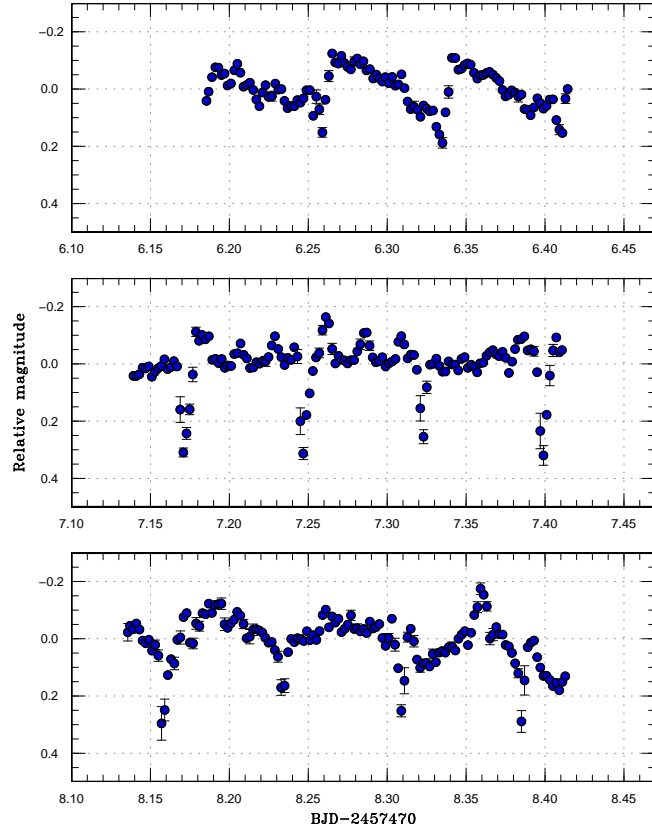


Fig. 17. Eclipses and superhumps in V893 Sco (2016). The data were binned to 0.002 d.

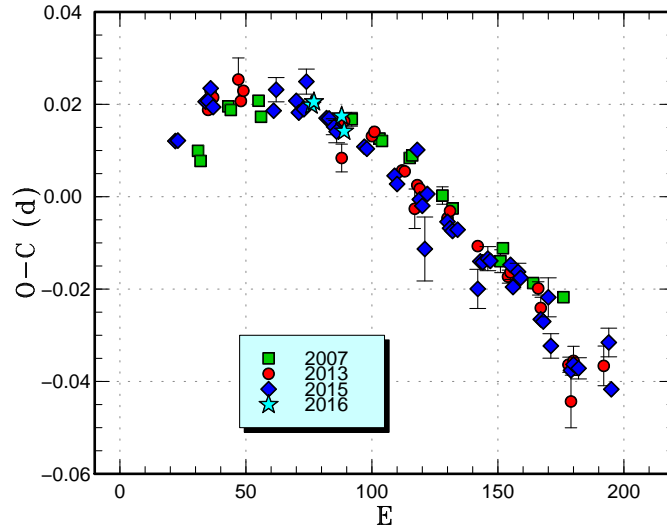


Fig. 18. Comparison of $O - C$ diagrams of V493 Ser between different superoutbursts. A period of 0.08310 d was used to draw this figure. Approximate cycle counts (E) after the start of the superoutburst were used.

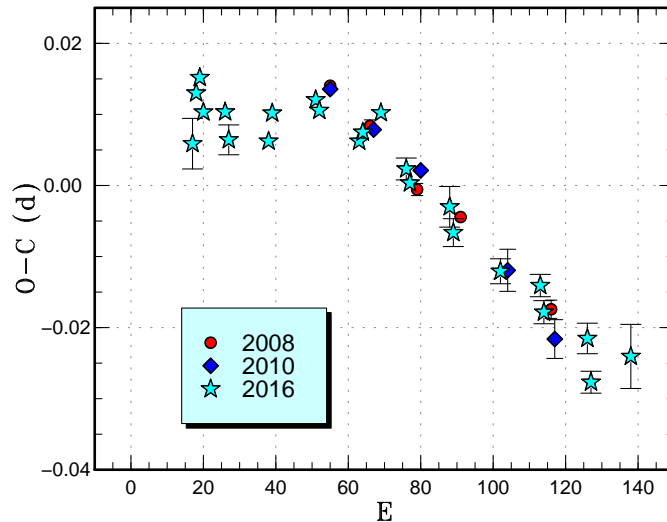


Fig. 19. Comparison of $O - C$ diagrams of V1389 Tau between different superoutbursts. A period of 0.08046 d was used to draw this figure. Approximate cycle counts (E) after the start of the superoutburst were used. Since the start of the 2010 superoutburst was not known, we have shifted the $O - C$ diagram to best fit the others.

on June 14. Time-resolved photometric observations were carried out on a single night and yielded the superhumps maxima: BJD 2457558.3859(5) ($N=75$) and 2457558.4606(9) ($N=50$).

3.22 V1389 Tauri

This object was discovered by K. Itagaki at an unfiltered CCD magnitude of 14.1 on 2008 August 7 (Yamaoka et al. 2008). There was an X-ray counterpart (1RXS J040700.2+005247) and the dwarf nova-type classification was readily suggested. The object was recorded already in outburst at $V=13.5$ on August 4 in the ASAS-3 (Pojmański 2002) data (vsnet-alert 10419). There were two past outbursts (2004 October 20 and 2006 March 16) recorded in the ASAS-3 data (vsnet-alert 10419). Subsequent observations detected superhumps (vsnet-alert 10422, 10423). This outburst was studied in Kato et al. (2009). Another superoutburst in 2010 was studied in Kato et al. (2010).

The 2016 superoutburst was detected by the ASAS-SN team at $V=13.52$ on October 23. Subsequent observations detected superhumps (vsnet-alert 20267). The times of superhump maxima are listed in e-table 18. As in other typical long- P_{SH} systems (cf. figure 4 in Kato et al. 2009), stage B was relatively short. A comparison of the $O - C$ diagrams has confirmed that the superhumps recorded in 2008 were indeed stage C ones (figure 19). Although individual superhump maxima were not measured, a PDM analysis of the post-superoutburst data (4.5 d segment after BJD 2457697) detected a period of 0.08000(11) d. This value suggests that stage C superhump lasted even after the termination of the superoutburst.

3.23 SU Ursae Majoris

This object is the prototype of SU UMa-type dwarf novae. See Kato et al. (2015a) for the history. The 2017 superoutburst was detected by E. Muyliaert at a visual magnitude of 11.3 on February 23. Only single superhump at BJD 2457810.5647(3) ($N=89$) was observed.

3.24 HV Virginis

HV Vir was originally discovered by Schneller (1931) in outburst on 1929 February 11. The object was also given a designation of NSV 6201 as a suspected variable. Duerbeck (1984) and Duerbeck (1987) classified it as a classical nova and provided a light curve of the 1929 outburst based on his examination of archival plates. Amateur observers, particularly by the Variable Star Observers' League in Japan (VSOLJ), suspected it to be a dwarf nova and started monitoring since 1987 [i.e. following the publication of Duerbeck (1987)]. The object was caught in outburst by P. Schmeer on 1992 April 20 at a visual magnitude of 12.0 (Schmeer et al. 1992). The 1992 outburst was extensively studied (Barwig et al. 1992; Leibowitz et al. 1994; Kato et al. 2001). It might be worth noting that Barwig et al. (1992) recorded low-amplitude variations with a period corresponding to the orbital period, their interpretation (originating from the hot spot as in quiescence) was strongly affected by Patterson et al. (1981). Although Szkody et al. (1992) reported the detection of superhumps, the detailed result has not been published. Leibowitz et al. (1994) reported the detection of historical outbursts in 1939, 1970 and 1981 in archival plates. Although Leibowitz et al. (1994) noted chaotic "early superhump variability", its period was not precisely determined. Leibowitz et al. (1994) recorded superhumps and reported a negative P_{dot} , which was incorrect due to an error in cycle counts probably misguided by the received wisdom at that time that SU UMa-type dwarf novae universally show negative P_{dot} (cf. Warner 1985; Patterson et al. 1993). Using additional observations and all available data, Kato et al. (2001) clarified that this object showed two types of superhumps (early superhumps and ordinary superhumps) and the P_{dot} for ordinary superhumps was positive. Kato et al. (2001) proposed the close similarity to AL Com (cf. Kato et al. 1996a) and WZ Sge, giving a basis of the modern concept of WZ Sge-type dwarf novae (Kato 2015).

The object underwent another superoutburst in 2002. This outburst was also extensively studied by Ishioka et al. (2003), who established the positive P_{dot} using a much more complete set of observations than in 1992. Patterson et al. (2003) also reported the superhump period of the same outburst and the orbital period of 0.057069(6) d from quiescent

photometry. There was another superoutburst in 2008, which was reported in Kato et al. (2009).

The 2016 superoutburst was detected by the ASAS-SN team at $V=12.0$ on March 10 (cf. vsnet-alert 19571). Initial observations already detected early superhumps (vsnet-alert 19573, 19576, 19589; e-figure 5). The object then developed ordinary superhumps (vsnet-alert 19581, 19599, 19633). The times of superhump maxima are listed in e-table 19. The data very clearly demonstrate the presence of stages A and B, although there was an observational gap in the middle of stage B. The superhump period of stage A was very ideally determined to be 0.05907(6) d (cf. figure 20). This period gives the fractional superhump excess of $\epsilon^*=0.034(1)$, which corresponds to $q=0.093(3)$. This value supersedes the earlier determination by the same method to be $q=0.072(1)$ using the less extensive 2002 data. The period was determined for the 2002 data from single-night observations assuming that stage A continued up to the first observation of stage B while the present observation obtained an almost complete coverage of stage A (see figure 20). It was likely that the error was underestimated in the 2002 superoutburst. The outburst started rapid fading on March 29–30 and the entire duration of the superoutburst was at least 20 d. Despite dense observations, no post-outburst rebrightening was recorded.

A PDM analysis of the post-superoutburst observations yielded a period of 0.05799(2) d (e-figure 6). This period corresponds to a disk radius of $0.33a$ assuming that the precession rate is not affected by the pressure effect. The value is in the range of $0.30\text{--}0.38a$ determined for well-observed WZ Sge-type dwarf novae (Kato, Osaki 2013).

The period of early superhumps [0.057000(8) d] is in agreement with 0.056996(9) d determined from the 2008 observation (from the observations reported in Kato et al. 2009). The quality of past observations were lower: 0.057085 d (without error estimate) for the 1992 outburst (Kato et al. 2001), which was based only on published times of maxima, and 0.0569(1) d for the 2002 outburst (Ishioka et al. 2003). The current observations, combined with the 2008 data, established the period of early superhumps of this object to a precision directly comparable to the orbital period for the first time. The 2016 and 2008 periods were 0.13(2)% and 0.13(3)% shorter than the orbital period, respectively.

3.25 NSV 2026

This object was discovered as a variable star (=HV 6907) by Hoffleit (1935). The SU UMa-type nature was confirmed during the 2015 superoutburst. For more history, see Kato et al.

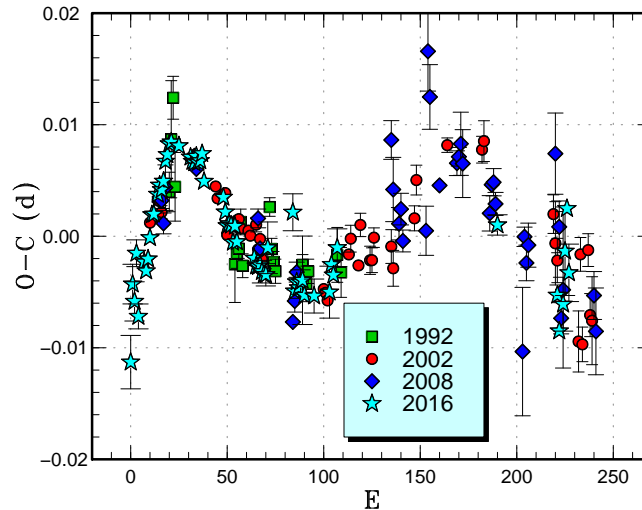


Fig. 20. Comparison of $O - C$ diagrams of HV Vir between different superoutbursts. A period of 0.05828 d was used to draw this figure. Approximate cycle counts (E) after the emergence of ordinary superhumps were used. After the high-quality observations in 2016, it became apparent that the emergence of ordinary superhumps was not well recorded in the past superoutbursts. The cycle counts were shifted by 20, 10 and 15 for the 1992, 2002 and 2008 superoutbursts, respectively, to match the 2016 observations.

(2016a).

There was a superoutburst in 2016 February (Kato et al. 2016a). Another superoutburst occurred in 2016 November, which was detected by J. Shears at an unfiltered CCD magnitude of 14.19 and by E. Muylaert at a visual magnitude of 14.0 on November 25. The object was further observed to brighten to a visual magnitude of 13.2 on November 26. The times of superhump maxima are listed in e-table 20. These superhumps were likely stage B ones (figure 21). As judged from the interval of two superoutbursts in 2016 and the supercycle of ~ 95 d (Kato et al. 2016a), two superoutbursts were likely missed between the two superoutbursts in 2016.

3.26 NSV 14681

NSV 14681 was discovered as a variable star (SVS 749) of unknown type with a photographic range of 14 to fainter than 14.5 (Belyavskii 1936). The CRTS team detected an outburst at an unfiltered CCD magnitude of 15.6 on 2007 June 13 and it was readily identified with NSV 14681 (Drake et al. 2014). The CV is a fainter component of a close pair (Kato et al. 2012b). The CRTS team detected another outburst at 16.4 mag on 2009 September 14.

The 2016 outburst was detected by the ASAS-SN team at $V=14.35$ on October 19. Subsequent observations detected superhumps (vsnet-alert 20245, 20256; e-figure 7). The times of superhump maxima are listed in e-table 21. The superhump stage is unknown. The

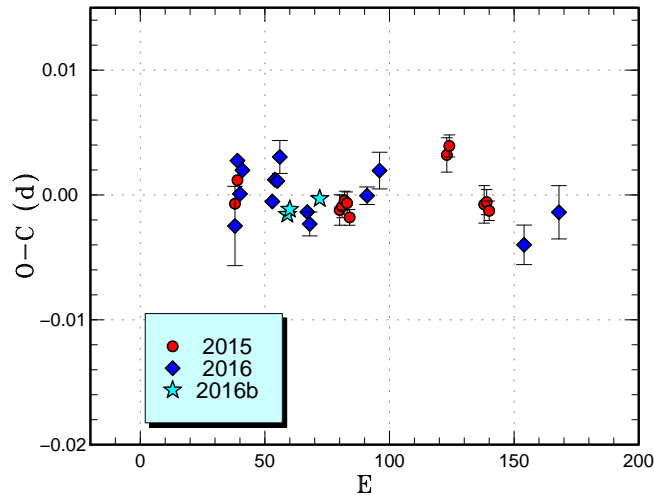


Fig. 21. Comparison of $O - C$ diagrams of NSV 2026 between different superoutbursts. A period of 0.06982 d was used to draw this figure. Approximate cycle counts (E) after the starts of the outbursts were used. The start of the 2016 outburst refers to the precursor outburst. Since the start of the 2015 outburst was not well constrained, the $O - C$ curve was shifted as in the 2016 one.

object is on the lower edge of the period gap.

3.27 1RXS J161659.5+620014

This object (hereafter 1RXS J161659) was initially identified as an X-ray selected variable (also given a name as MASTER OT J161700.81+620024.9), which was first detected in bright state on 2012 September 11 at an unfiltered CCD magnitude of 14.4 (Balanutsa et al. 2013). The dwarf nova-type variability was confirmed by analysis of the CRTS data (Balanutsa et al. 2013; see also vsnet-alert 16079, 16720).

The 2016 April outburst was detected by the ASAS-SN team at $V=14.74$ on April 22. Subsequent observations detected superhumps (vsnet-alert 19763, 19765, 19772; e-figure 8). The times of superhump maxima are listed in e-table 22. The nature of the humps for $E \geq 155$ (post-superoutburst) is unclear due to the gap in the observation. These humps may be either traditional late superhumps or the extension of stage C superhumps (if it is the case, the cycle count should be increased by one). We consider the latter possibility less likely, since this interpretation requires the period of stage C superhumps to be 0.07065(2) d, which appears to be too short (by $\sim 1\%$) shorter than that of stage B superhumps. We do not use these maxima in obtaining the periods in table 3.

The 2016 July outburst was detected by the CRTS team at an unfiltered CCD magnitude of 14.63 on July 10 (cf. vsnet-alert 19970). Although it was considered to be too early for a next superoutburst, subsequent observations detected superhumps (vsnet-alert 19996).

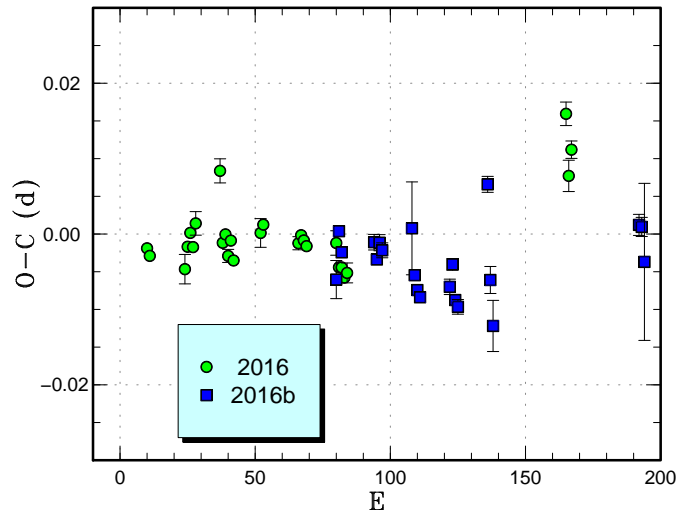


Fig. 22. Comparison of $O - C$ diagrams of 1RXS J161659 between different superoutbursts. A period of 0.07130 d was used to draw this figure. Approximate cycle counts (E) after the start of the superoutburst were used.

The times of superhump maxima are listed in e-table 23. As in the superoutburst in 2016 April, the nature of maxima for $E \geq 112$ (post-superoutburst) was unclear. A comparison of $O - C$ diagrams between two superoutbursts is given in figure 22.

These observations indicate that the supercycle is only ~ 80 d. We studied past ASAS-SN observations and detected outbursts (e-table 24). The outburst pattern became more regular since the 2015 July (it may have been due to the change in the variability in this system or the improvement of observations in ASAS-SN) and we obtained a mean supercycle of 89(1) d from five most recent superoutbursts (with $|O - C|$ values less than 8 d). Despite the shortness of the supercycle, normal outbursts are not as frequent as in ER UMa-type dwarf novae (Kato, Kunjaya 1995; Robertson et al. 1995) or active SU UMa-type dwarf novae, such as SS UMi (Kato et al. 2000; Olech et al. 2006) and BF Ara (Kato et al. 2001a). The object resembles V503 Cyg with a supercycle of 89 d with a few normal outbursts between superoutbursts (Harvey et al. 1995). V503 Cyg is known to show different states (Kato et al. 2002b), which is now considered to be a result of the disk tilt suppressing normal outbursts (Ohshima et al. 2012; Osaki, Kato 2013a; Osaki, Kato 2013b). A search for negative superhumps in 1RXS J161659 would be fruitful.

3.28 ASASSN-13ak

This object was detected as a transient at $V=15.4$ on 2013 May 23 by the ASAS-SN team (Stanek et al. 2013). There was an independent detection by the MASTER network (Shurpakov et al. 2013b). The SU UMa-type nature was identified during the 2015 superout-

burst (Kato et al. 2016a).

The 2016 superoutburst was detected by the ASAS-SN team at $V=14.43$ on August 2. We obtained time-resolved observations on two nights, yielding superhump maxima in e-table 25. The resultant period is longer than that in 2015 (Kato et al. 2016a) and these superhumps may have been stage A ones, despite that the amplitudes were already large since the 2016 observations were obtained in the earlier phase than in 2015.

3.29 ASASSN-13al

This object was detected as a transient at $V=15.2$ on 2013 June 1 by the ASAS-SN team (Prieto et al. 2013) (The ASAS-SN Transients page gave a magnitude of 16.03 with a “BADCAL” flag). The CV-type nature was confirmed by spectroscopy.¹³

The 2016 outburst was detected by the ASAS-SN team at $V=14.77$ on October 9. There was a previous detection in the ASAS-SN data at $V=14.75$ on 2012 June 7. Subsequent observations detected superhumps (vsnet-alert 20220; e-figure 9). The time of superhump maxima are listed in e-table 26. The period was not very well determined since the observations were undertaken only on a single night. The best superhump period by the PDM method is 0.0783(2) d.

3.30 ASASSN-13bc

This object was detected as a transient at $V=16.9$ on 2013 July 4 by the ASAS-SN team. A number of past outbursts were recorded in the CRTS data.

The 2015 outburst was detected by the ASAS-SN team at $V=14.83$ on July 30. Subsequent observations detected superhumps (vsnet-alert 18921, 18930). The times of superhump maxima are listed in e-table 27.

The 2016 outburst was detected by the ASAS-SN team at $V=15.19$ on May 24. Superhumps were also observed (vsnet-alert 19843, 19867). The object underwent a post-superoutburst rebrightening at $V=16.13$ on June 9 (cf. vsnet-alert 19883). The times of superhump maxima are listed in e-table 28. The superhump profile is given for the better observed 2016 one (e-figure 10). A combined $O - C$ diagram (figure 23) suggests that the 2015 observations covered the early phase of stage B and the 2016 ones recorded both stages B and C, although the later part of stage B was not well recorded due to the lack of observations.

¹³<http://www.astronomy.ohio-state.edu/~assassin/followup/spec_asassn13al.png>

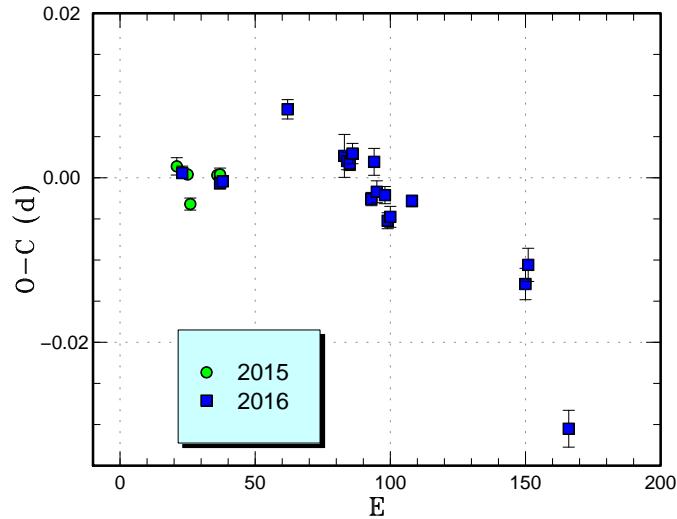


Fig. 23. Comparison of $O - C$ diagrams of ASASSN-13bc between different superoutbursts. A period of 0.07040 d was used to draw this figure. Approximate cycle counts (E) after the start of the superoutburst were used.

3.31 ASASSN-13bj

This object was detected as a transient at $V=16.2$ on 2013 July 10 by the ASAS-SN team. Two superhump maxima were obtained during the 2013 superoutburst (Kato et al. 2014b).

The 2016 superoutburst was detected by the ASAS-SN team at $V=14.98$ on July 3. Subsequent observations detected superhumps (vsnet-alert 19957, 19965, 19975; e-figure 11). The times of superhump maxima are listed in e-table 29. There was a marked decrease in the superhump period and we tentatively identified a stage B-C transition around $E = 22$. The accuracy of the resultant periods was not sufficiently high since they were determined by only short baselines.

3.32 ASASSN-13bo

This object was detected as a transient at $V=15.96$ on 2013 July 13 by the ASAS-SN team. The 2016 outburst was detected by the ASAS-SN team at $V=15.19$ on August 1. The 2016 outburst was the brightest recorded one and a superoutburst was suspected. Subsequent observations detected superhumps (vsnet-alert 20053, 20068). There was a 3-d gap in the observations and alias periods are possible (e-figure 12). The period in table 3 refers to the one giving smallest residuals and it was determined by the PDM method. The object faded to ~ 20 mag on August 13.

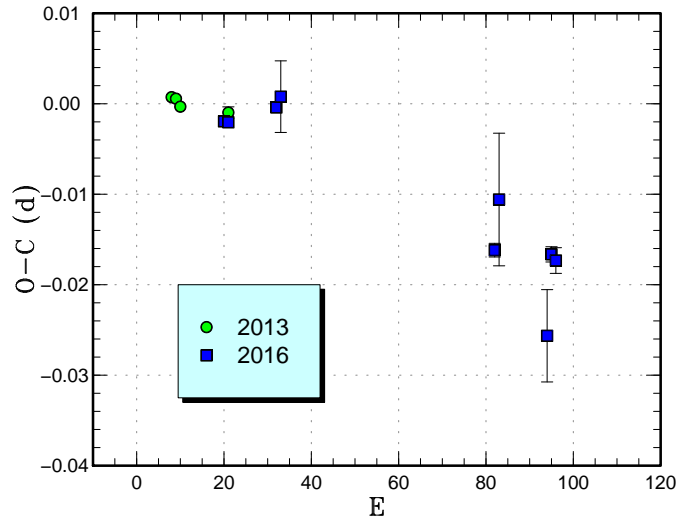


Fig. 24. Comparison of $O - C$ diagrams of ASASSN-13cz between different superoutbursts. A period of 0.07995 d was used to draw this figure. Approximate cycle counts (E) after the start of the superoutburst were used.

3.33 ASASSN-13cs

This object was detected as a transient at $V=14.9$ on 2013 September 2 by the ASAS-SN team. The object was spectroscopically identified as a dwarf nova in outburst.¹⁴

The 2016 outburst was detected by the ASAS-SN team at $V=15.03$ on June 21. The light curves of past outbursts suggested an SU UMa-type dwarf nova. Subsequent observations detected superhumps (vsnet-alert 19920, 19923; e-figure 13). The times of superhump maxima are listed in e-table 31.

3.34 ASASSN-13cz

This object was detected as a transient at $V=14.9$ on 2013 September 14 by the ASAS-SN team. The 2013 outburst turned out to be a superoutburst by the detection of superhumps (Kato et al. 2014a).

The 2016 superoutburst was detected by the ASAS-SN team at $V=14.47$ on July 27. Subsequent observations detected superhumps (vsnet-alert 20023, 20042). The times of superhump maxima are listed in e-table 32. We suspect that stages B and C were partially observed (cf. figure 24). We provide a superhump profile (e-figure 14), which was determined much better than in 2013.

¹⁴<http://www.astronomy.ohio-state.edu/~assassin/followup/spec_asassn13cs.png>.

3.35 ASASSN-14gg

This object was detected as a transient at $V=14.8$ on 2014 August 23 by the ASAS-SN team. The 2016 outburst was detected by the ASAS-SN team at $V=13.95$ on August 11. Subsequent observations detected superhumps (vsnet-alert 20079; e-figure 15). The times of superhump maxima are listed in e-table 33. The positive P_{dot} for stage B superhumps is a common feature in many short- P_{SH} systems.

3.36 ASASSN-15cr

This object was detected as a transient at $V=14.9$ on 2015 February 7 by the ASAS-SN team. The 2017 outburst was detected by the ASAS-SN team at $V=14.73$ on January 9. Subsequent observations detected superhumps (vsnet-alert 20558, 20590; e-figure 16). The times of superhump maxima are listed in e-table 34. Despite that observational coverage was not sufficient, all stages of A-C were recorded thanks to the early detection by the ASAS-SN team.

3.37 ASASSN-16da

This object was detected as a transient at $V=16.1$ on 2016 March 8 by the ASAS-SN team. The outburst was confirmed and announced on March 12, when the object was at $V=15.5$. The brightness peak was on March 10 at $V=15.1$. The object was identified with an $g=21.5$ mag SDSS object. The large outburst amplitude received attention.

The object showed double-wave early superhumps on March 13 and 14 (vsnet-alert 19579, 19592; e-figure 17). On March 15 (5 d after the brightness peak), the object started to show ordinary superhumps (vsnet-alert 19598, 19617, 19653; e-figure 18). The times of superhump maxima are listed in e-table 35. The epochs for $E \leq 2$ and $E \geq 203$ were apparently those of stage A and C superhumps, respectively. If we consider that stage A just ended at $E=10$ (which may not be a bad assumption as compared with $O - C$ diagrams of well-observed objects), the period of stage A superhumps was 0.05858(10) d. The resultant ϵ^* of 0.042(2) corresponds to $q=0.12(1)$. This relatively large q for a WZ Sge-type dwarf nova is consistent with the appearance of stage C superhumps, short duration of stage A, relatively large P_{dot} in stage B [$+7.5(0.9) \times 10^{-5}$], and relatively early appearance of ordinary superhumps. This object is probably close to the borderline of WZ Sge-type dwarf novae and ordinary SU UMa-type dwarf novae.

3.38 ASASSN-16dk

This object was detected as a transient at $V=16.4$ on 2016 March 21 by the ASAS-SN team. The outburst was confirmed and announced on March 24, when the object was at $V=15.1$. Subsequent observations detected superhumps. The times of superhump maxima are listed in e-table 36. Since the observations were apparently obtained during the late phase of the superoutburst, the superhump stage was probably C. The lack of period variation is consistent with this interpretation.

3.39 ASASSN-16ds

This object was detected as a transient at $V=14.7$ on 2016 April 1 by the ASAS-SN team. Subsequent observations detected growing superhumps (vsnet-alert 19680), which later became fully developed ones. The times of superhump maxima are listed in e-table 37. The $O - C$ values indicates typical stages A and B (vsnet-alert 19704). Although individual times of superhump maxima could not be measured after BJD 2457495, a PDM analysis of the corresponding segment yielded a signal of 0.06723(5) d, which is included in table 3.

3.40 ASASSN-16dz

This object was detected as a transient at $V=15.0$ on 2016 April 2 by the ASAS-SN team. The outburst was announced after the observation on April 3 at $V=14.2$. The object had been listed as an emission-line object IPHAS2 J064225.58+082546.7 (Witham et al. 2008). Although superhumps were detected, the period was not well determined due to short runs and the limited coverage only on two nights (e-figure 21). The times of superhump maxima are listed in e-table 38, which is based on one of the aliases giving the smallest $O - C$ scatter.

3.41 ASASSN-16ez

This object was detected as a transient at $V=14.3$ on 2016 May 6 by the ASAS-SN team. The large outburst amplitude suggested an SU UMa-type superoutburst (cf. vsnet-alert 19804).

On May 12, this object started to show large-amplitude superhumps (vsnet-alert 19823, 19829). The times of superhump maxima are listed in e-table 39. These superhumps were stage B ones and there was little period variation. The object was still in outburst on May 23 (17 d after the outburst detection and 11 d after the first detection of superhumps). Although there were some variations before May 12, we could not confidently detect stage A superhumps (probably due to a 1.5-d gap in the observation). Although the small P_{dot}

might suggest a small q (cf. Kato 2015), the relatively large amplitude of superhumps (e-figure 22) and the lack of long duration of stage A do not support this interpretation. The seemingly small P_{dot} may be a result of a relatively short observational coverage of 4 d.

3.42 ASASSN-16fr

This object was detected as a transient at $V=16.6$ on 2016 May 30 by the ASAS-SN team. Subsequent observations detected superhumps (vsnet-alert 19863; e-figure 23). The times of superhump maxima are listed in e-table 40. Due to the faintness of the object (17 mag around the observations), the statistics was not good.

3.43 ASASSN-16fu

This object was detected as a transient at $V=13.9$ on 2016 June 5 by the ASAS-SN team. The large outburst amplitude received attention (cf. vsnet-alert 19864). On June 14 (9 d after the outburst detection), this object showed fully developed superhumps (vsnet-alert 19899, 19901; e-figure 24). The times of superhump maxima are listed in e-table 41. Although the maxima for $E \leq 1$ were stage A superhumps, the period of stage A superhumps was not determined due to the unfortunate 2 d gap before the full growth of the superhumps. The relatively small P_{dot} in stage B [$+4.6(0.6) \times 10^{-5}$] suggests a relatively small q [$q \sim 0.08(1)$ according to equation (6) in Kato (2015)]. This expectation is consistent with the small amplitude of the superhumps (e-figure 24). A retrospective analysis of the data before ordinary superhumps appeared (BJD before 2457553) detected possible early superhumps with a period of 0.05623(3) d (e-figure 25). We consider that this object is a WZ Sge-type dwarf nova, which appears consistent with the small q as inferred from the small P_{dot} .

3.44 ASASSN-16gh

This object was detected as a transient at $V=15.5$ on 2016 June 16 by the ASAS-SN team. The outburst was announced on June 18, when the object further brightened to $V=14.3$. No strong superhumps were detected up to observations on June 24. Growing superhumps were recorded on June 28 (12 d after the outburst detection; vsnet-alert 19935). Further development of superhumps were observed (vsnet-alert 19943, 19952; e-figure 26). Although we could not detect early superhumps, the object may be a WZ Sge-type dwarf nova since the waiting time (12 d) of the growth of the superhumps was long. If this identification is true, the object appears to be a candidate for a period bouncer. The relatively small ampli-

tude of the superhumps (e-figure 26) and the large outburst amplitude (there was no known quiescent counterpart) would favor this possibility.

3.45 ASASSN-16gj

This object was detected as a transient at $V=13.3$ on 2016 June 18 by the ASAS-SN team (cf. vsnet-alert 19905). The object was also detected on June 17 by the MASTER network (independent detection, Balanutsa et al. 2016a). The object was undetected on June 12 (Balanutsa et al. 2016a) and June 11 (ASAS-SN data). Observations on June 21 already recorded superhumps (vsnet-alert 19927). The superhumps grew further (vsnet-alert 19934, 19936, 19953; e-figure 27, figure 25). It took, however, some time to establish the superhump period since nightly observations were short. The times of superhump maxima are listed in e-table 43. The maxima for $E \leq 23$ were most likely stage A superhumps as judged from the growing amplitudes and $O - C$ values (figure 25). The period of stage A superhumps, however, was not convincingly determined due to the shortness of nightly observations.

The object showed a likely plateau-type rebrightening (figure 25; the plateau-type rebrightening was favored by the lack of rising/fading trends in the nightly light curves in the rebrightening phase). Although we could not observe early superhumps, we consider that this object is a WZ Sge-type dwarf nova as judged from the long rebrightening (cf. Kato 2015). The duration of the phase of early superhumps, if it was present, must have been shorter than 9 d. This shortness suggests that this object may not be an extreme WZ Sge-type dwarf nova. There was, however, the case of the 2015 superoutburst of AL Com (Kimura et al. 2016), in which no early superhumps were observed despite that the same object showed long phases of early superhumps in previous superoutbursts. It may be premature to draw any conclusion about the evolutionary state of ASASSN-16gj only from the present observation.

3.46 ASASSN-16gl

This object was detected as a transient at $V=14.8$ on 2016 June 19 by the ASAS-SN team. The outburst was announced on June 22, when the object faded to $V=15.4$. Subsequent observations detected superhumps (vsnet-alert 19940, 19942, 19949; e-figure 28). The times of superhump maxima are listed in e-table 44. The object was still in outburst on July 11, and the entire duration of the superoutburst exceeded 22 d. Although our initial observation was already 8 d after the outburst detection, the possibility that we observed stage C super-

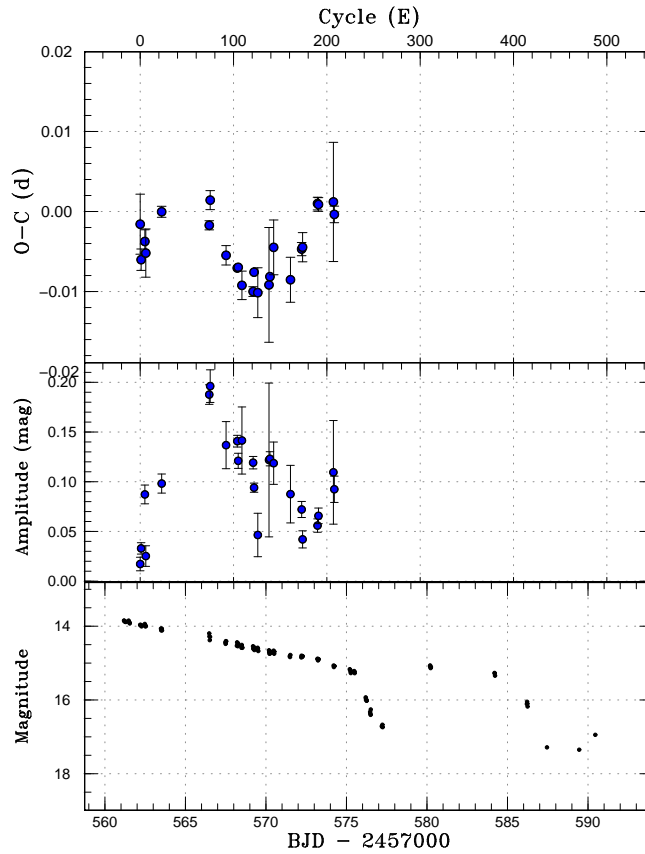


Fig. 25. $O - C$ diagram of superhumps in ASASSN-16gj (2016). (Upper:) $O - C$ diagram. We used a period of 0.05796 d for calculating the $O - C$ residuals. (Middle:) Amplitudes of superhumps. (Lower:) Light curve. The data were binned to 0.019 d.

humps may be rather small considering the long duration of the superoutburst (stage B-C transitions usually occur very late in such systems, e.g. SW UMa in figure 1).

3.47 ASASSN-16hi

This object was detected as a transient at $V=15.5$ on 2016 July 15 by the ASAS-SN team. Subsequent observations detected superhumps (vsnet-alert 20002, 20018; e-figure 29). The times of superhump maxima are listed in e-table 45. The observed maxima well illustrate typical stages B and C. Although the outburst was rather well recorded, the faintness (around 16 mag) made the quality of the averaged superhump profile rather poor.

3.48 ASASSN-16hj

This object was detected as a transient at $V=14.2$ on 2016 July 18 by the ASAS-SN team. Subsequent observations detected likely early superhumps and ordinary superhumps (vsnet-alert 20006, 20029; e-figure 30). On August 2–3, the object faded rapidly to a tem-

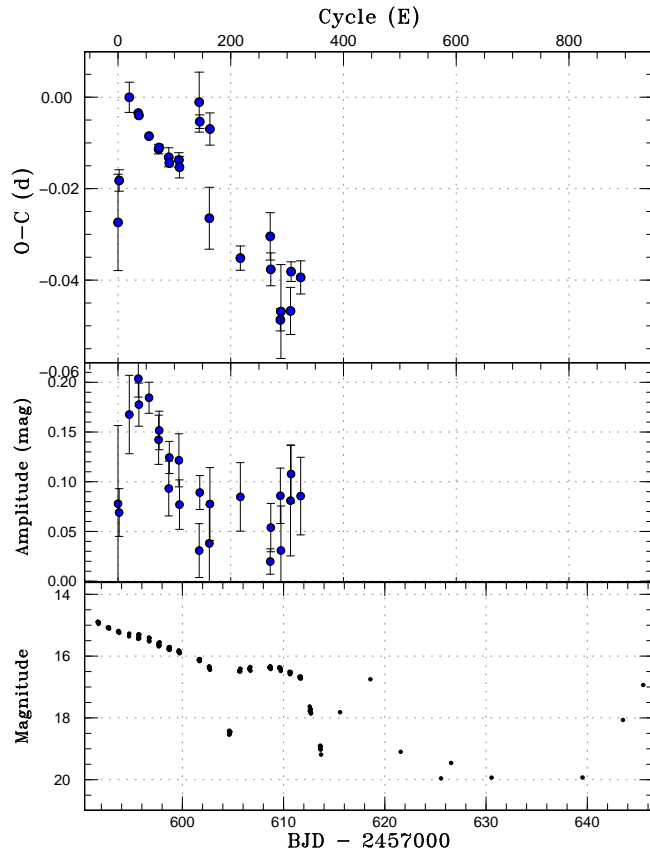


Fig. 26. $O - C$ diagram of superhumps in ASASSN-16hj (2016). (Upper:) $O - C$ diagram. We used a period of 0.05568 d for calculating the $O - C$ residuals. (Middle:) Amplitudes of superhumps. (Lower:) Light curve. The data were binned to 0.018 d.

porary dip (around 18.5 mag, figure 26). The object then entered a plateau-type rebrightening (vsnet-alert 20049), during which ordinary superhumps were present (e-figure 31). The object showed another separate rebrightening on August 18 (vsnet-alert 20089). Although later observations suggested another rebrightening on September 11–13, the reality of this rebrightening needs to be confirmed since it was long after the previous rebrightening and the observations were at the end of the observing season (figure 26).

The times of superhump maxima are listed in e-table 46. This table includes superhump maxima after a short dip. There were apparent stages A–C, although observations of stage C were rather poor (figure 26).

We give the possible signal of early superhumps in e-figure 32. Although the signal was close to the detection limit, the period appears to be consistent with the superhump period and the profile is also consistent with that of early superhumps. The period with the PDM method was 0.05499(6) d. The ϵ^* for stage A superhumps was 0.034(7), which corresponds to $q=0.09(2)$.

3.49 ASASSN-16ia

This object was detected as a transient at $V=14.6$ on 2016 August 1 by the ASAS-SN team. The object was also detected by Gaia (Gaia16azd) at a magnitude of 16.71 on August 7.¹⁵ The coordinates of the object were taken from this Gaia detection. The object once faded to $V=17.1$ on August 5. It was observed bright (16.0 mag) again on August 7 and showed strong early superhumps (vsnet-alert 20055, 20069, 20076). The object was followed until August 15, when early superhumps were still present. A transition to ordinary superhumps was not observed since the object became too faint.

The mean profile of early superhumps is shown in e-figure 33. The large (0.42 mag) full amplitude is exceptional and is largest among the known WZ Sge-type dwarf novae (cf. figure 15 in Kato 2015). The deeper minimum around phase 0.3 in figure e-figure 33 is somewhat flat-bottomed, which may be suggestive of an eclipsing component (see numerical model for MASTER OT J005740.99+443101.5 in Kato et al. 2014a). Nightly variation of early superhumps is shown in figure 27. It is noteworthy that the amplitudes of early superhump remained sufficiently large even 8 d after our initial observation. The systematic shift of the phase of the deeper minimum may reflect the varying degree of the contribution of the eclipsing component. Since the object is expected to have a very high inclination, detailed observations in quiescence are desired to determine the system parameters.

It is noteworthy that a precursor outburst was apparently present before the phase of the early superhumps. This is probably the first case in WZ Sge-type dwarf novae and the reason why the cooling wave started during the initial peak needs to be clarified.

3.50 ASASSN-16ib

This object was detected as a transient at $V=14.2$ on 2016 August 5 by the ASAS-SN team. Subsequent observations detected growing superhumps (vsnet-alert 20066, 20083). The times of superhump maxima are listed in e-table 47. During the epochs for $E \leq 14$, the amplitudes of superhumps grew, and these superhumps can be safely identified as stage A superhumps. The distinction of stages B and C was unclear. We listed a value for $47 \leq E \leq 133$ as stage B in table 3. The mean profile of the superhumps is shown in e-figure 34.

¹⁵<http://gsaweb.ast.cam.ac.uk/alerts/alert/Gaia16azd/>.

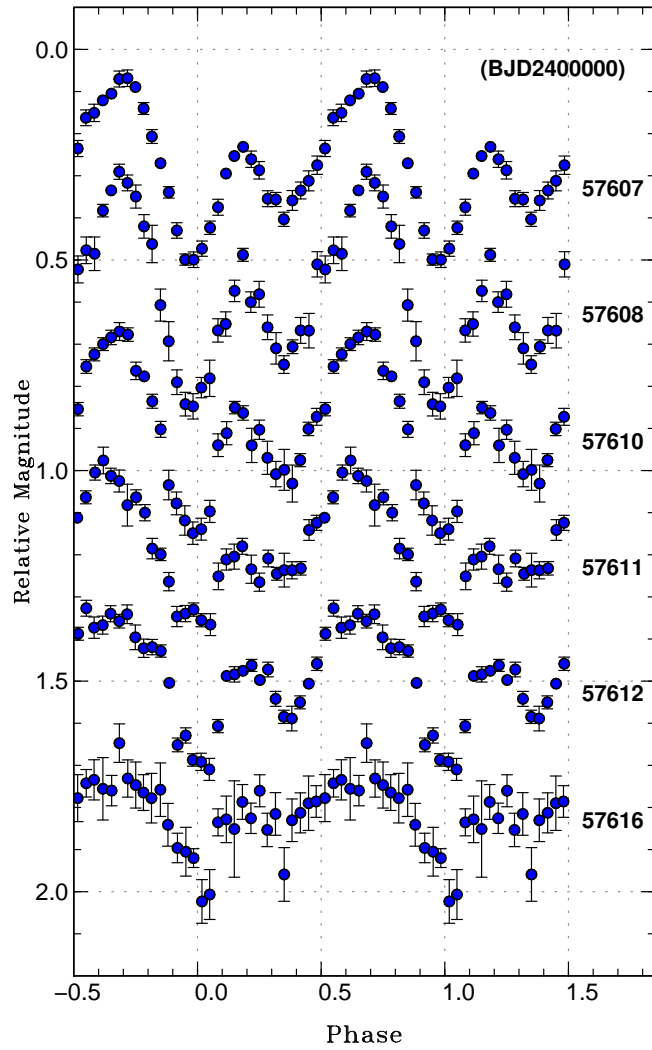


Fig. 27. Evolution of profile of early superhumps in ASASSN-16ia (2016). A period of 0.056962 d was used to draw this figure. The zero phase was defined to be BJD 2457607.428

3.51 ASASSN-16ik

This object was detected as a transient at $V=15.26$ on 2016 August 6 by the ASAS-SN team. The object further brightened to $V=13.9$ on August 8. The object started to show superhumps on August 11–12 (vsnet-alert 20082; e-figure 35). The times of superhump maxima are listed in e-table 48. The data very clearly show stages A (growing superhumps) and B. The object showed a rebrightening on August 25 (vsnet-alert 20109), which faded rapidly. During this rebrightening phase, a weak superhump signal was detected with a period of 0.0649(3) d.

3.52 ASASSN-16is

This object was detected as a transient at $V=14.9$ on 2016 August 9 by the ASAS-SN team. Initial observations detected double-wave modulations attributable to early superhumps (vsnet-alert 20078, 20084; e-figure 36). The period of early superhumps was 0.05762(2) d. The object started to show ordinary superhumps at least on August 20 (vsnet-alert 20101, 20106; e-figure 37). The times of superhump maxima are listed in e-table 49. The superoutburst plateau was terminated by rapid fading on August 28. The object is confirmed to be a WZ Sge-type dwarf nova.

3.53 ASASSN-16iu

This object was detected as a transient at $V=15.3$ on 2016 August 4 by the ASAS-SN team. The object once faded to fainter than $V=17.6$ on August 6 and brightened again to $V=15.2$ on August 9. The detection of the outburst was announced after this brightening. Superhumps were soon detected on August 11 (vsnet-alert 20075). The amplitudes of superhumps decreased and they became less prominent on subsequent nights. They became detectable again on August 15 (e-figure 38). The times of superhump maxima are listed in e-table 50. Due to the long period of undetectable superhumps, the P_{dot} for stage B superhumps is very uncertain. The period for stage C given in table 3 is very approximate due to the short baseline.

3.54 ASASSN-16iw

This object was detected as a transient at $V=13.9$ on 2016 August 10 by the ASAS-SN team. There was a faint ($g=21.9$) SDSS counterpart (there were 17 measurements in the SDSS data with a range of 21.8–22.2 in g) and the large outburst amplitude suggested a WZ Sge-type dwarf nova.

The object started to show superhumps on August 17 (vsnet-alert 20086, 20091, 20100; e-figure 39). The times of superhump maxima are listed in e-table 51. The superhumps grew slowly and it took at least 47 cycles to reach the full superhump amplitude. Based on $O - C$ variations, we have identified $E \leq 32$ to be stage A superhumps (figure 28).

The object showed at least five post-superoutburst rebrightenings (vsnet-alert 20129, 20147, 20164, 20167: figure 29).

An analysis of the early part of the light curve detected a possible signal of early superhumps (e-figure 40). Although the signal was weak (the amplitude was smaller than

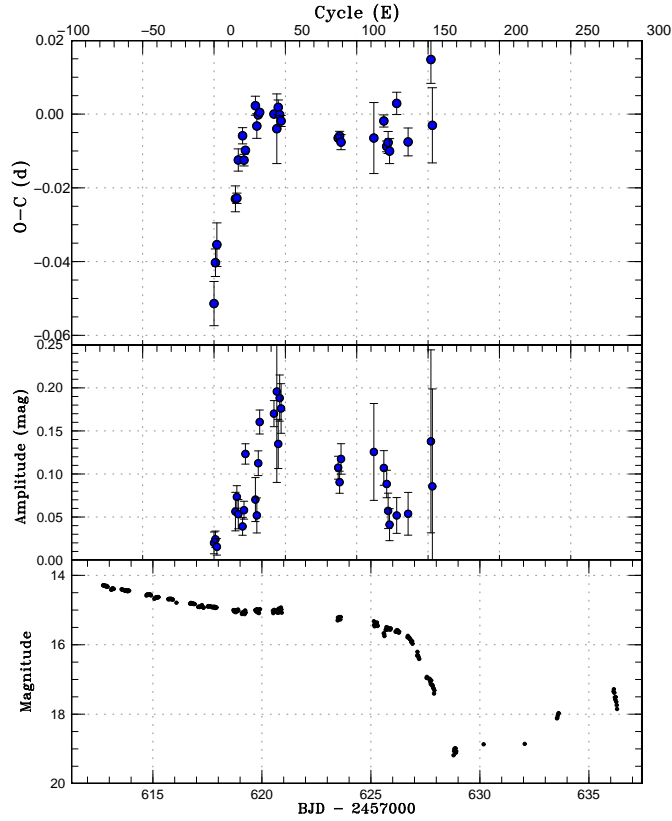


Fig. 28. $O - C$ diagram of superhumps in ASASSN-16iw (2016). (Upper:) $O - C$ diagram. We used a period of 0.06546 d for calculating the $O - C$ residuals. (Middle:) Amplitudes of superhumps. (Lower:) Light curve. The data were binned to 0.022 d. The final part of this figure (BJD 2457636) corresponds to the fading part from the first rebrightening.

0.01 mag) and the profile was not doubly humped as expected for early superhumps, we suspect that this is a candidate period of early superhumps since the period excess was close to what is expected for a WZ Sge-type dwarf nova. The period was 0.06495(5) d. The ϵ^* of 0.029(1) for stage A superhumps corresponds to $q=0.079(2)$. This q value is not as small as expected for a period bouncer at this orbital period. The relatively large P_{dot} for stage B superhump may also be suggestive for a relatively large q . The object may be similar to WZ Sge-type dwarf novae with multiple rebrightenings with relatively large q , such as MASTER OT J211258.65+242145.4 and MASTER OT J203749.39+552210.3 (Nakata et al. 2013).

3.55 ASASSN-16jb

This object was detected as a transient at $V=13.3$ on 2016 August 18 by the ASAS-SN team. The object was caught on the rise to the maximum. The object was initially suspected to be a Galactic nova (cf. vsnet-alert 20092). The object was confirmed to be blue, confirming the dwarf nova-type nature (vsnet-alert 20094). Subsequent observations detected early

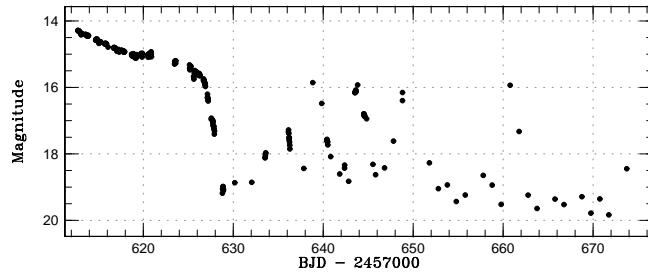


Fig. 29. Overall light curve of ASASSN-16iwl (2016). The data were binned to 0.022 d. The data on BJD 2457636 represent observations of the fading branch of the first rebrightening. There may have been a rebrightening on BJD 2457674, which was not well sampled.

superhumps (vsnet-alert 20098, 20095; e-figure 41). The object started to show ordinary superhumps (e-figure 42) on August 25 and showed behavior similar to a short-period SU UMa-type dwarf nova rather than an extreme WZ Sge-type dwarf nova (vsnet-alert 20112, 20125, 20154).

The times of superhump maxima are listed in e-table 52. All stages (A–C) are clearly seen. The period of stage A superhumps listed in table 3 was determined by the PDM method.

The period of early superhumps was 0.06305(2) d (e-figure 41). The fractional superhump excess of stage A superhumps ϵ^* was 0.0321(5), which corresponds to $q=0.088(1)$. This value is larger than what is expected for a period bouncer having this orbital period. The $O - C$ behavior (positive P_{dot} for stage B and the appearance of stage C) is also consistent with an object having an intermediately low q .

The object was also detected in outburst by ASAS-3 on 2006 March 10 ($V=13.66$, superoutburst), and possibly on 2009 November 3 ($V=13.63$, single observation at the end of the observing season). The presence of earlier outbursts also seems to exclude the possibility of a period bouncer.

The identification in AAVSO VSX with UGPS J175044.95–255837.2 appears to be doubtful considering its red color ($J - K=2.7$). This supposed identification likely came from the initial proposed classification as a classical nova. We adopted coordinates by the ASAS-SN team.

3.56 ASASSN-16jd

This object was detected as a transient at $V=13.6$ on 2016 August 20 by the ASAS-SN team. Superhumps started to appear on August 25 (vsnet-alert 20108, 20113; e-figure 43). The times of superhump maxima are listed in e-table 53. The period reported in vsnet-alert

20113 was a one-day alias of the true period. The period in this paper has been confirmed by the PDM analysis (e-figure 43) and the much smoother $O - C$ diagram than obtained using the former period [the case is the same as presented in subsection 2.2 in Kato et al. (2015a)].

3.57 ASASSN-16jk

This object was detected as a transient at $V=13.9$ on 2016 August 27 by the ASAS-SN team. The object has a blue $g=20.72$ SDSS counterpart. A neural network analysis of SDSS colors (Kato et al. 2012b) yielded an expected orbital period shorter than 0.06 d. One long outburst reaching 14.36 mag (unfiltered CCD) was recorded by the CRTS team on 2007 May 7. This outburst lasted at least until May 21. There was another detection at $r=13.87$ by the Carlsberg Meridian telescope (Niels Bohr Institute et al. 2014).

Subsequent observations of the 2016 outburst detected superhumps (vsnet-alert 20119, 20124; e-figure 44). The times of superhump maxima are listed in e-table 54. Although the maxima for $E < 16$ are clearly stage A superhumps, the period was not determined due to the shortness of the segment. Although there was apparent stage B-C transition around $E=146$, the period of stage C superhumps was not well determined.

3.58 ASASSN-16js

This object was detected as a transient at $V=13.0$ on 2016 August 30 by the ASAS-SN team. Early superhumps were immediately detected (vsnet-alert 20122, 20126, 20155; e-figure 45). Ordinary superhump emerged on September 9 (vsnet-alert 20165, 20187). The period of early superhumps was 0.060337(5) d. The times of superhump maxima are listed in e-table 55. The $O - C$ somewhat flattened after $E=32$ and there was a rather smooth transition to stage B, which started at around $E=48$. The mean profile of ordinary superhumps is given in e-figure 46.

The fractional superhump excess ϵ^* for stage A superhumps was 0.0213(16), which corresponds to $q=0.056(5)$. The small q and an orbital period significantly longer than the period minimum suggest that this object is a period bouncer. Although the mean superhump amplitude is larger than those of period bouncer candidates, this may have been due to the high orbital inclination as suggested by the strong early superhumps.

3.59 ASASSN-16jz

This object was detected as a transient at $V=15.7$ on 2016 September 5 by the ASAS-SN team. Observations immediately detected superhumps (vsnet-alert 20142; e-figure 47). The time of superhump maxima are listed in e-table 56. There was some hint of decrease in the $O - C$ values, which may reflect a stage transition. The exact identification of the superhump stage was impossible due to the short baseline.

3.60 ASASSN-16kg

This object was detected as a transient at $V=16.1$ on 2016 September 7 by the ASAS-SN team. The object brightened to $V=15.2$ on September 8 and the outburst was announced. There was no quiescent counterpart recorded in previous plates, and the large outburst amplitude received attention. Subsequent observations detected superhumps (vsnet-alert 20182; figure 30). The superhump period was around 0.10 d, which was not expected from the large outburst amplitude. Since there was a 3-d gap in the observation and individual runs were comparable to one superhump cycle, it was impossible to select the alias uniquely. The candidate periods by the PDM methods (e-figure 48) are 0.09676(4) d, 0.10013(4) d, 0.10373(5) d, 0.107610(5) d and 0.11178(5) d. Other aliases can be likely rejected because they give large $O - C$ scatters. Among them, we have selected 0.10013(4) d which gives the smallest θ in the PDM analysis to make cycle counts in e-table 57. One should note that there remains cycle count ambiguities due to the ambiguity in the alias selection. The object, however, is certainly located in the period gap. It might be worth noting that such a large-amplitude dwarf nova exists in the period gap.

The object was detected in outburst at an unfiltered CCD magnitude of 17.27 on September 26 by the CRTS team (=CSS160926:213630–251348). Since the object had already faded to 18.0 mag on September 20, this CRTS observation appears to have detected a post-superoutburst rebrightening.

3.61 ASASSN-16kx

This object was detected as a transient at $V=14.8$ on 2016 September 26 by the ASAS-SN team. Subsequent observations detected superhumps (vsnet-alert 20210; e-figure 49). The times of superhump maxima are listed in e-table 58.

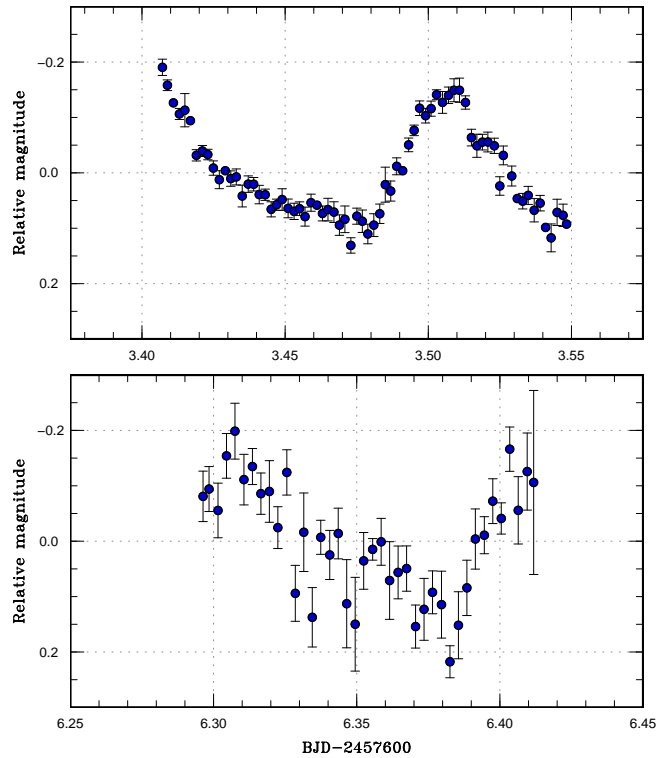


Fig. 30. Superhumps in ASASSN-16kg (2016). The data were binned to 0.003 d.

3.62 ASASSN-16le

This object was detected as a transient at $V=15.5$ on 2016 October 2 by the ASAS-SN team. Subsequent observations detected superhumps (vsnet-alert 20214). Since the object was observed only on one night, only three superhump maxima were recorded: BJD 2457668.1480(38) ($N=26$), 2457668.2486(13) ($N=176$) and 2457668.3286(20) ($N=147$). The best period determined by the PDM method was 0.0808(13) d (e-figure 50). The object faded to fainter than 17.5 mag on October 14.

3.63 ASASSN-16lj

This object was detected as a transient at $V=15.8$ on 2016 October 6 by the ASAS-SN team. Subsequent observations detected superhumps (vsnet-alert 20217). Since the object was observed only on one night, only three superhump maxima were recorded: BJD 2457670.3611(5) ($N=82$), 2457670.4447(5) ($N=87$) and 2457670.5325(22) ($N=45$). The best period determined by the PDM method was 0.0857(4) d (e-figure 51).

3.64 ASASSN-16lo

This object was detected as a transient at $V=14.3$ on 2016 October 8 by the ASAS-SN team. Subsequent observations detected early superhumps (vsnet-alert 20219, 20222; e-figure 52) confirming that this object is a WZ Sge-type dwarf nova. The best period of early superhump was 0.05416(1) d. Ordinary superhump developed on October 19 (vsnet-alert 20230, 20243; e-figure 53). The times of superhump maxima are listed in e-table 59. Although epochs $E \leq 2$ were stage A superhumps, the period of stage A superhumps could not be determined. Although observations were present after BJD 2457690, superhumps were not clearly detected since the object was very faint (16.5–17.0 mag). The outburst lasted at least until November 7.

3.65 ASASSN-16mo

This object was detected as a transient at $V=15.0$ on 2016 October 28 by the ASAS-SN team. Subsequent observations detected superhumps (vsnet-alert 20280, 20294, 20311; e-figure 54). The times of superhump maxima are listed in e-table 60. Although there was likely stage B-C transition after $E=84$, later observations could not detect superhumps very clearly and we did not determine the period of stage C superhumps.

3.66 ASASSN-16my

This object was detected as a transient at $V=14.4$ on 2016 November 6 by the ASAS-SN team. Subsequent observations detected superhumps (vsnet-alert 20325, 20357; e-figure 55). The times of superhump maxima are listed in e-table 61. Although the $O - C$ values suggest that $E \leq 12$ were still stage A superhumps, we did not determine the period of stage A superhumps since superhump amplitudes were already large (0.3–0.4 mag) and it is likely that the period was already affected by the pressure effect (i.e. transition to stage B).

3.67 ASASSN-16ni

This object was detected as a transient at $V=16.5$ on 2016 November 16 by the ASAS-SN team. The large outburst amplitude received attention. Subsequent observations detected long-period superhumps (vsnet-alert 20446; the period reported in vsnet-alert 20398 was probably in error). Such a long period [0.1152(4) d determined in this paper] was unexpected for a large-amplitude dwarf nova. Observations were, however, insufficient to determine the period uniquely due to the faintness. We selected the most likely alias in calculating

the $O - C$ values in e-table 62. The superhump amplitudes were growing on the first two nights, and the period reported here may refer to that of stage A superhumps. The small amplitudes (e-figure 56) may also support this stage identification.

The quiescent counterpart was originally proposed to be a very faint ($g=22.9$) object SDSS J050500.40+605455.3. This object, however, has a red color ($u - g=+2.6$) and it is unlikely a CV. The true quiescent counterpart should be fainter than $g=23$. We adopted the coordinates by the ASAS-SN team.

3.68 ASASSN-16nq

This object was detected as a transient at $V=15.0$ on 2016 November 26 by the ASAS-SN team. Observations on November 28 detected superhumps (vsnet-alert 20411; e-figure 57). Although the observations were obtained two nights after the outburst detection, stage A was already over (vsnet-alert 20431, 20472; figure 31). The times of superhump maxima are listed in e-table 63. Both stages B and C can be recognized. There was one post-superoutburst rebrightening on December 23 (figure 31), which is relatively rare for such a long P_{SH} system.

3.69 ASASSN-16nr

This object was detected as a transient at $V=15.1$ on 2016 November 26 by the ASAS-SN team. The outburst was announced after the observation on November 27 at $V=15.1$. The object showed superhumps (vsnet-alert 20420, 20432; e-figure 58). The times of superhump maxima are listed in e-table 64. Although a large outburst amplitude (~ 7 mag) was suggested, the object was not a WZ Sge-type dwarf nova since it showed well-developed ordinary superhumps immediately after the outburst detection.

3.70 ASASSN-16nw

This object was detected as a transient at $V=15.6$ on 2016 November 23 by the ASAS-SN team. The outburst was announced after the observation on November 27 at $V=16.1$ and November 29 at $V=16.3$. Superhumps were detected in observations on two nights (vsnet-alert 20445; e-figure 59). The alias selection is most likely based on the single long run on the first night giving a period of 0.073(1) d. The times of superhump maxima are listed in e-table 65.

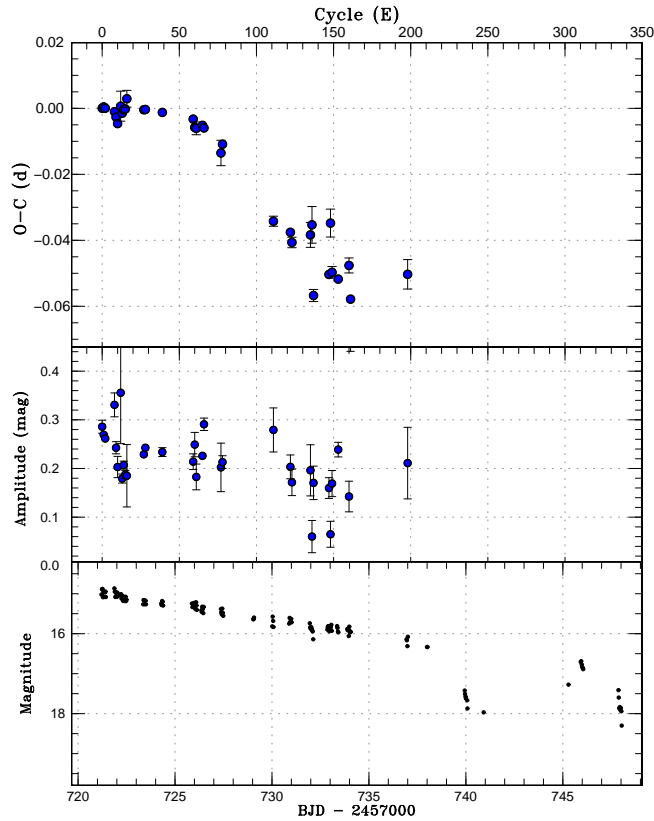


Fig. 31. $O - C$ diagram of superhumps in ASASSN-16nq (2016). (Upper:) $O - C$ diagram. We used a period of 0.05796 d for calculating the $O - C$ residuals. (Middle:) Amplitudes of superhumps. (Lower:) Light curve. The data were binned to 0.026 d.

3.71 ASASSN-16ob

This object was detected as a transient at $V=14.3$ on 2016 November 28 by the ASAS-SN team. The outburst was announced after its further brightening to $V=13.8$ on November 30. Although the object was initially identified with a $B=18.4$ mag star in USNO catalog, B. Monard obtained outburst astrometry which indicated that the true counterpart is much fainter (vsnet-alert 20438). The object was also detected by Gaia (Gaia16bz1)¹⁶ at a magnitude of 13.84 on November 30 and was announced (with an identification with ASASSN-16ob) on December 7. The large outburst amplitude suggested a WZ Sge-type dwarf nova. On December 11, low-amplitude superhumps were detected (vsnet-alert 20464, 20465, 20481), which grew to full superhumps (vsnet-alert 20484, 20498). The times of superhump maxima are listed in e-table 66. The maxima for $E \leq 36$ correspond to stage A superhumps. Although a PDM analysis of ordinary superhumps gave several candidate periods (e-figure 60), we consider them false signals due to low signal-to-noise ratio since an analysis restricted to better observation quality gave a single period (e-figure 61; one-day aliases can be safely

¹⁶<<http://gsaweb.ast.cam.ac.uk/alerts/alert/Gaia16bz1/>>.

ruled out by $O - C$ analysis).

By using the data before BJD 2457734, we could not detect early superhumps. The upper limit of the amplitude of early superhumps was 0.01 mag. Although we could not detect early superhumps, we consider that this object belongs to WZ Sge-type dwarf novae based on its long waiting time (13 d) for ordinary superhumps to appear and the large outburst amplitude. Using the empirical relation between q and P_{dot} for stage B superhumps [equation (6) in Kato 2015], the expected q is 0.069(3) (the error reflects the error in P_{dot}).

3.72 ASASSN-16oi

This object was detected as a transient at $V=13.4$ on 2016 December 3 by the ASAS-SN team (vsnet-alert 20443). Low-amplitude early superhumps were detected (vsnet-alert 20466; e-figure 62). The object subsequently showed ordinary superhumps (vsnet-alert 20466, 20485; e-figure 63). The object is confirmed to be a WZ Sge-type dwarf nova. The times of superhump maxima are listed in e-table 67. The best period of early superhumps with the PDM method is 0.05548(7) d. The fractional superhump excess ϵ^* for stage A superhumps is 0.033(2), which gives $q=0.091(7)$. The relatively large q is consistent with a relatively large P_{dot} for stage B superhumps and the relatively large amplitude of superhumps.

3.73 ASASSN-16os

This object was detected as a transient at $V=13.6$ on 2016 December 10 by the ASAS-SN team. The large outburst amplitude (~ 8 mag) attracted attention. The object started to show ordinary superhumps on December 18 (vsnet-alert 20501). These superhumps grew further (vsnet-alert 20504, 20508; e-figure 64). The times of superhump maxima are listed in e-table 68. Both stages A and B were very clearly recorded (figure 32).

A PDM analysis of the early part of the data yielded a signal which may be early superhumps (e-figure 65). This period was close to that of ordinary superhumps and we checked a possible contamination of ordinary superhumps by testing different segments. Although the test suggested that the period was not from a contamination of ordinary superhumps, we were not very confident about the reality of the signal since the amplitude was small and mostly only low time-resolution observations were obtained. If the detected period, 0.05494(6) d, is that of early superhumps, the fractional superhump excess for stage A superhumps is $\epsilon^*=0.018(1)$. Although this value corresponds to $q=0.047(3)$, it needs to be treated with caution due to the limitation of the quality of observations. The overall behav-

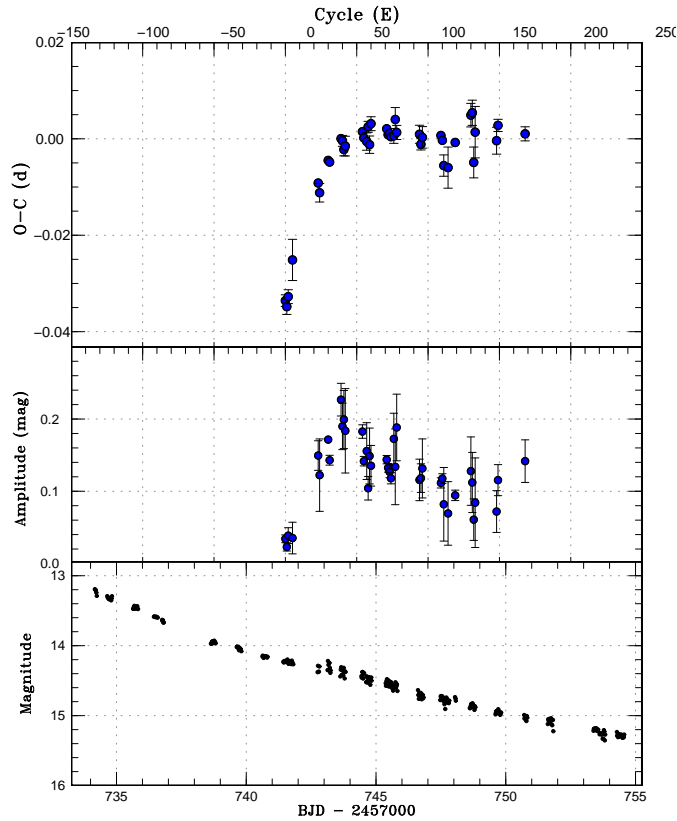


Fig. 32. $O - C$ diagram of superhumps in ASASSN-16os (2016). (Upper:) $O - C$ diagram. We used a period of 0.05499 d for calculating the $O - C$ residuals. (Middle:) Amplitudes of superhumps. (Lower:) Light curve. The data were binned to 0.017 d.

ior, however, suggests that this object is a rather extreme WZ Sge-type dwarf nova.

3.74 ASASSN-16ow

This object was detected as a transient at $V=13.9$ on 2016 December 13 by the ASAS-SN team. Since the object was near the Galactic plane, it was also suspected to be a nova. The presence of a GALEX UV counterpart and an $H\alpha$ emission in IPHAS catalog (IPHAS2 J063047.05+023931.4) suggested a dwarf nova (vsnet-alert 20474, 20476). The dwarf nova-type nature was confirmed by spectroscopy (Siviero, Munari 2016). Subsequent observations detected superhumps (vsnet-alert 20483, 20497, 20503, 20510; e-figure 66). The times of superhump maxima are listed in e-table 69. The superoutburst lasted at least up to December 25.

In contrast to many long- P_{SH} SU UMa-type dwarf novae, this object showed a post-superoutburst rebrightening on December 29–31 (vsnet-alert 20571). Although modulations were detected during this rebrightening, we could not detect a secure signal of superhumps.

3.75 ASASSN-17aa

This object was detected as a transient at $V=13.9$ on 2017 January 2 by the ASAS-SN team (vsnet-alert 20527). On January 11, superhumps were finally observed (vsnet-alert 20562; e-figure 67). Although these superhumps were originally suspected to be stage A ones (vsnet-alert 20572, 20573), the large superhump amplitudes suggest that they were already stage B ones. The cycle numbers in e-table 70 follows this interpretation. There were possibly low-amplitude early superhumps (e-figure 68) with a period of 0.05393(3) d. These properties suggest the WZ Sge-type classification.

3.76 ASASSN-17ab

This object was detected as a transient at $V=13.4$ on 2017 January 2 by the ASAS-SN team (vsnet-alert 20527). The object was already in outburst at $V=13.1$ on January 1. Subsequent observations detected superhumps (vsnet-alert 20531; e-figure 69). The times of superhump maxima are listed in e-table 71. Although the maxima for $E \leq 2$ were stage A superhumps, we could not determine the period. The object was also detected by Gaia (Gaia17aep)¹⁷ at a magnitude of 17.33 on January 18.

3.77 ASASSN-17az

This object was detected as a transient at $V=14.4$ on 2017 January 19 by the ASAS-SN team. Subsequent observations detected superhumps (vsnet-alert 20626; e-figure 70). The times of superhump maxima are listed in e-table 72. Since there was a 2-d gap between observations, there remained viable aliases. Among these aliases, the listed period gave the smallest $O - C$ values and we selected it as the most likely one.

3.78 ASASSN-17bl

This object was detected as a transient at $V=13.7$ on 2017 January 24 by the ASAS-SN team. On February 4, the object started to show superhumps (vsnet-alert 20641). The long waiting time (11 d) of superhumps strongly suggested a WZ Sge-type object. Further development of superhumps was recorded (vsnet-alert 20646; e-figure 71). The times of superhump maxima are listed in e-table 73. Although individual superhumps were not very well covered (most of them had only 10 observations or even less; the maxima could be reasonably determined since the object was bright), the overall $O - C$ diagram indicates the clear presence of

¹⁷<http://gsaweb.ast.cam.ac.uk/alerts/alert/Gaia17aep/>.

stage A and stage B with a positive P_{dot} . The stage A-B transition was rather uncertain due to the lack of observations in the initial part.

An analysis of the early part of the superoutburst yielded a possible signal of early superhumps (e-figure 72). Although there was a stronger signal around 0.0563 d, we consider it a false alias since it does not match the period of ordinary superhumps (the period of early superhumps should be shorter than that of ordinary superhumps). The suggested period by the PDM method was 0.05467(5) d. The ϵ^* of stage A superhumps determined using this period was 0.0235(9), which corresponds to $q=0.062(3)$. This value, however, could have a larger uncertainty since both the orbital period and the period of stage A superhumps were determined from insufficient observations. The small q value, however, appears to be consistent with the WZ Sge-type behavior, the small amplitude of ordinary superhumps and the small P_{dot} for stage B superhumps.

3.79 ASASSN-17bm

This object was detected as a transient at $V=15.9$ on 2017 January 25 by the ASAS-SN team. The outburst was announced after confirmation on January 27. Subsequent observations detected superhumps (vsnet-alert 20627; e-figure 73). The times of superhump maxima are listed in e-table 74. The period in table 3 was determined by the PDM method since individual maxima were not very well determined.

3.80 ASASSN-17bv

This object was detected as a transient at $V=15.0$ on 2017 January 31 by the ASAS-SN team. The outburst was announced after confirmation at $V=14.9$ on February 1. Subsequent observations starting on February 3 detected superhumps (vsnet-alert 20634; e-figure 74). The times of superhump maxima are listed in e-table 75. The $O - C$ values suggest that the maxima for $E \leq 1$ were stage A superhumps, although the amplitudes were already large. The period of stage C superhumps in table 3 is rather uncertain due to the large scatter in the final part of observations. The object faded to 19 mag on February 13.

3.81 ASASSN-17ce

This object was detected as a transient at $V=14.6$ on 2017 February 13 by the ASAS-SN team. Subsequent observations detected superhumps (vsnet-alert 20668, 20676; e-figure 75). The times of superhump maxima are listed in e-table 76. The maxima for $E \leq 6$ likely correspond

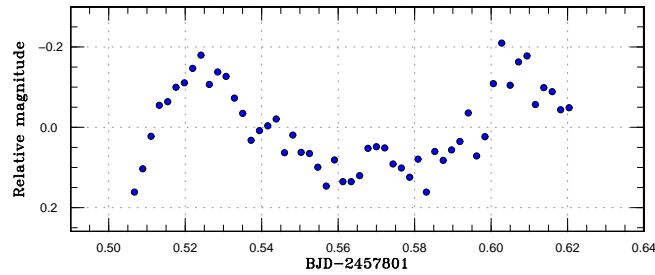


Fig. 33. Superhumps in ASASSN-17ck (2017).

to a short stage B usually seen in long- P_{orb} systems (Kato et al. 2009). The object faded close to 18 mag on February 26.

3.82 ASASSN-17ck

This object was detected as a transient at $V=16.6$ on 2017 February 15 by the ASAS-SN team. The object was already in outburst at $V=16.5$ on February 13. Single-night observations on February 17 detected superhumps (vsnet-alert 20680, figure 33). The times of maxima were BJD 2457801.5269(7) ($N=25$) and 2457801.6099(17) ($N=21$). The superhump period by the PDM analysis was 0.083(1) d.

3.83 ASASSN-17cn

This object was detected as a transient at $V=13.7$ on 2017 February 13 by the ASAS-SN team. The outburst announcement was made after an observation of $V=13.2$ on February 16. The object showed low-amplitude double-wave early superhumps (e-figure 76) and then ordinary superhumps (vsnet-alert 20750, 20755; e-figure 77). The behavior was typical for a WZ Sge-type dwarf nova. There was a 7 d gap in the observations, which hindered the detection of stage A superhumps. The times of superhump maxima are listed in e-table 77. Although the maxima after $E=137$ were stage C superhumps, we could not determine the period due to the limited quality of the data. The period of early superhumps by the PDM method was 0.05303(2) d. The object was also detected by Gaia (Gaia17arq)¹⁸ at a magnitude of 16.07 on March 14. This detection was made during the superoutburst plateau.

The long waiting time to develop ordinary superhumps (≥ 9 d counted from the outburst peak, ≥ 12 d from the outburst detection) and the large outburst amplitude ($\gtrsim 9$ mag) suggest that the object is a rather extreme WZ Sge-type dwarf nova.

¹⁸<http://gsaweb.ast.cam.ac.uk/alerts/alert/Gaia17arq/>.

3.84 ASASSN-17cx

This object was detected as a transient at $V=16.4$ on 2017 February 21 by the ASAS-SN team. The object was already in outburst at $V=16.6$ on February 18 and the outburst was announced after an observation at $V=16.7$ on February 23. Single-night observations on February 24 detected superhumps. The maxima were BJD 2457809.0621(9) ($N=52$), 2457809.1406(6) ($N=48$) and 2457809.2151(14) ($N=50$). The superhump period by the PDM method was 0.0761(7) d.

3.85 ASASSN-17dg

This object was detected as a transient at $V=13.8$ on 2017 March 7 by the ASAS-SN team. The object was already in outburst at $V=13.8$ on March 6. The last negative observation was on February 23. There is an ROSAT X-ray counterpart 1RXS J160232.8–603240. There was also an outburst with a maximum of $V=13.03$ on 2002 September 25, which lasted at least for 6 d in the ASAS-3 data. The actual maximum may have been even brighter since ASAS-3 did not observe this field for 6 d before this detection. The object has a bright ($J=13.68$) and blue ($J - K=+0.10$) 2MASS counterpart, indicating that the object was in outburst during 2MASS scans.

Observations started on March 9 and superhumps were immediately detected (vsnet-alert 20760; e-figure 79). The object started fading rapidly already on March 11. It was most likely the true maximum was missed by ASAS-SN observations for more than ~ 5 d. The times of superhump maxima are listed in e-table 78. These superhumps were most likely stage C ones since observations were performed in the final phase of the superoutburst. The low amplitudes of superhumps (vsnet-alert 20760) suggested that superhumps were already decaying.

There was one post-superoutburst rebrightening on March 19 ($V=14.3$, vsnet-alert 20809). A PDM analysis of the post-superoutburst data (BJD 2457825.7–2457842.9) yielded a period of 0.06655(5) d, which is likely a continuation of stage C superhumps.

3.86 ASASSN-17dq

This object was detected as a transient at $V=15.4$ on 2017 March 11 by the ASAS-SN team. The outburst was announced after the observation at $V=15.2$ on March 14. Observations starting on March 15 recorded superhumps (vsnet-alert 20791, 20810; e-figure 80). The times of superhump maxima are listed in e-table 79. The object started fading rapidly on March

24.

3.87 CRTS J000130.5+050624

This object (=CSS101127:000130+050624, hereafter CRTS J000130) was detected by the CRTS team at an unfiltered CCD magnitude of 15.68 on 2010 November 27.

The 2016 outburst was detected by the ASAS-SN team at $V=16.73$ on September 3 while the object was still rising. The detection announcement was made when it reached $V=15.47$ on September 9. The past outbursts in the ASAS-SN data suggested an SU UMa-type dwarf nova. Subsequent observations detected superhumps (vsnet-alert 20152, 20176). The times of superhump maxima are listed in e-table 80. The data were insufficient to give a solid value of P_{dot} . The superhump period of 0.09477(1) d (by the PDM method) places the object in the period gap.

3.88 CRTS J015321.5+340857

This object (=CSS081026:015321+340857, hereafter CRTS J015321) was discovered by the CRTS team on 2008 October 26. The SU UMa-type nature was established during the 2012 superoutburst (see Kato et al. 2014b for more history). The 2016 superoutburst was detected by the ASAS-SN team at $V=15.95$ on November 16. One superhump maximum at BJD 2457710.3850(10) ($N=72$) was observed.

3.89 CRTS J023638.0+111157

This object (=CSS091106:023638+111157, hereafter CRTS J023638) was detected by the CRTS team at an unfiltered CCD magnitude of 16.23 on 2009 November 6. Seven outbursts were detected in the CRTS data and there was a brighter ($V=15.17$) outburst in 2013 (vsnet-alert 16477).

The 2016 outburst was detected by the ASAS-SN team at $V=14.90$ on August 29. Subsequent observations detected superhumps (vsnet-alert 20118, 20128, 20153; e-figure 82). The times of superhump maxima are listed in e-table 81. The maxima for $E \geq 137$ were post-superoutburst ones. There was most likely a phase jump between $E=80$ and $E=137$ and the humps for $E \geq 137$ were likely traditional late superhumps. The transition between stages B and C was rather smooth as in other relatively long P_{SH} systems.

Table 6. List of superoutbursts of CRTS J033349

Year	Month	Day	max*	V-mag
2014	10	28	56959	14.26
2015	2	16	57070	14.49
2015	9	16	57282	14.50
2015	12	29	57386	14.38
2016	8	17	57618	14.41
2016	11	18	57711	14.46

*JD–2400000.

3.90 CRTS J033349.8–282244

This object (=SSS110224:033350–282244, hereafter CRTS J033349) was discovered by the CRTS team at an unfiltered CCD magnitude of 15.06 on 2011 February 24. The bright outburst in 2016 November was detected by the ASAS-SN team at $V=14.46$ on November 19. Subsequent observations detected superhumps (vsnet-alert 20400, 20403; e-figure 83). The times of superhump maxima are listed in e-table 82. The observations were performed during the later course of the superoutburst and the period probably refers to stage C one.

We listed well-defined superoutbursts in the ASAS-SN data since 2014 in table 6. These superoutbursts can be well expressed by a supercycle of 108(1) d with maximum $|O - C|$ values of 10 d. There have been typically two normal outbursts between superoutbursts. These features closely resemble those of V503 Cyg (Harvey et al. 1995) (vsnet-alert 20386). V503 Cyg, however, sometimes showed frequent normal outbursts (e.g. Kato et al. 2002b) and these alternations between phases of different number of normal outbursts have been considered to be a result of a disk tilt, which is considered to suppress normal outbursts (see the subsection of 1RXS J161659, subsection 3.27). Detection of negative superhumps is expected in CRTS J033349.

3.91 CRTS J044636.9+083033

This object (=CSS130201:044637+083033, hereafter CRTS J044637) was detected by the CRTS team at an unfiltered CCD magnitude of 17.70 on 2013 February 1. There was a bright outburst at $V=15.12$ on 2017 January 12 detected by the ASAS-SN team. Subsequent observations detected two superhumps on a single night (vsnet-alert 20580). The maxima were BJD 2457768.9773(11) ($N=97$) and 2457769.0716(14) ($N=98$). A PDM analysis yielded a period of

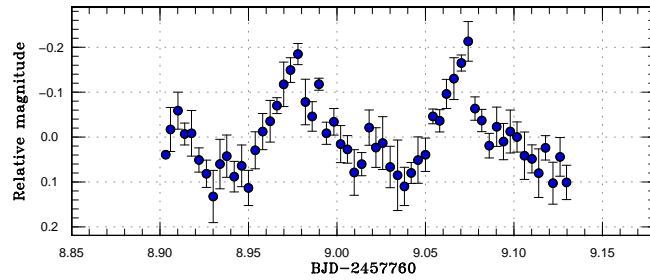


Fig. 34. Superhump in CRTS J044637 (2017). The data were binned to 0.004 d.

0.093(1) d. Although there were single-night observations 4 d later, the observing condition was not sufficient to detect superhumps.

3.92 CRTS J082603.7+113821

This object (=CSS110124:082604+113821, hereafter CRTS J082603) was detected by the CRTS team at an unfiltered CCD magnitude of 15.95 on 2011 January 24 (Drake et al. 2014).

The 2017 outburst was detected by the ASAS-SN team at $V=14.9$ on January 3. The observation on January 5 detected superhumps (vsnet-alert 20542). The best period with the PDM method was 0.0719(4) d. Two superhump maxima were measured: BJD 2457759.4542(5) ($N=72$) and 2457759.5245(5) ($N=68$).

3.93 CRTS J085113.4+344449

This object (=CSS080401:085113+344449, hereafter CRTS J085113) was detected by the CRTS team at an unfiltered CCD magnitude of 16.4 on 2008 April 1 (Drake et al. 2008). The past data suggested that there was a bright ($I=14$) outburst in the past (vsnet-alert 10009). There was a bright outburst at unfiltered CCD magnitudes of 14.14–14.73 on 2008 November 20, detected by the CRTS team (cf. vsnet-alert 10717). The outburst was suspected to be a super-outburst. Subsequent observations detected a superhump with a period of ~ 0.08 d (vsnet-alert 10723; figure 35). There have been eight outbursts (up to 2016) in the CRTS database. The SDSS colors in quiescence suggested an orbital period of 0.08–0.12 d (Kato et al. 2012b).

The 2016 superoutburst was detected by the ASAS-SN team at $V=13.85$ on November 1. Subsequent observations detected superhumps (vsnet-alert 20315; e-figure 85). The times of superhump maxima were BJD 2457697.2246(2) ($N=181$) and 2457697.3114(3) ($N=176$). The best superhump period by the PDM method was 0.08750(9) d.

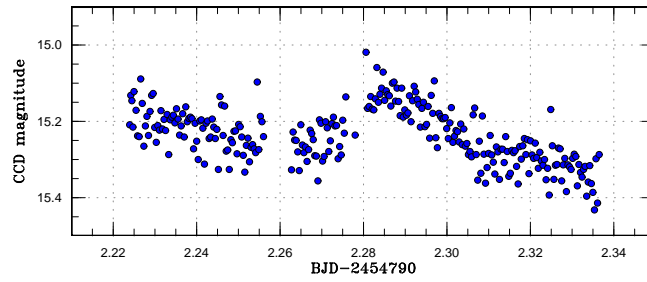


Fig. 35. Superhump in CRTS J085113 (2008).

Table 7. List of likely superoutbursts of CRTS J085603

Year	Month	Day	max*	V-mag
2014	5	10	56788	15.67
2015	2	17	57071	15.67
2015	10	22	57317	15.61
2016	5	17	57526	15.75
2016	11	26	57718	16.62

*JD-2400000.

3.94 CRTS J085603.8+322109

This object (=CSS100508:085604+322109, hereafter CRTS J085603) was detected by the CRTS team at an unfiltered CCD magnitude of 16.20 on 2010 May 8. There is a $g=19.6$ -mag SDSS counterpart and its colors yielded an expected orbital period of 0.067(1) d (Kato et al. 2012b).

The 2016 outburst was detected by the ASAS-SN team at $V=16.62$ on November 26. Subsequent observations detected superhumps (vsnet-alert 20428; e-figure 86). The times of superhump maxima are listed in e-table 83.

The ASAS-SN data indicate that past outbursts occurred rather regularly. We listed outburst maxima (they are likely superoutburst as judged from the brightness) in table 7. These maxima can be expressed by a supercycle of 232(10) d, with the maximum $|O - C|$ of 33 d. It was likely that the peak of the 2016 superoutburst was not covered by ASAS-SN observations.

3.95 CRTS J164950.4+035835

This object (=CSS100707:164950+035835, hereafter CRTS J164950) was detected by the CRTS team at an unfiltered CCD magnitude of 14.1 on 2010 July 7. There were seven outbursts recorded in the CRTS data.

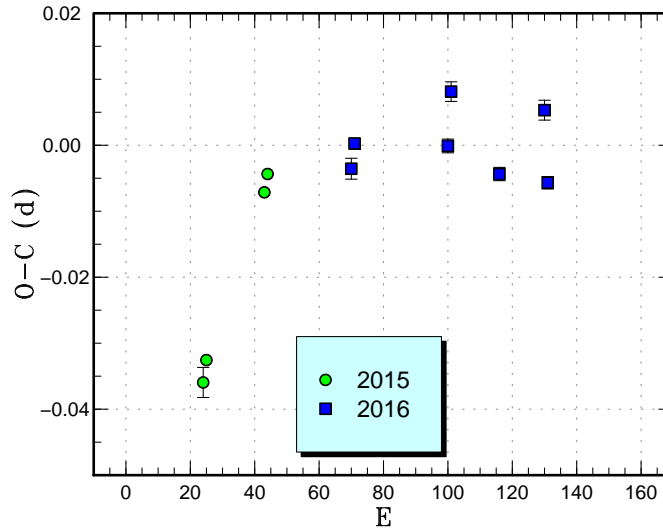


Fig. 36. Comparison of $O - C$ diagrams of CRTS J164950 between different superoutbursts. A period of 0.06490 d was used to draw this figure. Approximate cycle counts (E) after the start of the superoutburst were used.

The 2015 superoutburst was detected by the ASAS-SN team at $V=13.80$ on April 13. Subsequent observations detected superhumps (vsnet-alert 18545). The times of superhump maxima are listed in e-table 84.

The 2016 superoutburst was detected by the ASAS-SN team at $V=13.41$ on August 31. Subsequent observations detected superhumps (vsnet-alert 20132). The times of superhump maxima are listed in e-table 85.

The period for the 2015 observations was much longer than in 2016. The 2015 observations were carried out soon after the outburst detection and they may have recorded stage A superhumps. This interpretation is illustrated in figure 36. A mean superhump profile is given for the better observed 2016 superoutburst (e-figure 87).

3.96 CSS J062450.1+503114

This object (=CSS131223:062450+503111, hereafter CSS J062450) was detected by the CRTS team at an unfiltered CCD magnitude of 14.76 on 2013 December 23. The 2017 outburst was detected by the ASAS-SN team at $V=14.59$ on March 11. Subsequent observations detected superhumps (vsnet-alert 20766, 20770; e-figure 88). The times of superhump maxima are listed in e-table 86.

According to the ASAS-SN data, this object showed relatively regular superoutbursts (table 8). These superoutburst can be expressed by a supercycle of 128(2) d with maximum $|O - C|$ of 20 d. The interval between the 2016 September and 2017 March superoutbursts

Table 8. List of likely superoutbursts of CSS J062450 in the ASAS-SN data

Year	Month	Day	max*	V-mag
2013	12	24	56651	14.31
2014	9	7	56908	14.61
2015	1	12	57035	14.70
2015	9	17	57283	14.79
2016	1	29	57416	14.74
2016	9	25	57657	14.94
2017	3	11	57823	14.59

*JD-2400000.

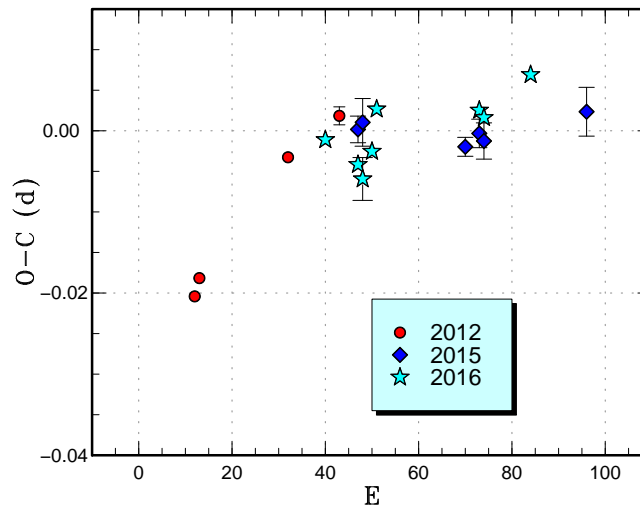


Fig. 37. Comparison of $O - C$ diagrams of DDE 26 between different superoutbursts. A period of 0.08860 d was used to draw this figure. Approximate cycle counts (E) after the start of the superoutburst were used.

was 166 d, which was rather unusually long for this object.

3.97 DDE 26

DDE 26 is a dwarf nova discovered by Denisenko (2012). See Kato et al. (2014b) for more information. The 2016 superoutburst was detected by the ASAS-SN team at $V=15.95$ on August 1. Superhumps were recorded (vsnet-alert 20067). The times of superhump maxima are listed in e-table 87. The observation probably covered stage B (figure 37).

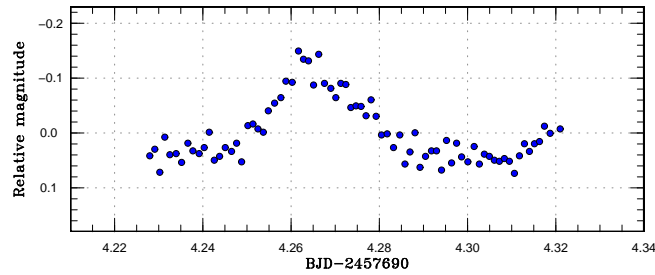


Fig. 38. Superhump in DDE 48 (2016).

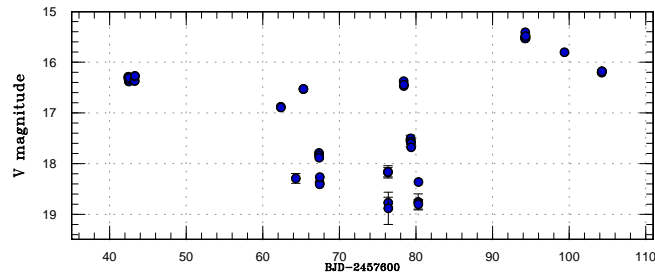


Fig. 39. Light curve of DDE 48 (2016). The data were binned to 0.002 d.

3.98 DDE 48

DDE 48 is a dwarf nova discovered by D. Denisenko (vsnet-alert 20146) in the vicinity of the dwarf nova MASTER OT J204627.96+242218.0 (Shumkov et al. 2016a). N. Mishevskiy monitored this object in 2016 and detected a bright outburst at $V=15.5$ on November 1 (vsnet-alert 20290). Subsequent observations detected a superhump (vsnet-alert 20291). Although this superhump was recorded only on a single night, the profile suggests a genuine superhump (figure 38). The superhump maximum was at BJD 2457694.2662(6) ($N=43$). The superhump became undetectable on two nights during the same superoutburst.

This object shows frequent outbursts (cf. vsnet-alert 20291; figure 39). The shortest interval of outbursts was 3 d. The initial long outburst in figure 39 was also likely a superoutburst recorded in its the final phase. If it is indeed the case, the supercycle is around 62 d. The object may belong to ER UMa-type dwarf novae (Kato, Kunjaya 1995; Robertson et al. 1995). (see also vsnet-alert 20291). Future continuous observations to determine the outburst characteristics, duty cycle and superhump period are desired.

3.99 MASTER OT J021315.37+533822.7

This object (hereafter MASTER J021315) was discovered as a transient at an unfiltered CCD magnitude of 16.8 mag on 2013 November 1 by the MASTER network (Yecheistov et al. 2013). The 2016 outburst was detected by the ASAS-SN team at $V=16.39$ on October 2. The

ASAS-SN also detected the 2013 outburst and its duration was long (at least 8 d). During the 2016 outburst, long-period superhumps were detected (vsnet-alert 20218; e-figure 89). The period indicates that the object is in the period gap. The times of superhump maxima are listed in e-table 88. The period markedly decreased with a global P_{dot} of $-205(35) \times 10^{-5}$. As recently recognized in many long- P_{orb} objects, such a large period decrease is most likely a result of stage A-B transition (cf. V1006 Cyg and MN Dra: Kato et al. 2016b; CRTS J214738.4+244554 and OT J064833.4+065624: Kato et al. 2015a; KK Tel, possibly V452 Cas and ASASSN-15cl: Kato et al. 2016a). The case is also likely since the initial observation of MASTER J021315 started only 1 d after the outburst detection. We gave values in table 3 following this interpretation. The ASAS-SN data suggest that outbursts in this system were relatively rare (only two were known with a separation of ~ 3 yr). The object should have a low mass-transfer rate.

3.100 MASTER OT J030205.67+254834.3

This object (hereafter MASTER J030205) was discovered as a transient at an unfiltered CCD magnitude of 13.7 mag on 2016 December 4 by the MASTER network (Balanutsa et al. 2016b). Although initial observations suggested the presence of early superhumps of the WZ Sge-type dwarf nova (vsnet-alert 20447), they were later identified as developing superhumps (stage A) with double maxima (vsnet-alert 20449, 20451). Further development of superhumps were reported (vsnet-alert 20456, 20471; e-figure 90). The times of superhump maxima are listed in e-table 89. Stages A and B can be recognized and the P_{dot} of stage B superhumps is positive, which is expected for this P_{SH} . The period of stage A superhump in table 3 was determined by the PDM method for the data before BJD 2457728.7.

Short-term periodic oscillations were reported (vsnet-alert 20452, 20457). An analysis of the entire data confirmed the presence of a coherent signal with a period 0.0035420(2) d [306.03(2) s] as originally reported (vsnet-alert 20457) (figure 40). Given the sharpness (high coherence) of the signal, it may be an intermediate-polar (IP) signal rather than quasi-periodic oscillations (vsnet-alert 20458). Since IPs are relatively rare in SU UMa-type dwarf novae [see table 1 in Hameury, Lasota (2017); the only well-established SU UMa-type dwarf nova (not including WZ Sge-type one) is CC Scl (Kato et al. 2015b)], further confirmation of the signal in this system is desired.

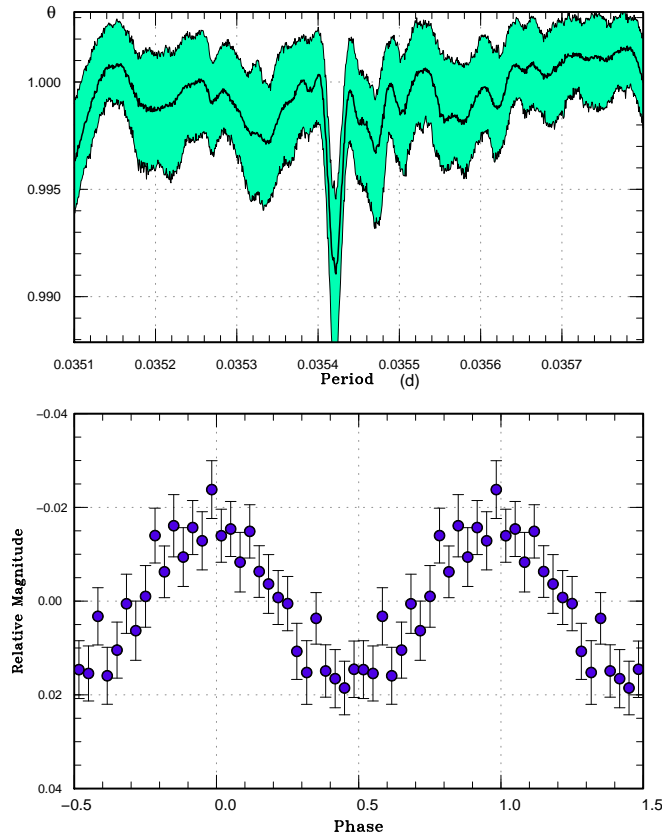


Fig. 40. Possible intermediate-polar-type signal in MASTER J030205 (2016). (Upper): PDM analysis. (Lower): Phase-averaged profile.

3.101 MASTER OT J042609.34+354144.8

This object (hereafter MASTER J042609) was discovered as a transient at an unfiltered CCD magnitude of 12.9 on 2012 September 30 by the MASTER network (Denisenko et al. 2012). The SU UMa-type nature was confirmed during this superoutburst (Kato et al. 2014b). This object is also a grazing eclipser. For more information and history, see Kato et al. (2014b).

The 2016 superoutburst was detected by E. Muylaert at a visual magnitude of 13.8 on December 26. The last observation before this detection was on $V=15.35-15.51$ on December 23 (ASAS-SN). It was not clear when the outburst started. Superhumps were observed with a period change (vsnet-alert 20532, 20533). The times of superhump maxima are listed in e-table 90. The period change observed during the 2016 superoutburst probably reflected stage B-C transition (figure 41). Although the last two points may have been traditional late superhumps, no clear superhumps were observed after them despite relatively good observational coverage. Although no clear eclipses were visible during this superoutburst, a phase-averaged light curve with a period of 0.06550168 d and an epoch of BJD 2456276.6430 (Kato et al. 2014b) yielded a shallow eclipse (0.03 mag) at the expected phase (figure 42). We

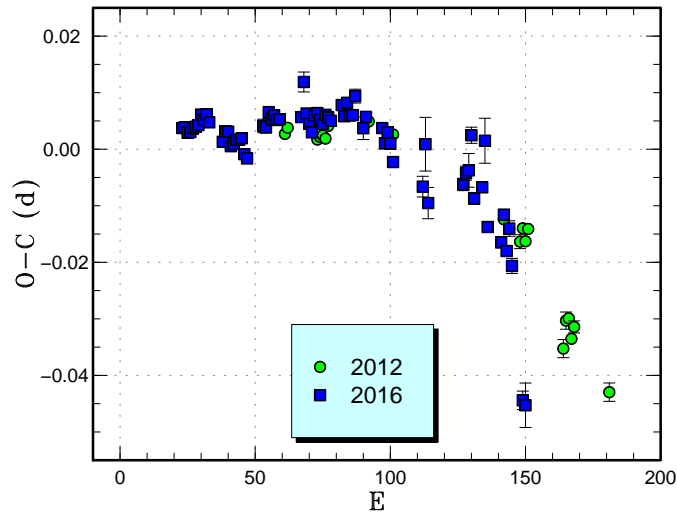


Fig. 41. Comparison of $O - C$ diagrams of MASTER J042609 between different superoutbursts. A period of 0.06756 d was used to draw this figure. Approximate cycle counts (E) after the outburst detection were used. The 2012 superoutburst was shifted by 20 cycles to match the 2016 one.

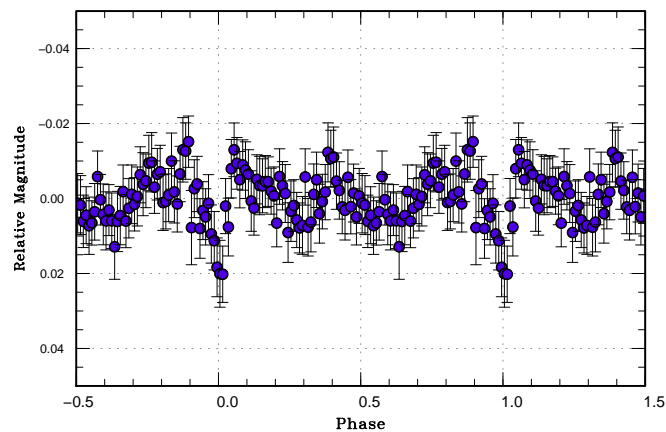


Fig. 42. Eclipse profile in MASTER J042609 (2016). The superhumps were mostly removed by using LOWESS. The phase-averaged profile was drawn against the ephemeris $\text{BJD } 2456276.6430 + 0.06550168E$.

consider 0.06550168(1) d to be the refined orbital period.

3.102 MASTER OT J043220.15+784913.8

This object (hereafter MASTER J043220) was discovered as a transient at an unfiltered CCD magnitude of 16.8 on 2013 December 12 by the MASTER network (Shurpakov et al. 2013a). The 2017 outburst was detected by the ASAS-SN team at $V=16.29$ on January 25. The object was already seen in outburst at $V=16.52$ in the ASAS-SN data. Subsequent observations detected superhumps (vsnet-alert 20614; figure 43). The times of superhump maxima were $\text{BJD } 2457780.4941(5)$ ($N=64$) and $2457780.5584(5)$ ($N=64$). A PDM analysis yielded a period of 0.0640(6) d.

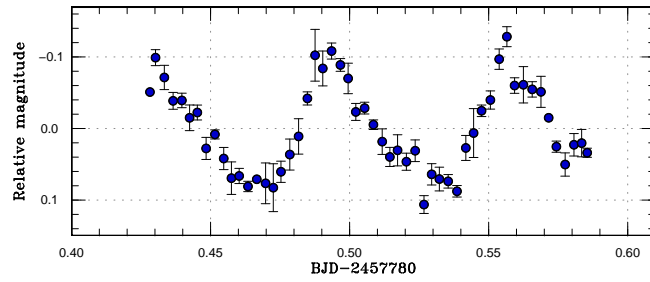


Fig. 43. Superhump in MASTER J043220 (2017). The data were binned to 0.003 d.

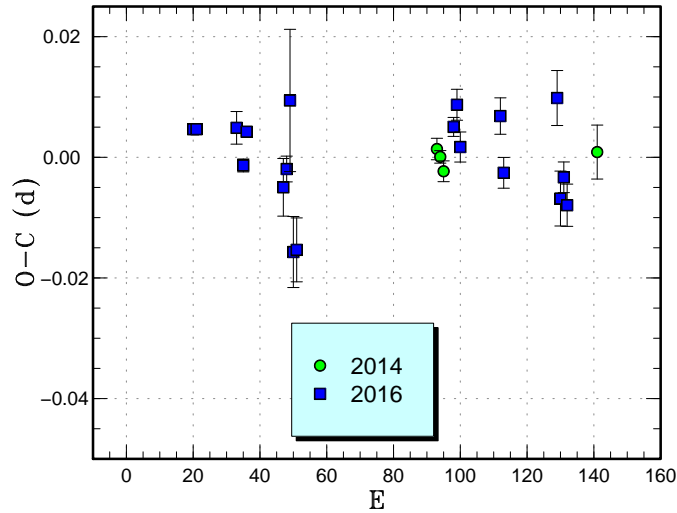


Fig. 44. Comparison of $O - C$ diagrams of MASTER J043915 between different superoutbursts. A period of 0.06243 d was used to draw this figure. Approximate cycle counts (E) after the start of the superoutburst were used.

3.103 MASTER OT J043915.60+424232.3

This object (hereafter MASTER J043915) was discovered as a transient at an unfiltered CCD magnitude of 15.7 on 2014 January 21 by the MASTER network (Balanutsa et al. 2014). The SU UMa-type nature was confirmed during this superoutburst (Kato et al. 2015a). For more history, see Kato et al. (2015a).

The 2016 superoutburst was detected by the ASAS-SN team at $V=16.38$ on December 22. Superhumps were subsequently recorded (vsnet-alert 20509). The times of superhump maxima are listed in e-table 91. Although there was no disagreement between the 2014 and 2016 observations, we could not detect clear stages B and C, which are expected for this short P_{SH} (figure 44).

3.104 MASTER OT J054746.81+762018.9

This object (hereafter MASTER J054746) was discovered as a transient at an unfiltered CCD magnitude of 16.7 mag on 2016 October 12 by the MASTER network (Shumkov et al. 2016b).

Subsequent observations detected superhumps (vsnet-alert 20227; e-figure 91). The times of superhump maxima are listed in e-table 92. The best superhump period with the PDM method is listed in table 3.

3.105 MASTER OT J055348.98+482209.0

This object (hereafter MASTER J055348) was discovered as a transient at an unfiltered CCD magnitude of 16.5 mag on 2014 March 13 by the MASTER network (Vladimirov et al. 2014). The 2017 outburst was detected by the ASAS-SN team at $V=16.52$ on February 16. Subsequent observations detected superhumps (vsnet-alert 20681). Although observations on two nights were reported, neither data were of sufficient quality to determine the superhump period (the object already faded below 17 mag). The period used to calculate epochs in e-table 93 was one of the possibilities giving smallest $O - C$ residuals. Other candidate aliases were 0.0784(1) d and 0.0720(1) d (e-figure 92). The period of 0.0666 d reported in vsnet-alert 20681 could not express the second-night observation.

3.106 MASTER OT J055845.55+391533.4

This optical transient (hereafter MASTER J055845) was detected on 2014 February 19 at a magnitude of 14.4 (Yecheistov et al. 2014). During the 2014 superoutburst, single-night observations detected superhumps (likely stage C ones) with a period of 0.0563(4) d (Kato et al. 2015a).

The 2016 outburst was detected by the ASAS-SN team at $V=15.24$ on September 14. The object was on the rise at $V=16.51$ on September 7. Rather queerly, the object was also detected at $V=14.16$ on August 30. There were no observations between August 30 and September 7. Three-night observations starting on September 16 detected superhumps (vsnet-alert 20186). During these observations, the object brightened from 15.4 mag (September 16) to 15.2 mag (September 18). Superhumps were recorded on the first two nights (e-table 94). The period in table 3 was determined by the PDM method (e-figure 93). Since the recorded outburst behavior was rather strange, we could not determine the superhump stage. The reason of the large difference of superhump periods between 2014 and 2016 is unclear. The 2014 observations were single-night ones and there were no possibility of an alias and the 2014 period could not satisfy the 2016 data. More observations are apparently needed.

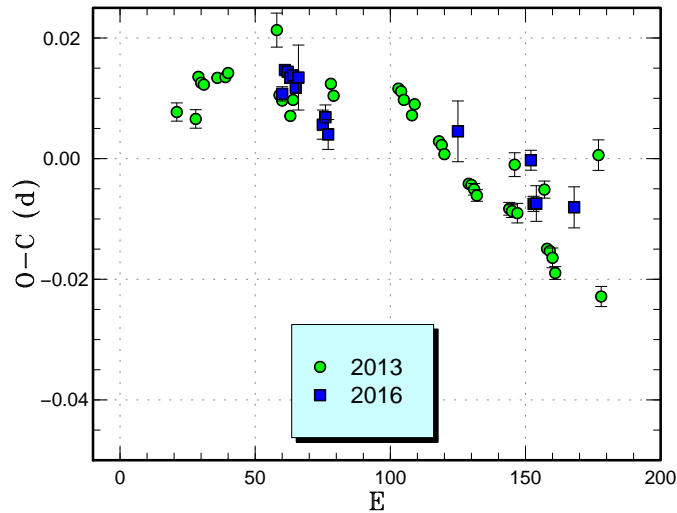


Fig. 45. Comparison of $O - C$ diagrams of MASTER J064725 between different superoutbursts. A period of 0.06777 d was used to draw this figure. Approximate cycle counts (E) after the start of the superoutburst were used.

3.107 MASTER OT J064725.70+491543.9

This object (hereafter MASTER J064725) was discovered as a transient at an unfiltered CCD magnitude of 13.2 mag on 2013 March 7 by the MASTER network (Tiurina et al. 2013). Subsequent observations detected superhumps (Kato et al. 2014b).

The 2016 superoutburst was detected by the ASAS-SN team at $V=13.99$ on December 13. Time-resolved photometry started on December 17 and stage A superhumps were not recorded. The times of superhump maxima are listed in e-table 95. The 2016 observations, which were obtained in poorer conditions than in the 2013 observations, likely resulted a mixture of stages B and C (figure 45). Due to the limited number of superhumps maxima, we could not determine the periods for these stages individually.

3.108 MASTER OT J065330.46+251150.9

This object (hereafter MASTER J065330) was discovered as a transient at an unfiltered CCD magnitude of 15.9 mag on 2014 February 16 by the MASTER network (Echeistov et al. 2014). The 2017 outburst was detected by the ASAS-SN team at $V=15.89$ on January 23. Subsequent observations detected superhumps (vsnet-alert 20612; e-figure 94). The times of superhump maxima are listed in e-table 96. According to the ASAS-SN data, there was another long outburst (superoutburst) on 2015 September 17.

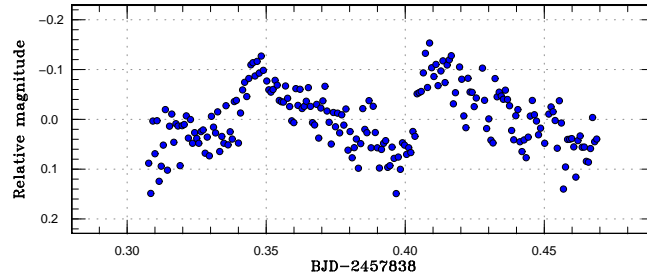


Fig. 46. Superhump in MASTER J075450 (2017).

3.109 MASTER OT J075450.18+091020.2

This object (hereafter MASTER J075450) was discovered as a transient at an unfiltered CCD magnitude of 16.0 mag on 2013 November 7 by the MASTER network (Vladimirov et al. 2013). The 2017 outburst was detected by the ASAS-SN team at $V=16.36$ on March 24. The object was then found to be already in outburst at $V=16.39$ on March 22. Observations on March 25–26 detected superhumps (vsnet-alert 20821; figure 46). The times of superhump maxima were BJD 2457838.3515(8) ($N=71$) and 2457838.4172(8) ($N=68$). The superhump period determined by the PDM method was 0.0664(5) d. There was also a most likely super-outburst in the ASAS-SN data on 2015 January 20 with a maximum of $V=16.08$.

3.110 MASTER OT J150518.03–143933.6

This object (hereafter MASTER J150518) was discovered as a transient at an unfiltered CCD magnitude of 15.5 mag on 2017 February 8 by the MASTER network (Gress et al. 2017). This transient was also detected by the ASAS-SN team (ASASSN-17cb) at $V=15.4$ on the same night, but the announcement was made after confirmation at $V=15.1$ on February 11. Although only the late course of the outburst was observed, superhumps were recorded (vsnet-alert 20660). Since observations only recorded one superhump maximum on each night, the one-day alias could not be resolved. We selected one of them to minimize the θ of the PDM analysis to make cycle counts in table e-table 97. Although the large negative global P_{dot} may have reflected stage B-C transition, the quality of the data were insufficient to confirm it.

3.111 MASTER OT J151126.74–400751.9

This object (hereafter MASTER J151126) was discovered as a transient at an unfiltered CCD magnitude of 14.0 mag on 2016 March 18 by the MASTER network (Popova et al. 2016). Subsequent observations detected superhumps (vsnet-alert 19614, 19630; e-figure 96). The

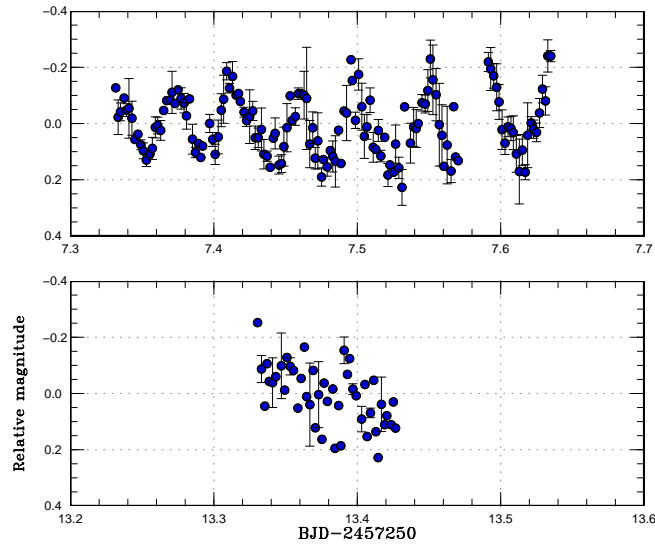


Fig. 47. Superhump-like double wave modulations in MASTER J162323 (2015). The data were binned to 0.002 d. The variations were only recorded on BJD 2457255 (August 22) and they disappeared 6 d later.

times of superhump maxima are listed in e-table 98. We interpreted that most of our observations recorded stage B as judged from a positive P_{dot} expected for this P_{SH} . The outburst faded on April 3. The duration of the outburst was at least 16 d.

3.112 MASTER OT J162323.48+782603.3

This object (hereafter MASTER J162323) was detected as a transient at an unfiltered CCD magnitude of 13.2 mag on 2013 December 9 by the MASTER network (Denisenko et al. 2013a). The 2013 superoutburst was well observed (Kato et al. 2014a).

The 2015 superoutburst was detected at $V=13.49$ on August 10 by the ASAS-SN team. Double-wave modulations were recorded on August 22 (vsnet-alert 19004). These variations disappeared 6 d later (see figure 47). Since these observations covered only the last (and likely post-superoutburst) phase of the superoutburst and the nature of humps is unclear, we did not use these data for comparison with other superoutbursts.

There was an outburst at $V=13.46$ on 2016 April 22 (ASAS-SN detection). Subsequent observations did not detect superhumps (observers: Shugarov team and Akazawa). There was another outburst at $V=13.34$ on 2016 September 26 (ASAS-SN detection). Three superhumps were recorded during this superoutburst (e-table 99). These superhumps were likely obtained around transition from stage A to B (figure 48) and the period [0.09013(7) d, PDM method] is not listed in table 3.

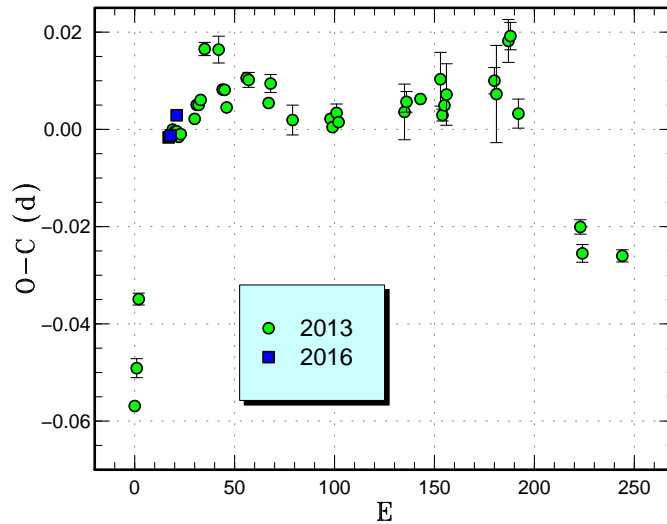


Fig. 48. Comparison of $O - C$ diagrams of MASTER J162323 between different superoutbursts. A period of 0.08866 d was used to draw this figure. Approximate cycle counts (E) after the start of the superoutburst were used. We shifted the 2016 $O - C$ diagram by 25 cycles to match the well-observed 2015 one.

3.113 MASTER OT J165153.86+702525.7

This object (hereafter MASTER J165153) was detected as a transient at an unfiltered CCD magnitude of 15.9 on 2013 May 23 by the MASTER network (Shurpakov et al. 2013b).

The 2017 outburst was detected by the ASAS-SN team at $V=14.64$ on February 4. Subsequent observations detected superhumps (vsnet-alert 20659; e-figure 97). The times of superhump maxima are listed in e-table 100.

3.114 MASTER OT J174816.22+501723.3

This object (hereafter MASTER J174816) was discovered as a transient at an unfiltered CCD magnitude of 15.6 mag on 2013 June 28 by the MASTER network (Denisenko et al. 2013b). The object has a blue SDSS counterpart ($g=17.59$). At least nine outbursts were recorded in the CRTS data. The object has a bright ($J=15.55$) 2MASS counterpart, suggesting that the object was in outburst during 2MASS scans.

The 2016 outburst was detected by the ASAS-SN team at $V=15.50$ on March 25. Subsequent observations detected superhumps (vsnet-alert 19642; e-figure 98). The times of superhump maxima are listed in e-table 101. Although we adopted a period of 0.08342(4) d (PDM method), an alias of 0.07950(4) d could not be excluded.

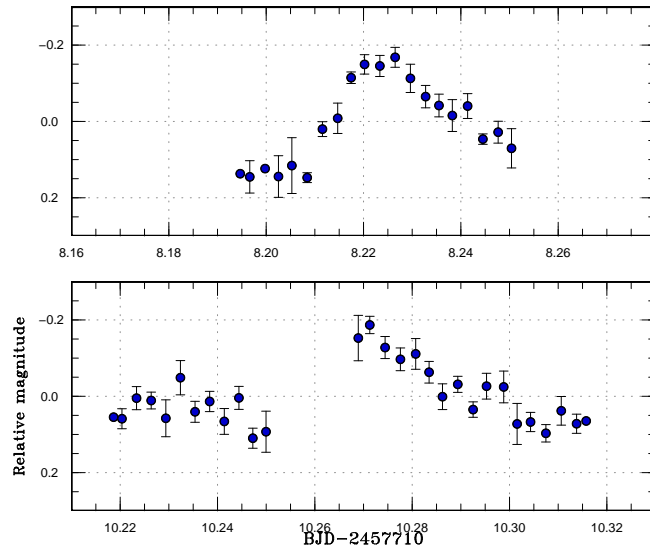


Fig. 49. Superhump in MASTER J211322 (2016).

3.115 MASTER OT J211322.92+260647.4

This object (hereafter MASTER J211322) was discovered by the MASTER network at an unfiltered CCD magnitude of 15.2 on 2012 December 21 (Shurpakov et al. 2012). The 2016 outburst was detected by the ASAS-SN team at $V=15.53$ on November 24. There was another bright outburst reaching $V=14.91$ on 2015 May 29 according to the ASAS-SN data. Subsequent observations detected superhumps (vsnet-alert 20453; figure 49). Although two superhump maxima were measured to be BJD 2457718.2276(8) ($N=73$) and 2457720.2718(14) ($N=66$, the maximum was missed and was estimated by template fitting), only one superhump maximum was recorded on each night and the period is $2.04(1)/n$, where n is an integer.

3.116 MASTER OT J220559.40–341434.9

This object (hereafter MASTER J220559) was discovered by the MASTER network at an unfiltered CCD magnitude of 14.5 on 2016 September 19 (Pogrosheva et al. 2016a; correction in Pogrosheva et al. 2016b). The object was also detected by the ASAS-SN team (ASASSN-16kr) at $V=14.3$ on September 11. The ASAS-SN detection was announced after the object brightened to $V=13.9$ on September 22, 2 d after the MASTER announcement. Although the object was initially considered to be an SS Cyg-type object from the low outburst amplitude (cf. vsnet-alert 20189), time-resolved photometry detected superhumps and eclipses (vsnet-alert 20190, 20196, 20206; figure 50, e-figure 99).

We obtained the eclipse ephemeris using the MCMC analysis (Kato et al. 2013):

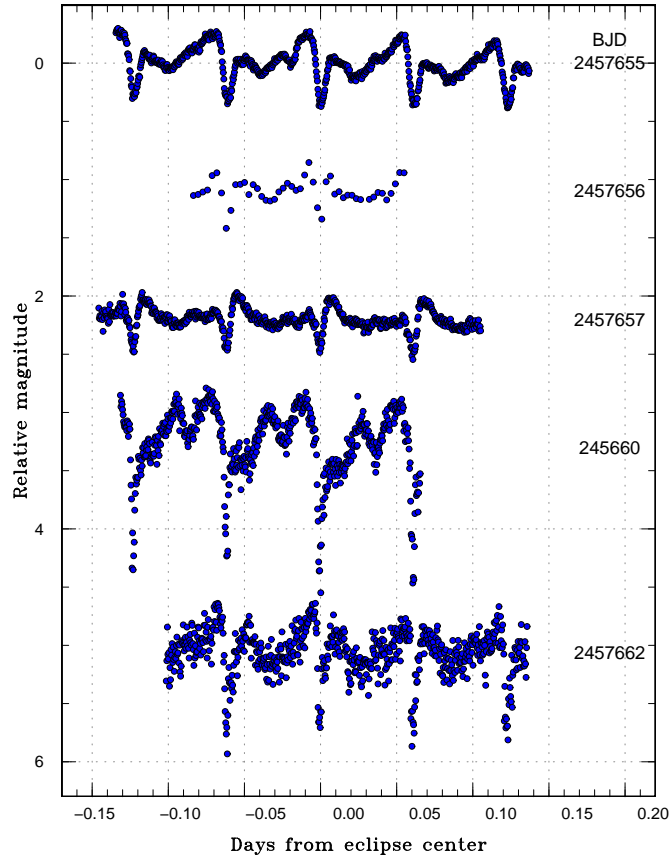


Fig. 50. Eclipses and superhumps in MASTER J220559.

$$\text{Min(BJD)} = 2457658.72016(3) + 0.0612858(3)E. \quad (4)$$

This ephemeris is not intended for long-term prediction of eclipses. The epoch refers to the center of the observation. The times of superhump maxima outside the eclipses are listed in e-table 102. Although the $O - C$ diagram suggests stage B-C transition, the periods and P_{dot} may have not been well determined since the actual start of the outburst was much earlier than the detection announcement and determination of superhump maxima should have been affected by overlapping eclipses and orbital humps in the late epochs. A large positive P_{dot} , however, is usual for such a short- P_{orb} SU UMa-type dwarf nova.

The small outburst amplitude (~ 4.5 mag) was probably a result of the high orbital inclination. Since the object has deep eclipses and apparently shows a large positive P_{dot} , it surely deserves further detailed observations to clarify the origin of increasing P_{SH} during stage B. Observations of the early phase of a superoutburst are also desired to determine q by the stage A superhump method.

3.117 SBS 1108+574

This object (hereafter SBS 1108) was originally selected as an ultraviolet-excess object during the course of the Second Byurakan Survey (SBS, Markarian, Stepanian 1983). An outburst detected by CRTS on 2012 April 22 (=CSS120422:111127+571239) led to an identification as an SU UMa-type dwarf nova having a period below the period minimum (cf. Kato et al. 2013). Littlefield et al. (2013) studied this object by spectroscopy and found He I emission of comparable strength to the Balmer lines, indicating a hydrogen abundance less than 0.1 of ordinary hydrogen-rich CVs but still at least 10 times higher than that in AM CVn stars. The object received special attention since it is considered to be a candidate progenitor of an AM CVn system (also known as EI Psc-type objects) (Littlefield et al. 2013).

The 2016 outburst was detected by the ASAS-SN team at $V=15.44$ on March 17. Although subsequent observations detected superhumps (vsnet-alert 19615, 19674), the 2016 outburst was not as well observed as in 2012 and superhumps were detected only on two nights (e-table 103). We could not make a comparison of $O - C$ diagrams between the 2012 and 2016 observations due to the insufficiency of observations in 2016.

3.118 SDSS J032015.29+441059.3

This object (hereafter SDSS J032015) was originally selected as a CV by Wils et al. (2010) based on SDSS variability. The SDSS colors suggested an object below the period gap (Kato et al. 2012b).

The 2016 outburst was detected by the ASAS-SN team at $V=14.84$ on September 19. Subsequent observations detected superhumps (vsnet-alert 20209; e-figure 100). The times of superhump maxima are listed in e-table 104. Since the observations were obtained during the final part of the superoutburst, these superhumps probably consisted of both stage B and C ones.

Although there were single-night observations by C. Littlefield on 2014 October 3, the nature of this outburst and detected variations were unknown (cf. vsnet-alert 17801, 17818).

3.119 SDSS J091001.63+164820.0

This object (hereafter SDSS J091001) was originally selected as a CV by the SDSS (Szkody et al. 2009). The SDSS colors suggested an object below the period gap (Kato et al. 2012b). There was an outburst in 2016 February–March (cf. vsnet-alert 19539), but CCD observations by T. Vanmunster and Y. Maeda showed that the outburst was a rapidly fading normal one.

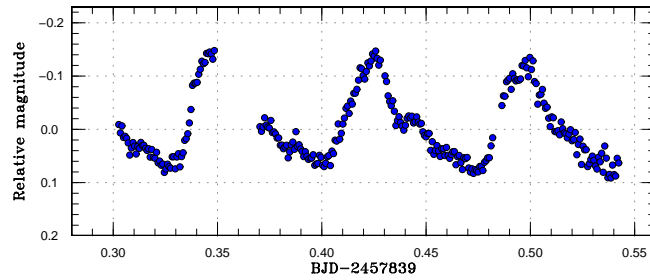


Fig. 51. Superhump in SDSS J091001 (2017).

The 2017 outburst was detected by the ASAS-SN team at $V=14.39$ on March 25. The ASAS-SN data indicated that the outburst started at $V=16.28$ on March 21 and peaked at $V=14.04$ on March 23. Subsequent observations detected superhumps (vsnet-alert 20830). Three superhump maxima were recorded: BJD 2457839.3524(3) ($N=50$), 2457839.4252(3) ($N=76$) and 2457839.4980(3) ($N=73$). The superhump period determined by the PDM method was 0.0734(2) d.

3.120 SDSS J113551.09+532246.2

This object (hereafter SDSS J113551) was reported as an outbursting object discovered by ROTSE-IIIb telescope at an unfiltered CCD magnitude of 15.1 on 2006 March 24 (Quimby, Mondol 2006). Kato et al. (2012b) expected an orbital period of 0.112(6) d based on SDSS colors.

The 2017 outburst was detected by the ASAS-SN team at $V=15.34$ on February 16. Although observations on two nights were reported, neither data were of sufficient quality to determine the superhump period (due to cloud gaps). The period used to calculate epochs in e-table 105 was one of the possibilities giving smallest $O - C$ residuals. Other candidate aliases were 0.1023(1) d and 0.0914(1) d (e-table 105). In any case, SDSS J113551 is in or close to the period gap and should be studied further. According to the ASAS-SN data, there were past (most likely) superoutbursts on 2012 March 10 ($V=15.53$) and 2016 May 15 ($V=15.68$). There were additional possible ones which were not well recorded. The frequency of superoutbursts was not probably especially low.

3.121 SDSS J115207.00+404947.8

This object (hereafter SDSS J115207) was originally selected as a CV by the SDSS (Szkody et al. 2007). Although Szkody et al. (2007) suspected an eclipsing system, its nature was established by Southworth et al. (2010), who determined the orbital period of 0.06770(28) d

and an mass ratio of 0.14(3). Savoury et al. (2011) obtained further observations and refined the values to be 0.067721356(3) d and 0.155(6), respectively.

The object was confirmed to be an SU UMa-type dwarf nova by the detection of superhumps during the 2009 superoutburst (Kato et al. 2010). Due to the poor coverage of the 2009 superoutburst and the limited knowledge of the orbital period at that time, we could not determine superhump and orbital periods precisely in Kato et al. (2010).

The 2017 superoutburst was detected by the ASAS-SN team at $V=15.51$ on February 14. Superhumps were subsequently detected (vsnet-alert 20664, 20671, 20688).

We noticed that the ephemeris by Savoury et al. (2011) could not express our eclipse observations and found that the period 0.0677497 d satisfy all the data (Southworth et al. 2010; Savoury et al. 2011; Kato et al. 2010 and the present observations). By using our data in 2009 and 2017, we have updated the eclipse ephemeris using the MCMC analysis (Kato et al. 2013):

$$\text{Min(BJD)} = 2457578.07695(6) + 0.0677497014(14)E. \quad (5)$$

The epoch corresponds to the center of the entire combined observation of 2009 and 2017. This period corresponds to 4797 cycles between Southworth et al. (2010) and Savoury et al. (2011), which was assumed to be 4799 cycles in Savoury et al. (2011). The $O - C$ values against this ephemeris are listed in table 9. The times of eclipse centers by our observations in table 9 were determined by the same MCMC method against the data segments (2007 and 2017) by fixing the orbital period. The eclipse profiles used to determine these minima are shown in figure 52 and figure 53.

The times of superhump maxima are listed in e-table 106. Although superhumps were initially suspected to be stage A ones (vsnet-alert 20671), they were more likely already stage B ones (figure 54). Stage B-C transition occurred around $E=52$. We also provide an updated table of superhump maxima of the 2009 superoutburst in e-table 107. This table is based on the identification of the true superhump period and based on the updated orbital ephemeris. The 2009 observations likely recorded a combination of stages B and C.

3.122 SDSS J131432.10+444138.7

This object (hereafter SDSS J131432) was originally selected as a CV by Wils et al. (2010) based on SDSS colors and variability. The 2017 outburst was detected by the ASAS-SN team at $V=15.63$ on March 28. Subsequent observations detected superhumps (vsnet-alert 20841; e-figure 102). The times of superhump maxima are listed in e-table 108.

Table 9. List of eclipse minima in SDSS J115207

E	BJD-2400000	$O - C$	Source*
-39831	54879.5387(2)	0.0001	1
-39830	54879.6065(2)	0.0002	1
-38125	54995.11953(6)	-0.00005	2
-35033	55204.601324(6)	-0.00034	3
3321	57803.07370(2)	-0.00001	2

*1: Southworth et al. (2010), 2: this work, 3:

Savoury et al. (2011)

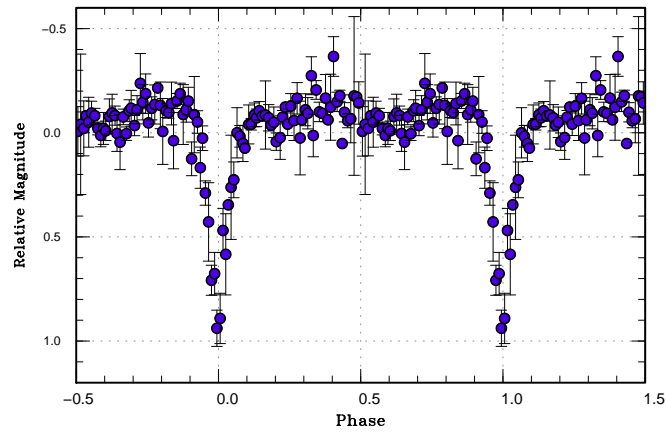


Fig. 52. Eclipse profile in SDSS J115207 (2009). The superhumps were mostly removed by using LOWESS. The phase-averaged profile was drawn against the ephemeris equation (5).

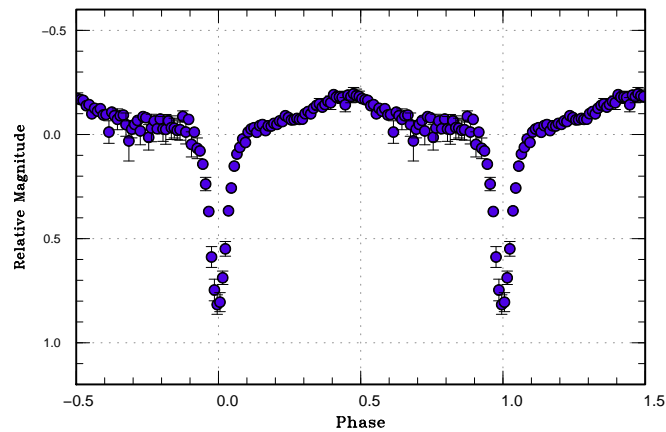


Fig. 53. Eclipse profile in SDSS J115207 (2017). The superhumps were mostly removed by using LOWESS. The phase-averaged profile was drawn against the ephemeris equation (5).

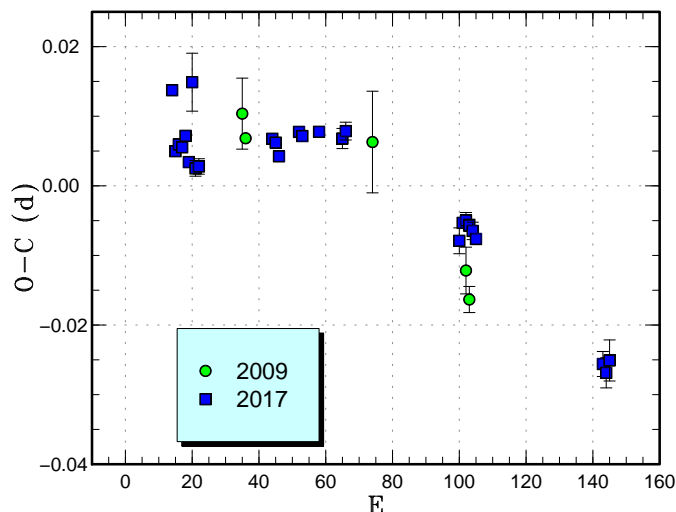


Fig. 54. Comparison of $O - C$ diagrams of SDSS J115207 between different superoutbursts. A period of 0.07036 d was used to draw this figure. Approximate cycle counts (E) after the start of the superoutburst were used.

3.123 SDSS J153015.04+094946.3

This object (hereafter SDSS J153015) was originally selected as a CV by the SDSS (Szkody et al. 2009). The dwarf nova-type variation was confirmed by CRTS observations (Drake et al. 2014). The 2017 outburst was detected by the ASAS-SN team at $V=15.84$ on March 7. Based on ASAS-SN observations, this outburst was likely a precursor one. The peak was observed on March 10. Subsequent observations detected superhumps (vsnet-alert 20769; e-figure 103). The times of superhump maxima are listed in e-table 109. The period in table 3 was obtained by the PDM analysis. Since these superhump observations were made during the early phase, the period may refer to that of stage A superhumps.

ASAS-SN observations indicate that this object shows superoutburst relatively regularly. The times of recent (likely) superoutburst are listed in table 10. Assuming that two superoutbursts were not recorded between 2016 July and 2017 March, all the superoutbursts were well expressed by a supercycle of 84.7(1.2) d with the maximum $|O - C|$ of 18 d. The long-term light curve does not look like that of an ER UMa-type dwarf nova but resembles that of V503 Cyg (cf. subsections 3.14, 3.27 and 3.90). Further observations to search for negative superhumps are recommended.

3.124 SDSS J155720.75+180720.2

This object (hereafter SDSS J155720) was originally selected as a CV by the SDSS (Szkody et al. 2009). The spectrum was that of a dwarf nova in quiescence and Szkody et al. (2009) suggested a period of ~ 2.1 hr. There is an ROSAT X-ray counterpart of 1RXS

Table 10. List of likely superoutbursts of SDSS J153015 since 2015

Year	Month	Day	max*	V-mag
2015	2	17	57070	15.93
2015	5	12	57155	15.79
2015	7	31	57235	15.57
2016	1	22	57409	15.97
2016	4	15	57493	15.91
2016	7	28	57597	15.77
2017	3	10	57823	15.76

*JD–2400000.

J155720.3+180715. The object was detected in outburst on 2007 June 12 (14.8 mag) and 2008 September 5 (16.1 mag) by the CRTS team¹⁹

The 2016 outburst was detected by the CRTS team at an unfiltered CCD magnitude of 15.37 on March 17 (=CSS160317:155721+180720) and by the ASAS-SN team at $V=15.12$ on the same night. Subsequent observations detected superhumps (vsnet-alert 19613; e-figure 104). The times of superhump maxima are listed in e-table 110.

3.125 SSS J134850.1–310835

This object (hereafter SSS J134850) was discovered by Stan Howerton during the course of the CRTS SNHunt (supernova hunt).²⁰ The object showed a number of outbursts in the ASAS-3 data in the past.

The 2016 outburst was detected by R. Stubbings at a visual magnitude of 11.8 on April 17. Subsequent observations detected superhumps (vsnet-alert 19751; e-figure 105). The times of superhump maxima are listed in e-table 111. The period variation was rather smooth and we gave a global P_{dot} rather than giving stages. An analysis of the post-superoutburst data did not yield a superhump period.

¹⁹<<http://nesssi.cacr.caltech.edu/catalina/20160317/1603171180824123493.html>>.

²⁰<<https://www.aavso.org/sssj1348501-310835-bright-dwarf-nova-centaurus>>.

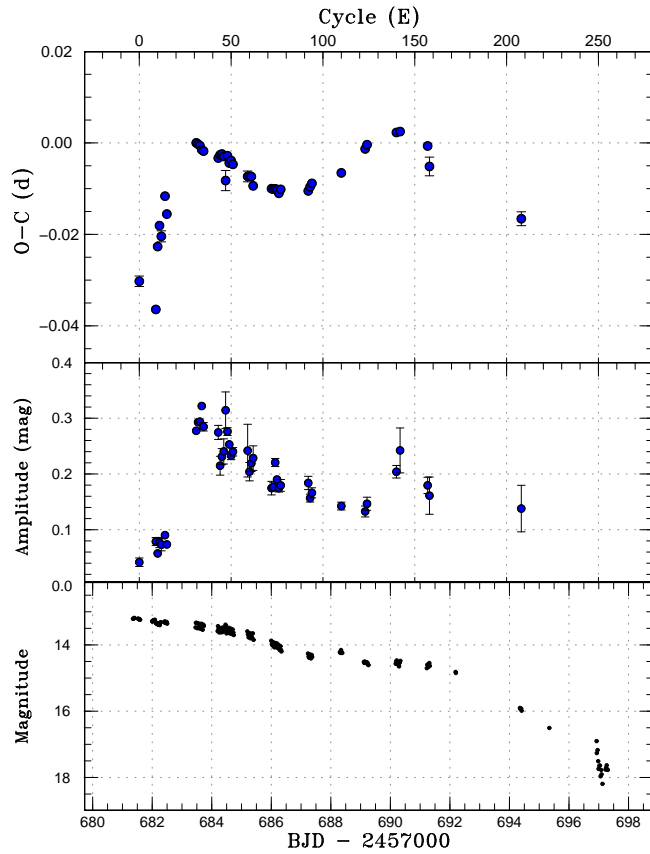


Fig. 55. $O - C$ diagram of superhumps in TCP J013758 (2016). (Upper:) $O - C$ diagram. We used a period of 0.06169 d for calculating the $O - C$ residuals. (Middle:) Amplitudes of superhumps. (Lower:) Light curve. The data were binned to 0.021 d.

3.126 TCP J01375892+4951055

This object (hereafter TCP J013758) was discovered by K. Itagaki at an unfiltered CCD magnitude of 13.2 on 2016 October 19.²¹ There is a blue SDSS counterpart ($g=19.85$ and $u - g=0.15$) and also a GALEX UV counterpart. The object was suspected to be a dwarf nova. Subsequent observations detected growing superhumps (vsnet-alert 20238). Superhumps with a stable period were observed 2 d after the discovery (vsnet-alert 20242, 20268; e-figure 106). The times of superhump maxima are listed in e-table 112. The data show clear stages A–C, with a positive P_{dot} for stage B characteristic to this short P_{SH} (figure 55). The period of stage A superhumps was not very well determined due to a gap around the stage A–B transition. The behavior suggests a typical SU UMa-type dwarf nova.

²¹<<http://www.cbat.eps.harvard.edu/unconf/followups/J01375892+4951055.html>>.

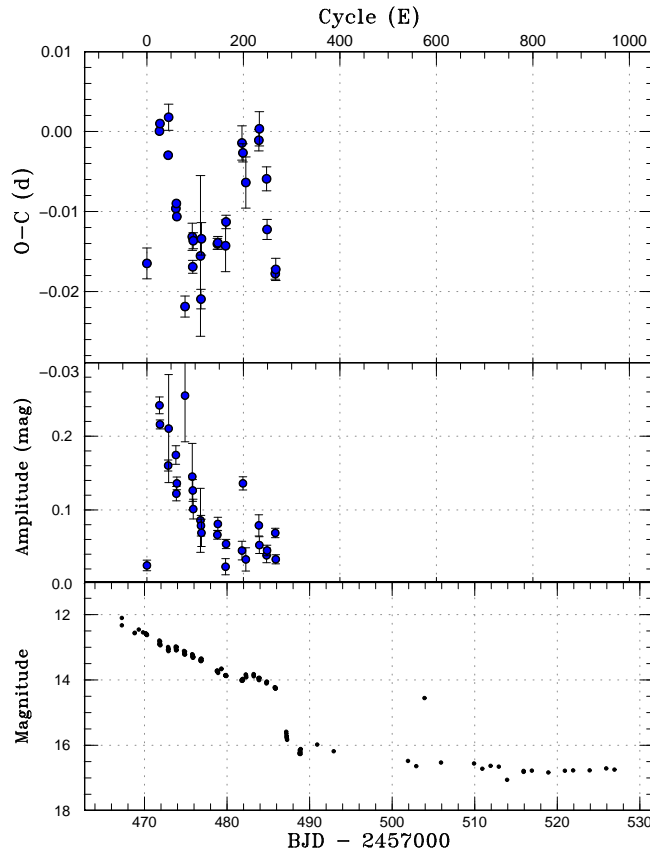


Fig. 56. $O - C$ diagram of superhumps in TCP J180018 (2016). (Upper:) $O - C$ diagram. We used a period of 0.05844 d for calculating the $O - C$ residuals. (Middle:) Amplitudes of superhumps. (Lower:) Light curve. The data were binned to 0.019 d.

3.127 TCP J18001854–3533149

This object (hereafter TCP J180018) was discovered as a transient by K. Nishiyama and F. Kabashima at an unfiltered CCD magnitude of 12.2 on March 16.²² Multicolor photometry by S. Kiyota showed a blue color, suggesting a dwarf nova-type outburst. A spectroscopic study by K. Ayani on March 20 showed Balmer absorption lines ($H\beta$ to $H\delta$). The $H\alpha$ line was not clear probably because the absorption is filled with the emission. The spectrum indicated a dwarf nova in outburst. Subsequent observations detected superhumps (vsnet-alert 19635, 19646, 19662, 19684, 19703; e-figure 107). The times of superhump maxima are listed in e-table 113. There were clear stages A–C, with a positive P_{dot} for stage B, characteristic to a short- P_{SH} SU UMa-type dwarf nova (figure 56).

The outburst faded on April 8 and the duration of the total outburst was at least 23 d. The object showed a single post-superoutburst rebrightening on April 25 at 14.5 mag (figure 56).

²²<<http://www.cbat.eps.harvard.edu/unconf/followups/J18001854-3533149.html>>.

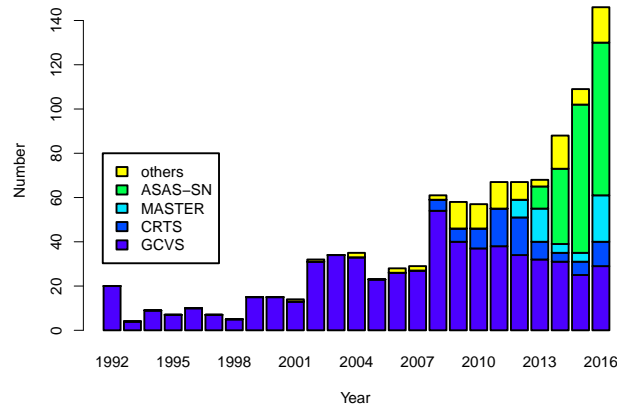


Fig. 57. Object categories in our survey. Superoutbursts with measured superhump periods are included. The year represents the year of outburst. The year 1992 represents outbursts up to 1992 and the year 2016 includes the outbursts in 2017, respectively. The category GCVS includes the objects named in the General Catalog of Variable Stars Kholopov et al. (1985) in the latest version and objects named in New Catalog of Suspected Variable Stars (NSV: Kukarkin et al. 1982). The categories CRTS, MASTER, ASAS-SN represent objects which were discovered in respective surveys. A fraction of objects discovered by these surveys are already named in GCVS and are included in the category GCVS.

4 Discussion

4.1 Statistics of objects

Following Kato et al. (2015a) and Kato et al. (2016a), we present statistics of sources of the objects studied in our surveys (figure 57). Although ASAS-SN CVs remained the majority of the objects we studied, there have also been an increase in MASTER CVs and CRTS CVs. The noteworthy recent tendency is the increase of objects in the Galactic plane discovered by ASAS-SN. This region had usually been avoided by the majority of surveys (the best examples being SDSS and CRTS) and we can expect a great increase of dwarf novae if the Galactic plane is thoroughly surveyed by ASAS-SN. This increase of CV candidates in the Galactic plane, however, has made it difficult to distinguish dwarf novae and classical novae. Indeed, there have been four Galactic novae discovered by the ASAS-SN team: ASASSN-16ig = V5853 Sgr (Stanek et al. 2016a; Williams, Darnley 2016), ASASSN-16kb (Prieto et al. 2016), ASASSN-16kd (Stanek et al. 2016c; Bohlsen 2016), and ASASSN-16ma = V5856 Sgr (Stanek et al. 2016b; Luckas 2016) in 2016. Several dwarf novae studied in this paper were also flagged as “could also be a nova” on the ASAS-SN Transients page. Some objects in this paper (ASASSN-16jb and ASASSN-16ow) were initially suspected to be Galactic novae. Although they have not been a serious problem in studying dwarf novae, the supposed nova classification might cause a delay in time-resolved photometry to detect superhumps in the earliest phase, and observers should keep in mind the dwarf nova-type possibilities of nova candidate in the Galactic plane.

Table 11. Ephemerides of eclipsing systems.

Object	Epoch (BJD)	Period (d)
OY Car	2457120.49413(2)	0.0631209131(5)
GP CVn	2455395.37115(4)	0.0629503676(9)
V893 Sco	2454173.3030(3)	0.0759614600(16)
MASTER J220559	2457658.72016(3)	0.0612858(3)
SDSS J115207	2457578.07695(6)	0.0677497014(14)

4.2 Period distribution

In figure 58, we give distributions of superhump and estimated orbital periods (see the caption for details) since Kato et al. (2009). For readers' convenience, we also listed ephemerides of eclipsing systems newly determined or used in this study in table 11. When there are multiple observations of superoutbursts of the same object, we adopted an average of the measurements. This figure can be considered to be a good representation of the distribution of orbital periods for non-magnetic CVs below the period gap, since the majority of CVs below the period gap are SU UMa-type dwarf novae. The following features reported in Kato et al. (2016a) are apparent: (1) the sharp cut-off at a period of 0.053 d and (2) accumulation of objects ("period spike") just above the cutoff.

We determined the location of the sharp cut-off (period minimum) by using the Bayesian approach. We assumed the following period distribution $D(P_{\text{orb}})$:

$$D(P_{\text{orb}}) \propto \begin{cases} c_1, & (P_{\text{orb}} \leq P_{\text{min}}) \\ 1/(P_{\text{orb}} - c_2), & (P_{\text{orb}} > P_{\text{min}}). \end{cases} \quad (6)$$

P_{min} is the cut-off and c_1, c_2 are parameters to be determined. We defined the likelihood to obtain the entire sample of our SU UMa-type dwarf novae by using this distribution (the distribution is normalized for a range of 0.01–0.13 d). We obtained the parameters by the MCMC method as follows: $c_1 = 1.93(25)$, $c_2 = 0.0471(7)$ and $P_{\text{min}} = 0.052897(16)$. The value of P_{min} is insensitive to the functional form above P_{min} . The resulting distribution is drawn as a line in the lower panel of figure 58.

Although the model does not properly reproduce the location of the period spike, the numbers of dwarf novae are lower than the best fit curve above $P_{\text{orb}} \sim 0.09$ d. This appears to correspond to the period gap, contrary to our finding in Kato et al. (2016a).

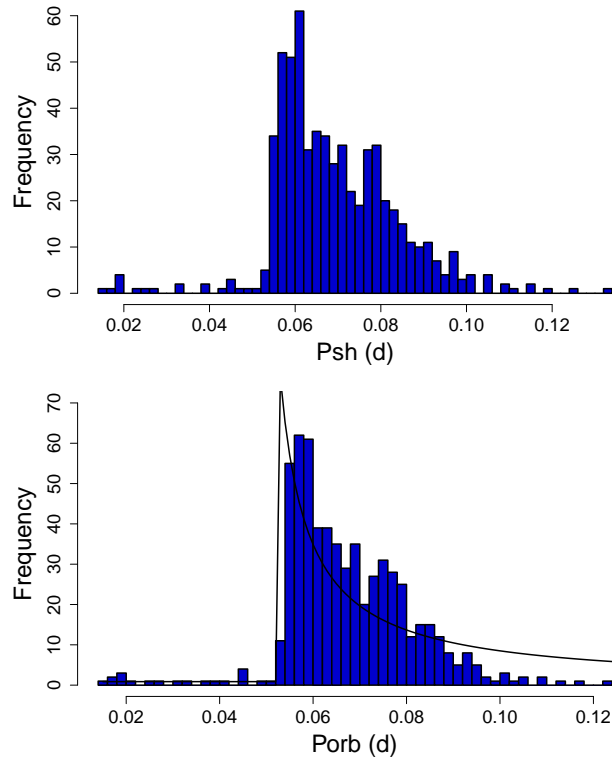


Fig. 58. Distribution of superhump periods in this survey. The data are from Kato et al. (2009), Kato et al. (2010), Kato et al. (2012a), Kato et al. (2013), Kato et al. (2014b), Kato et al. (2014a), Kato et al. (2015a), Kato et al. (2016a) and this paper. The mean values are used when multiple superoutbursts were observed. (Upper) distribution of superhump periods. (Lower) distribution of orbital periods. For objects with superhump periods shorter than 0.053 d, the orbital periods were assumed to be 1% shorter than superhump periods. For objects with superhump periods longer than 0.053 d, we used the calibration in Kato et al. (2012a) to estimate orbital periods. The line is the model distribution to determine the period minimum (equation 6, see text for the details).

4.3 Period derivatives during stage B

Figure 59 represents updated relation between P_{dot} for stage B versus P_{orb} . We have omitted poor quality observation (quality C) since Kato et al. (2016a) and simplified the symbols. The majority of new objects studied in this paper follow the trend presented in earlier papers.

4.4 Mass ratios from stage A superhumps

We list new estimates for q from stage A superhumps (Kato, Osaki 2013) in table 12. This table includes measurements of the objects in separate papers, which are listed in table 1. In table 13, we list all stage A superhumps recorded in the present study.

An updated distribution of mass ratios is shown in figure 60 [for the list of objects, see Kato, Osaki (2013), Kato et al. (2015a) and Kato et al. (2016a)]. We have newly added SDSS J105754.25+275947.5 (hereafter SDSS J105754) with $P_{\text{orb}}=0.062792$ d and $q=0.0546(20)$ (McAllister et al. 2017b, eclipse observation) and ASASSN-14ag with $P_{\text{orb}}=0.060311$ d and

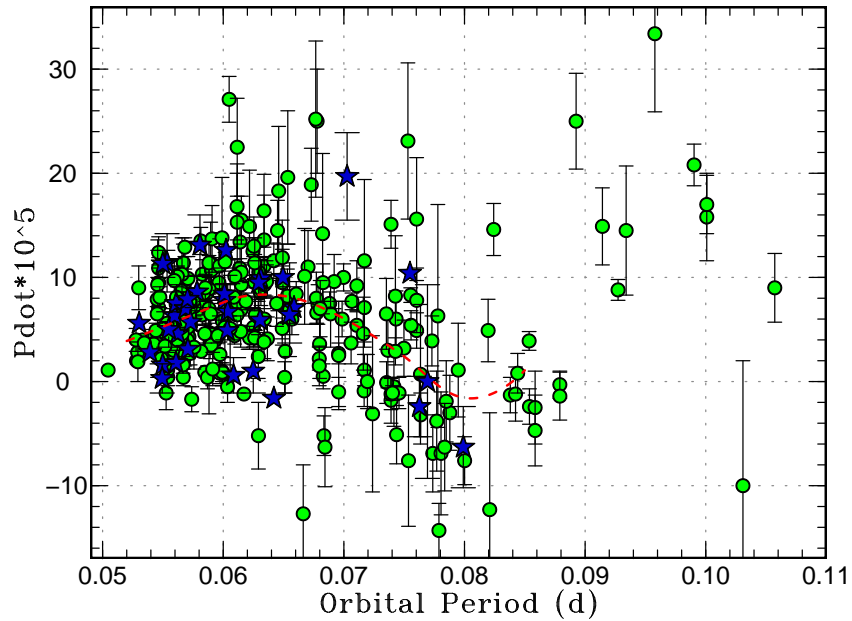


Fig. 59. $P_{\dot{\text{orb}}}$ for stage B versus P_{orb} . Filled circles and filled stars represent samples in Kato et al. (2009)–Kato et al. (2016a) and this paper, respectively. The curve represents the spline-smoothed global trend.

$q=0.149(16)$ (McAllister et al. 2017a, eclipse observation). It would be worth mentioning that McAllister et al. (2017b) classified SDSS J105754 as a period bouncer and we have two objects (ASASSN-16dt and ASASSN-16js) near the location of SDSS J105754. Both objects are likely identified as period bouncers and these detections demonstrate the efficiency of the stage A superhump method. The present study has strengthened the concentration of WZ Sge-type dwarf novae around $q = 0.07$ just above the period minimum, as reported in Kato et al. (2015a) and Kato et al. (2016a).

4.5 WZ Sge-type objects

WZ Sge-type dwarf novae are a subclass of SU UMa-type dwarf novae characterized by the presence of early superhumps (Kato et al. 1996a; Kato 2002; Ishioka et al. 2002; see a recent review Kato 2015). They are seen during the earliest stages of a superoutburst, and have period almost equal to the orbital periods.

These early superhumps are considered to be a result of the 2:1 resonance (Osaki, Meyer 2002). These objects usually show very rare outbursts (once in several years to decades) with large outburst amplitudes (6–9 mag or even more, Kato 2015) and often have complex light curves (Kato 2015). The WZ Sge-type dwarf novae are of special astrophysical interest for several reasons. We list two of them: (1) From the point of view of outburst physics, the origin of the complex light curves, including repetitive rebrightenings, is not

Table 12. New estimates for the binary mass ratio from stage A superhumps

Object	e^* (stage A)	q from stage A
HT Cas	0.0566(5)	0.171(2)
GS Cet	0.0288(8)	0.078(2)
GZ Cnc	0.081(3)	0.27(2)
IR Gem	0.068(11)	0.22(4)
HV Vir	0.034(1)	0.093(3)
ASASSN-16da	0.042(2)	0.12(1)
ASASSN-16dt	0.0135(7)	0.036(2)
ASASSN-16eg	0.0552(6)	0.166(2)
ASASSN-16hj	0.034(7)	0.09(2)
ASASSN-16iw	0.029(1)	0.079(2)
ASASSN-16jb	0.0321(5)	0.088(1)
ASASSN-16js	0.0213(16)	0.056(5)
ASASSN-16oi	0.033(2)	0.091(7)
ASASSN-16os	0.018(1)	0.047(3)
ASASSN-17bl	0.0235(9)	0.062(3)

well understood. They are also considered to be analogous to black-hole X-ray transients which often show rebrightenings (cf. Kuulkers et al. 1996) and there may be common underlying physics between WZ Sge-type dwarf novae and black-hole X-ray transients. (2) From the point of view of CV evolution, they are considered to represent the terminal stage of CV evolution and they may have brown-dwarf secondaries. Studies of WZ Sge-type dwarf novae are indispensable when discussing the terminal stage of CV evolution, such as the period minimum and period bouncers (e.g. Knigge 2006; Knigge et al. 2011; Patterson 2011; Kato 2015). We used the period of early superhumps as the approximate orbital period (Kato et al. 2014a; Kato 2015; labeled as ‘E’ in table 3). In table 14, we list the parameters of WZ Sge-type dwarf novae (including likely ones).

It has been known that P_{dot} and P_{orb} are correlated with the rebrightening type [starting with figure 36 in Kato et al. 2009 and refined in Kato et al. (2009)–Kato et al. (2015a) and Kato (2015), and updated in Kato et al. (2016a)]. The five types of outbursts based on rebrightenings are: type-A outbursts [long-duration rebrightening; we include type-A/B introduced in Kato (2015)], type-B outbursts (multiple rebrightenings), type-C outbursts (sin-

Table 13. Superhump Periods during Stage A

Object	Year	period (d)	err
BB Ari	2016	0.07514	0.00007
HT Cas	2016	0.07807	0.00004
GS Cet	2016	0.05763	0.00027
GZ Cnc	2017	0.09599	–
V1113 Cyg	2016	0.08030	0.00018
IR Gem	2017	0.07315	0.00000
HV Vir	2016	0.05824	0.00001
ASASSN-13ak	2016	0.08884	0.00047
ASASSN-15cr	2017	0.06258	0.00014
ASASSN-16da	2016	0.05858	0.00010
ASASSN-16ds	2016	0.06856	0.00015
ASASSN-16dt	2016	0.06512	0.00001
ASASSN-16eg	2016	0.07989	0.00004
ASASSN-16hj	2016	0.05691	0.00031
ASASSN-16ib	2016	0.06036	0.00007
ASASSN-16ik	2016	0.06656	0.00010
ASASSN-16iw	2016	0.06691	0.00012
ASASSN-16jb	2016	0.06514	0.00003
ASASSN-16jd	2016	0.05840	0.00012
ASASSN-16js	2016	0.06165	0.00010
ASASSN-16ob	2016	0.05785	0.00016
ASASSN-16oi	2016	0.05738	0.00009
ASASSN-16os	2016	0.05596	0.00006
ASASSN-17bl	2017	0.05599	0.00004
CRTS J164950	2015	0.06641	0.00006
MASTER J021315	2016	0.10712	0.00025
MASTER J030205	2016	0.06275	0.00015
OT J002656	2016	0.13320	0.00003
TCP J013758	2016	0.06290	0.00056

Table 14. Parameters of WZ Sge-type superoutbursts.

Object	Year	P_{SH}^*	P_{orb}^\dagger	P_{dot}^\ddagger	err^\ddagger	ϵ	Type [§]	N_{reb}^\parallel	delay [#]	Max	Min
GS Cet	2016	0.056645	0.05597	6.3	0.6	0.012	–	–	8	13.0	20.4
ASASSN-16da	2016	0.057344	0.05610	7.5	0.9	0.022	–	–	5	15.1	21.5
ASASSN-16dt	2016	0.064507	0.064197	–1.6	0.5	0.005	E+C	2	23	13.4	21.1:
ASASSN-16eg	2016	0.077880	0.075478	10.4	0.8	0.032	C	1	6	12.7	19.4
ASASSN-16fu	2016	0.056936	0.05623	4.6	0.6	0.013	–	–	6	13.9	21.6
ASASSN-16gh	2016	0.061844	–	6.7	2.7	–	–	–	12	14.3	[22
ASASSN-16gj	2016	0.057997	–	7.0	1.0	–	A:	1	≤ 9]13.3	21.3
ASASSN-16hg	2016	0.062371	–	0.6	1.7	–	A:	1	≥ 6]14.1	21.6:
ASASSN-16hj	2016	0.055644	0.05499	11.3	1.3	0.012	A+B?	3	9	14.2	21.1:
ASASSN-16ia	2016	–	0.05696	–	–	–	–	–	–	14.6	[22
ASASSN-16is	2016	0.058484	0.05762	4.2	1.7	0.015	–	–	11	14.9	20.4
ASASSN-16iw	2016	0.065462	0.06495	10.0	3.2	0.008	B	5	7	13.9	21.9
ASASSN-16jb	2016	0.064397	0.06305	5.9	0.7	0.021	–	–	7	13.3	[21
ASASSN-16js	2016	0.060934	0.06034	4.9	1.0	0.010	–	–	10	13.0	20.1
ASASSN-16lo	2016	0.054608	0.05416	–	–	0.008	–	–	11	14.3	20.7:
ASASSN-16ob	2016	0.057087	–	1.8	0.5	–	–	–	13	13.8	[22
ASASSN-16oi	2016	0.056241	0.05548	5.0	1.7	0.014	–	–	8	13.4	22.0:
ASASSN-16os	2016	0.054992	0.05494	0.3	1.4	0.001	–	–	8	13.6	21.4:
ASASSN-17aa	2017	0.054591	0.05393	2.8	0.3	0.012	–	–	9	13.9	[22
ASASSN-17bl	2017	0.055367	0.05467	3.6	0.6	0.013	–	–	11	13.7	[22
ASASSN-17cn	2017	0.053991	0.05303	5.6	0.8	0.018	–	–	≥ 9	13.2	[22

*Representative value (P_1).

[†]Period of early superhumps.

[‡]Unit 10^{-5} .

[§]A: long-lasting rebrightening; B: multiple rebrightenings; C: single rebrightening; D: no rebrightening.

^{||}Number of rebrightenings.

[#]Days before ordinary superhumps appeared.

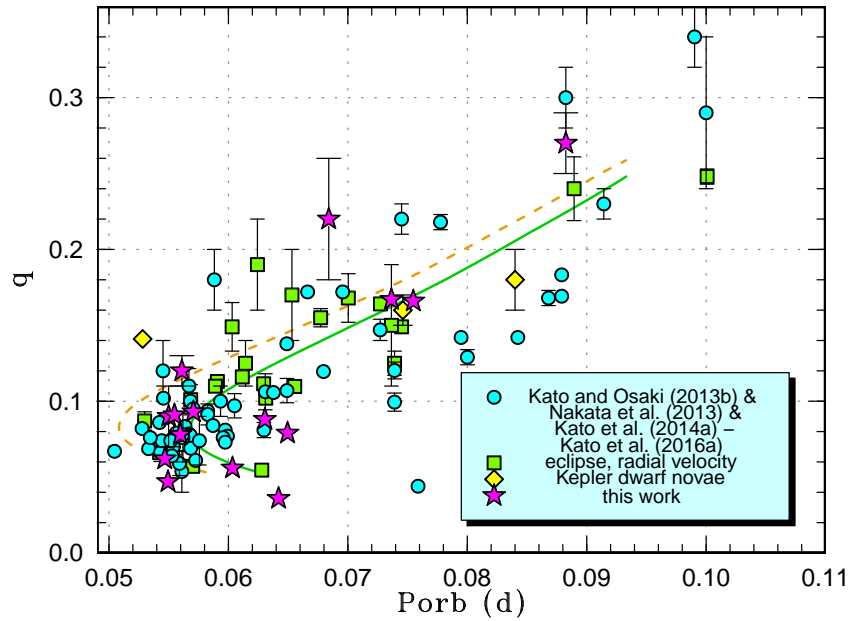


Fig. 60. Mass ratio versus orbital period. The dashed and solid curves represent the standard and optimal evolutionary tracks in Knigge et al. (2011), respectively. The filled circles, filled squares, filled stars, filled diamonds represent q values from a combination of the estimates from stage A superhumps published in four preceding sources (Kato, Osaki 2013; Nakata et al. 2013; Kato et al. 2014b; Kato et al. 2014a; Kato et al. 2015a; Kato et al. 2016a and references therein), known q values from quiescent eclipses or radial-velocity study, q estimated in this work and dwarf novae in the Kepler data (see text for the reference), respectively. The objects in “this work” includes objects studied in separate papers but listed in table 1.

gle rebrightening), type-D outbursts (no rebrightening) and type-E outbursts (double super-outburst, with ordinary superhumps only during the second one). In figure 61, we show the updated result up to this paper. In this figure, we also added objects without known rebrightening types. These objects have been confirmed to follow the same trend, which we consider to represent the evolutionary track [see subsection 7.6 in Kato (2015)]. The outlier around $P_{\text{orb}}=0.050$ d is ASASSN-15po, the object below the period minimum (Namekata et al. 2017). The two points around $P_{\text{orb}}=0.079$ d is RZ Leo. As shown in subsection 3.17 in Kato et al. (2016a), the two superoutbursts in 2000 and 2016 were not sufficiently covered and P_{dot} values had large errors and we consider that these points are not very reliable.

4.6 Objects with Very Short Supercycles

In this study, there were a group of four object with very short supercycles: NY Her [supercycle 63.5(2) d, subsection 3.14], 1RXS J161659 [89(1) d, subsection 3.27], CRTS J033349 [108(1) d, subsection 3.90] and SDSS J153015 [84.7(1.2) d, subsection 3.123]. We are not aware whether such a large number of detections were by chance or as a result of the recent change in detection policies of transients such as ASAS-SN. The most notable common features of

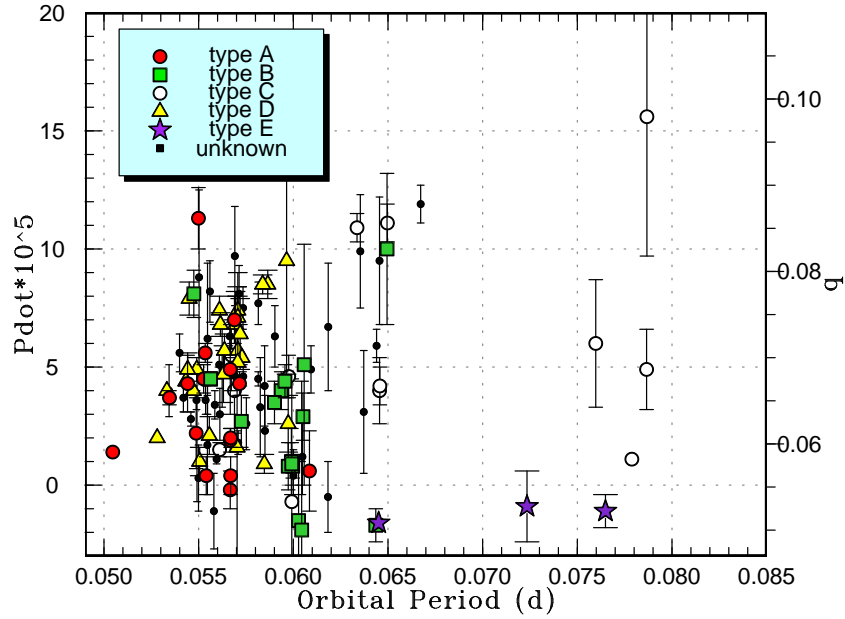


Fig. 61. P_{dot} versus P_{orb} for WZ Sge-type dwarf novae. Symbols represent the type of outburst: type-A (filled circles), type-B (filled squares), type-C (filled triangles), type-D (open circles) and type-E (filled stars) (see text for details). On the right side, we show mass ratios estimated using equation (6) in Kato (2015). We can regard this figure as to represent an evolutionary diagram.

these objects are the small number of normal outbursts. Since the short supercycle reflects the high mass-transfer rate (cf. Osaki 1996), the small number of normal outbursts is unexpected.

A likely solution to this apparent inconsistency is the disk tilt, which would prevent the accreted matter accumulating in the outer edge of the disk and it would suppress normal outbursts (Ohshima et al. 2012; Osaki, Kato 2013a; Osaki, Kato 2013b). It has been also demonstrated that the prototypical example V503 Cyg (supercycle 89 d) showed negative superhumps (Harvey et al. 1995), which are considered to be a consequence of a disk tilt (e.g. Wood, Burke 2007; Montgomery, Bisikalo 2010). The temporary emergence of frequent normal outbursts in V503 Cyg (Kato et al. 2002b) also suggests that normal outbursts were somehow suppressed, most likely by a disk tilt. More recent examples in Kepler dwarf novae V1504 Cyg and V344 Lyr in relation to transiently appearing negative superhumps were discussed in Osaki, Kato (2013a), Osaki, Kato (2013b) and it has become more evident that the state with negative superhumps (i.e. the disk is likely tilted) is associated with the reduced number of normal outbursts.

It has been proposed that a high mass-transfer rate is prone to produce a disk tilt in a hydrodynamical model (Montgomery, Martin 2010). If it is indeed the case, the large number of SU UMA-type dwarf novae with few normal outbursts but with short supercycles

may be a result of easy occurrence of a disk tilt in high-mass transfer systems and may not be surprising. A search for negative superhumps in the four systems reported in this paper is recommended. Long-term monitoring is also encouraged to see whether these objects switch the outburst mode as in V503 Cyg.

We should make a comment on another SU UMa-type dwarf nova V4140 Sgr with a short supercycle (80–90 d, Borges, Baptista 2005). Borges, Baptista (2005) and Baptista et al. (2016) used the eclipse mapping method and derived a conclusion that the distribution of the disk temperature in quiescence is incompatible with the disk-instability model and they interpreted that the outbursts in this object are caused by mass-transfer bursts from the secondary. We noticed that, despite its short supercycle, this object rarely shows normal outbursts (for example, there were no outburst between 2017 March 12 and April 16, observations by J. Hambusch). The object appears to be a V503 Cyg-like one and we can expect a disk tilt. The apparent deviation of the distribution of the disk temperature may have been caused by an accretion stream hitting the inner parts of the disk when the disk is tilted and may not be contradiction with the picture of the disk-instability model. Since no other V503 Cyg-like objects are eclipsing, we have had no observation about the structure of the disk in V503 Cyg-like objects. We propose to study V4140 Sgr more closely for detecting negative superhumps, and searching for a switch in the outburst mode to test the possibility of the V503 Cyg-like nature.

5 Summary

We provided updated statistics of the period distribution. We obtained the period minimum of 0.05290(2) d and confirmed the presence of the period gap above $P_{\text{orb}} \sim 0.09$ d. We refined the $P_{\text{orb}}-P_{\text{dot}}$ relation of SU UMa-type dwarf novae, the updated evolutionary track using stage A superhumps and refined relationship between $P_{\text{orb}}-P_{\text{dot}}$ versus the rebrightening type in WZ Sge-type dwarf novae. We also provide basic observational data of superoutbursts we studied for SU UMa-type dwarf novae.

The objects of special interest in this paper can be summarized as follows:

- Four objects (NY Her, 1RXS J161659, CRTS J033349 and SDSS J153015) have supercycles shorter than 100 d. These objects do not resemble ER UMa-type dwarf novae but show infrequent normal outbursts as in V503 Cyg. We consider that these properties may be caused by a tilted disk and we expect to detect negative superhumps in these systems.
- DDE 48 is likely an ER UMa-type dwarf nova. NSV 2026 also has a short supercycle but

with frequent normal outbursts.

- ASASSN-16ia and ASASSN-16js are WZ Sge-type dwarf novae with large-amplitude early superhumps.
- ASASSN-16ia showed a precursor outburst prior to the WZ Sge-type superoutburst. This is the first certain case of such a precursor outburst in a WZ Sge-type superoutburst.
- ASASSN-16js has a low mass ratio and is most likely a period bouncer. ASASSN-16gh is also a candidate for a period bouncer.
- ASASSN-16iw is a WZ Sge-type dwarf nova with five post-superoutburst rebrightenings.
- MASTER J021315 is located in the period gap. This object likely showed long-lasting phase of stage A. Outbursts in this system were relatively rare and it should have a low mass-transfer rate.
- ASASSN-16kg, ASASSN-16ni, CRTS J000130 and SDSS J113551 are also SU UMa-type dwarf novae in the period gap. ASASSN-16ni is possibly an SU UMa-type dwarf nova in or above the period gap.
- ASASSN-16kg and ASASSN-16ni have large outburst amplitudes. ASASSN-16kg showed a rebrightening. These properties are uncommon among dwarf novae in the period gap.
- MASTER J030205 showed a likely spin period and it is likely a rare intermediate polar among SU UMa-type dwarf novae.
- Five objects OY Car, GP CVn, V893 Sco, MASTER J220559 and SDSS J115207 are eclipsing and we present refined eclipse ephemerides for some of them.

Acknowledgements

This work was supported by the Grant-in-Aid “Initiative for High-Dimensional Data-Driven Science through Deepening of Sparse Modeling” (25120007) from the Ministry of Education, Culture, Sports, Science and Technology (MEXT) of Japan. This work was also partially supported by Grant VEGA 2/0008/17 and APVV-15-0458 (by Shugarov, Chochol, Sekeráš), NSh-9670.2016.2 (Voloshina, Katysheva) RFBR 17-52-175300 (Voloshina), RSF-14-12-00146 (Golysheva for processing observations data from Slovak Observatory) and APVV-15-0458 (Dubovsky, Kudzej). ASAS-SN is supported by the Gordon and Betty Moore Foundation through grant GBMF5490 to the Ohio State University and NSF grant AST-1515927. The authors are grateful to observers of VSNET Collaboration and VSOLJ observers who supplied vital data. We acknowledge with thanks the variable star observations from the AAVSO International Database contributed by observers worldwide and used in this research. We

are also grateful to the VSOLJ database. This work is helped by outburst detections and announcement by a number of variable star observers worldwide, including participants of CVNET and BAA VSS alert. The CCD operation of the Bronberg Observatory is partly sponsored by the Center for Backyard Astrophysics. We are grateful to the Catalina Real-time Transient Survey team for making their real-time detection of transient objects and the past photometric database available to the public. We are also grateful to the ASAS-3 team for making the past photometric database available to the public. This research has made use of the SIMBAD database, operated at CDS, Strasbourg, France. This research has made use of the International Variable Star Index (VSX) database, operated at AAVSO, Cambridge, Massachusetts, USA.

Supporting information

Additional supporting information can be found in the online version of this article: Tables. Figures.

Supplementary data is available at PASJ Journal online.

References

- Ahn, C. P., et al. 2012, *ApJS*, 203, 21
- Antipin, S. V. 1999, *IBVS*, 4673, 1
- Arenas, J., & Mennickent, R. E. 1998, *A&A*, 337, 472
- Balanutsa, P., Denisenko, D., Gorbovskoy, E., & Lipunov, V. 2013, *Perem. Zvezdy*, submitted (arXiv/1307.7396)
- Balanutsa, P., et al. 2014, *Astron. Telegram*, 5787
- Balanutsa, P., et al. 2016a, *Astron. Telegram*, 9174
- Balanutsa, P., et al. 2016b, *Astron. Telegram*, 9824
- Baptista, R., Borges, B. W., & Oliveira, A. S. 2016, *MNRAS*, 463, 3799
- Barwig, H., Mantel, K. H., & Ritter, H. 1992, *A&A*, 266, L5
- Belyavskii, S. I. 1936, *Perem. Zvezdy*, 5, 36
- Bernhard, K., Lloyd, C., Berthold, T., Kriebel, W., & Renz, W. 2005, *IBVS*, 5620, 1
- Bohlsen, T. 2016, *Astron. Telegram*, 9477
- Bond, H. E. 1978, *PASP*, 90, 526
- Borges, B. W., & Baptista, R. 2005, *A&A*, 437, 235

- Boyce, E. H. 1942, *Annals of the Astron. Obs. of Harvard Coll.* 109, 11
- Boyd, D., Krajci, T., Shears, J., & Poyner, G. 2007, *J. Br. Astron. Assoc.*, 117, 198
- Bruch, A., Steiner, J. E., & Gneiding, C. D. 2000, *PASP*, 112, 237
- Burenkov, A. N., & Voikhanskaia, N. F. 1979, *Soviet Astronomy Letters*, 5, 452
- Cleveland, W. S. 1979, *J. Amer. Statist. Assoc.*, 74, 829
- Coppejans, D. L., K rding, E. G., Knigge, C., Pretorius, M. L., Woudt, P. A., Groot, P. J., Van Eck, C. L., & Drake, A. J. 2016, *MNRAS*, 456, 4441
- Cutri, R. M., et al. 2003, 2MASS All Sky Catalog of point sources (NASA/IPAC Infrared Science Archive)
- Davis, A. B., Shappee, B. J., Archer Shappee, B., & ASAS-SN 2015, *American Astron. Soc. Meeting Abstracts*, 225, #344.02
- Denisenko, D., et al. 2013a, *Astron. Telegram*, 5643
- Denisenko, D., et al. 2012, *Astron. Telegram*, 4441
- Denisenko, D., et al. 2013b, *Astron. Telegram*, 5182
- Denisenko, D. V. 2012, *Astron. Lett.*, 38, 249
- Drake, A. J., et al. 2009, *ApJ*, 696, 870
- Drake, A. J., et al. 2014, *MNRAS*, 441, 1186
- Drake, A. J., Mahabal, A., Djorgovski, S. G., Graham, M. J., Williams, R., Beshore, E. C., Larson, S. M., & Christensen, E. 2008, *Astron. Telegram*, 1479
- Duerbeck, H. W. 1984, *IBVS*, 2502
- Duerbeck, H. W. 1987, *Space Sci. Rev.*, 45, 1
- Echeistov, V., et al. 2014, *Astron. Telegram*, 5898
- Feinswog, L., Szkody, P., & Garnavich, P. 1988, *AJ*, 96, 1702
- Fernie, J. D. 1989, *PASP*, 101, 225
- Gaia Collaboration 2016, *VizieR Online Data Catalog*, 1337
- Gorbovskoy, E. S., et al. 2013, *Astron. Rep.*, 57, 233
- Gress, O., et al. 2017, *Astron. Telegram*, 61
- Hameury, J.-M., & Lasota, J.-P. 2017, *A&A*, in press (arXiv/1703.03563)
- Han, Z.-T., Qian, S.-B., Fern andez Laj us, E., Liao, W.-P., & Zhang, J. 2015, *New Astron.*, 34, 1
- Harvey, D., Skillman, D. R., Patterson, J., & Ringwald, F. A. 1995, *PASP*, 107, 551
- Hirose, M., & Osaki, Y. 1990, *PASJ*, 42, 135
- Hirose, M., & Osaki, Y. 1993, *PASJ*, 45, 595
- Hoffleit, D. 1935, *Harvard Coll. Obs. Bull.*, 901, 20
- Hoffmeister, C. 1949, *Erg. Astron. Nachr.*, 12, 12

Hoffmeister, C. 1964, *Astron. Nachr.*, 288, 49
Hoffmeister, C. 1966, *Astron. Nachr.*, 289, 139
Howell, S. B., Szkody, P., Kreidl, T. J., Mason, K. O., & Puchnarewicz, E. M. 1990, *PASP*, 102, 758
Imada, A., et al. 2009, *PASJ*, 61, L17
Imada, A., et al. 2006, *PASJ*, 58, 143
Ishioka, R., Kato, T., Uemura, M., Iwamatsu, H., Matsumoto, K., Martin, B. E., Billings, G. W., & Novak, R. 2001, *PASJ*, 53, L51
Ishioka, R., et al. 2003, *PASJ*, 55, 683
Ishioka, R., Sekiguchi, K., & Maehara, H. 2007, *PASJ*, 59, 929
Ishioka, R., et al. 2002, *A&A*, 381, L41
Kapusta, A. B., & Thorstensen, J. R. 2006, *PASP*, 118, 1119
Kato, T. 1994, *IBVS*, 4136
Kato, T. 2001, *IBVS*, 5122
Kato, T. 2002, *PASJ*, 54, L11
Kato, T. 2015, *PASJ*, 67, 108
Kato, T., et al. 2014a, *PASJ*, 66, 90
Kato, T., et al. 2015a, *PASJ*, 67, 105
Kato, T., et al. 2002a, *A&A*, 396, 929
Kato, T., et al. 2013, *PASJ*, 65, 23
Kato, T., et al. 2014b, *PASJ*, 66, 30
Kato, T., et al. 2016a, *PASJ*, 68, 65
Kato, T., Hambsch, F.-J., Oksanen, A., Starr, P., & Henden, A. 2015b, *PASJ*, 67, 3
Kato, T., Hanson, G., Poyner, G., Muyliaert, E., Reszelski, M., & Dubovsky, P. A. 2000, *IBVS*, 4932
Kato, T., Haseda, K., Takamizawa, K., Kazarovets, E. V., & Samus, N. N. 1998, *IBVS*, 4585
Kato, T., et al. 2009, *PASJ*, 61, S395
Kato, T., Ishioka, R., & Uemura, M. 2002b, *PASJ*, 54, 1029
Kato, T., & Kunjaya, C. 1995, *PASJ*, 47, 163
Kato, T., et al. 2012a, *PASJ*, 64, 21
Kato, T., Maehara, H., & Uemura, M. 2012b, *PASJ*, 64, 62
Kato, T., et al. 2010, *PASJ*, 62, 1525
Kato, T., Nogami, D., Baba, H., Matsumoto, K., Arimoto, J., Tanabe, K., & Ishikawa, K. 1996a, *PASJ*, 48, L21
Kato, T., Nogami, D., Masuda, S., & Hirata, R. 1996b, *PASJ*, 48, 45
Kato, T., & Osaki, Y. 2013, *PASJ*, 65, 115

- Kato, T., et al. 2016b, PASJ, 68, L4
- Kato, T., Sekine, Y., & Hirata, R. 2001, PASJ, 53, 1191
- Kato, T., Stubbings, R., Pearce, A., Nelson, P., & Monard, B. 2001a, IBVS, 5119, 1
- Kato, T., et al. 2017, PASJ, in press (arXiv/1703.00650)
- Kato, T., Uemura, M., Buczynski, D., & Schmeer, P. 2001b, IBVS, 5123
- Kato, T., Uemura, M., Ishioka, R., Nogami, D., Kunjaya, C., Baba, H., & Yamaoka, H. 2004, PASJ, 56, S1
- Kholopov, P. N., et al. 1985, General Catalogue of Variable Stars, fourth edition (Moscow: Nauka Publishing House)
- Kimura, M., et al. 2017, PASJ, submitted
- Kimura, M., et al. 2016, PASJ, 68, L2
- Knigge, C. 2006, MNRAS, 373, 484
- Knigge, C., Baraffe, I., & Patterson, J. 2011, ApJS, 194, 28
- Kukarkin, B. V., et al. 1982, New Catalogue of Suspected Variable Stars (Moscow: Nauka Publishing House)
- Kuulkers, E., Howell, S. B., & van Paradijs, J. 1996, ApJ, 462, L87
- Lasker, B., Lattanzi, M. G., McLean, B. J., & et al. 2007, VizieR Online Data Catalog, 1305
- Lazaro, C., Martinez-Pais, I. G., Arevalo, M. J., & Solheim, J. E. 1991, AJ, 101, 196
- Lázaro, C., Martinez-Pais, I. G., Solheim, J. E., & Arévalo, M. J. 1990, Ap&SS, 169, 257
- Leibowitz, E. M., Mendelson, H., Bruch, A., Duerbeck, H. W., Seitter, W. C., & Richter, G. A. 1994, ApJ, 421, 771
- Littlefair, S. P., Dhillon, V. S., Marsh, T. R., Gänsicke, B. T., Southworth, J., Baraffe, I., Watson, C. A., & Copperwheat, C. 2008, MNRAS, 388, 1582
- Littlefield, C., et al. 2013, AJ, 145, 145
- Liu, Wu., Hu, J. Y., Li, Z. Y., & Cao, L. 1999, ApJS, 122, 257
- Lubow, S. H. 1991, ApJ, 381, 259
- Lubow, S. H. 1992, ApJ, 401, 317
- Luckas, P. 2016, Astron. Telegram, 9678
- Markarian, B. E., & Stepanian, D. A. 1983, Astrofizika, 19, 639
- Mason, E., & Howell, S. 2003, A&A, 403, 699
- Matsumoto, K., Mennickent, R. E., & Kato, T. 2000, A&A, 363, 1029
- Mayall, M. W. 1968, JRASC, 62, 141
- Maza, J., Hamuy, M., Wischnjewsky, M., Wells, L., Phillips, M., & Barros, S. 1990, IAU Circ., 5073
- McAllister, M. J., et al. 2017a, MNRAS, 464, 1353

McAllister, M. J., et al. 2017b, *MNRAS*, 467, 1024

Meinunger, L. 1976, *Mitteil. Veränderl. Sterne*, 7

Mennickent, R. E., Nogami, D., Kato, T., & Worraker, W. 1996, *A&A*, 315, 493

Miller, W. J. 1971, *Ricerche Astronomiche*, 8, 167

Montgomery, M. M. 2001, *MNRAS*, 325, 761

Montgomery, M. M., & Bisikalo, D. V. 2010, *MNRAS*, 405, 1397

Montgomery, M. M., & Martin, E. L. 2010, *ApJ*, 722, 989

Morgenroth, O. 1933, *Astron. Nachr.*, 250, 75

Murray, J. R. 1998, *MNRAS*, 297, 323

Nakata, C., et al. 2013, *PASJ*, 65, 117

Namekata, K., et al. 2017, *PASJ*, 69, 2

Niels Bohr Institute, U. o. C., Institute of Astronomy, UK, C., & Real Instituto y Observatorio de La Armada en San Fernando 2014, *VizieR Online Data Catalog*, 1327

Ohshima, T., et al. 2012, *PASJ*, 64, L3

Olech, A., Mularczyk, K., Kędzierski, P., Złoczewski, K., Wiśniewski, M., & Szaruga, K. 2006, *A&A*, 452, 933

Olech, A., Złoczewski, K., Mularczyk, K., Kedzierski, P., Wisniewski, M., & Stachowski, G. 2004, *Acta Astron.*, 54, 57

Osaki, Y. 1989, *PASJ*, 41, 1005

Osaki, Y. 1996, *PASP*, 108, 39

Osaki, Y., & Kato, T. 2013a, *PASJ*, 65, 50

Osaki, Y., & Kato, T. 2013b, *PASJ*, 65, 95

Osaki, Y., & Meyer, F. 2002, *A&A*, 383, 574

Otulakowska-Hypka, M., Olech, A., de Miguel, E., Rutkowski, A., Koff, R., & Bąkowska, K. 2013, *MNRAS*, 429, 868

Pastukhova, E. N. 1988, *Astron. Tsirk.*, 1534, 17

Patterson, J. 2011, *MNRAS*, 411, 2695

Patterson, J., Bond, H. E., Grauer, A. D., Shafter, A. W., & Mattei, J. A. 1993, *PASP*, 105, 69

Patterson, J., McGraw, J. T., Coleman, L., & Africano, J. L. 1981, *ApJ*, 248, 1067

Patterson, J., et al. 2003, *PASP*, 115, 1308

Pearson, K. J. 2006, *MNRAS*, 371, 235

Pogrosheva, T., et al. 2016a, *Astron. Telegram*, 9509

Pogrosheva, T., et al. 2016b, *Astron. Telegram*, 9510

Pojmański, G. 2002, *Acta Astron.*, 52, 397

Popova, A. 1960, *Mitteil. Veränderl. Sterne*, 464

Popova, E., et al. 2016, *Astron. Telegram*, 8843

Popowa, M. 1961, *Astron. Nachr.*, 286, 81

Pretorius, M. L., Woudt, P. A., Warner, B., Bolt, G., Patterson, J., & Armstrong, E. 2004, *MNRAS*, 352, 1056

Prieto, J. L., Chomiuk, L., Strader, J., Morrell, N., Stanek, K. Z., & Shappee, B. J. 2016, *Astron. Telegram*, 9479

Prieto, J. L., et al. 2013, *Astron. Telegram*, 5102

Quimby, R., & Mondol, P. 2006, *Astron. Telegram*, 787

Robertson, J. W., Honeycutt, R. K., & Turner, G. W. 1995, *PASP*, 107, 443

Ross, F. E. 1927, *AJ*, 37, 155

Satyvoldiev, V. 1972, *Astron. Tsirk.*, 711, 7

Savoury, C. D. J., et al. 2011, *MNRAS*, 415, 2025

Schmeer, P., Hurst, G. M., Kilmartin, P. M., & Gilmore, A. C. 1992, *IAU Circ.*, 5502

Schneller, H. 1931, *Astron. Nachr.*, 243, 335

Shafter, A. W., Cowley, A. P., & Szkody, P. 1984, *ApJ*, 282, 236

Shappee, B. J., et al. 2014, *ApJ*, 788, 48

Shears, J., Brady, S., Foote, J., Starkey, D., & Vanmunster, T. 2008, *J. Br. Astron. Assoc.*, 118, 288

Shumkov, V., et al. 2016a, *Astron. Telegram*, 9470

Shumkov, V., et al. 2016b, *Astron. Telegram*, 9616

Shurpakov, S., et al. 2012, *Astron. Telegram*, 4675

Shurpakov, S., et al. 2013a, *Astron. Telegram*, 5657

Shurpakov, S., et al. 2013b, *Astron. Telegram*, 5083

Simonsen, M. 2011, *J. American Assoc. Variable Star Obs.*, 39, 66

Siviero, A., & Munari, U. 2016, *Astron. Telegram*, 9862

Smart, R. L. 2013, *VizieR Online Data Catalog*, 1324

Southworth, J., Copperwheat, C. M., Gänsicke, B. T., & Pyrzas, S. 2010, *A&A*, 510, A100

Southworth, J., Marsh, T. R., Gänsicke, B. T., Aungwerojwit, A., Hakala, P., de Martino, D., & Lehto, H. 2007, *MNRAS*, 382, 1145

Stanek, K. Z., et al. 2016a, *Astron. Telegram*, 9343

Stanek, K. Z., et al. 2016b, *Astron. Telegram*, 9669

Stanek, K. Z., et al. 2016c, *Astron. Telegram*, 9469

Stanek, K. Z., et al. 2013, *Astron. Telegram*, 5082

Stellingwerf, R. F. 1978, *ApJ*, 224, 953

- Szkody, P., et al. 2002, *AJ*, 123, 430
- Szkody, P., et al. 2009, *AJ*, 137, 4011
- Szkody, P., et al. 2003, *AJ*, 126, 1499
- Szkody, P., et al. 2006, *AJ*, 131, 973
- Szkody, P., et al. 2005, *AJ*, 129, 2386
- Szkody, P., et al. 2007, *AJ*, 134, 185
- Szkody, P., & Howell, S. B. 1992, *ApJS*, 78, 537
- Szkody, P., Ingram, D., Schmeer, P., Midtskogen, O., Dahle, H., & Bortle, J. E. 1992, *IAU Circ.*, 5516
- Tappert, C., & Bianchini, A. 2003, *A&A*, 401, 1101
- Thorstensen, J. R., Fenton, W. H., Patterson, J. O., Kemp, J., Krajci, T., & Baraffe, I. 2002, *ApJ*, 567, L49
- Thorstensen, J. R., Taylor, C. J., Peters, C. S., Skinner, J. N., Southworth, J., & Gänsicke, B. T. 2015, *AJ*, 149, 128
- Tiurina, N., et al. 2013, *Astron. Telegram*, 4871
- Tsesevich, V. P. 1967, *Second Supplement to General Catalogue of Variable Stars*, second edition (Moscow: Astronomical Council of the Academy of Sciences in the USSR)
- Uemura, M., et al. 2002, *PASJ*, 54, L15
- Uemura, M., Mennickent, R., & Stubbings, R. 2004, *IBVS*, 5569
- Vladimirov, V., et al. 2013, *Astron. Telegram*, 5585
- Vladimirov, V., et al. 2014, *Astron. Telegram*, 5983
- Vogt, N. 1983, *A&A*, 118, 95
- Vogt, N., & Bateson, F. M. 1982, *A&AS*, 48, 383
- Wakamatsu, Y., et al. 2017, *PASJ*, submitted
- Walker, A. D., & Olmsted, M. 1958, *PASP*, 70, 495
- Warner, B. 1985, in *Interacting Binaries*, ed. P. P. Eggleton, & J. E. Pringle (Dordrecht: D. Reidel Publishing Company), p. 367
- Warner, B. 1995, *Cataclysmic Variable Stars* (Cambridge: Cambridge University Press)
- Wenzel, W. 1993a, *Mitteil. Veränderl. Sterne*, 12, 153
- Wenzel, W. 1993b, *IBVS*, 3921
- Whitehurst, R. 1988, *MNRAS*, 232, 35
- Williams, G. 1983, *ApJS*, 53, 523
- Williams, S. C., & Darnley, M. J. 2016, *Astron. Telegram*, 9375
- Wils, P., Gänsicke, B. T., Drake, A. J., & Southworth, J. 2010, *MNRAS*, 402, 436
- Witham, A. R., Knigge, C., Drew, J. E., Greimel, R., Steeghs, D., Gänsicke, B. T., Groot, P. J., & Mampaso, A. 2008, *MNRAS*, 384, 1277

- Wolf, M., & Wolf, G. 1906, *Astron. Nachr.*, 170, 361
- Wood, M. A., & Burke, C. J. 2007, *ApJ*, 661, 1042
- Wood, M. A., Still, M. D., Howell, S. B., Cannizzo, J. K., & Smale, A. P. 2011, *ApJ*, 741, 105
- Yamaoka, H., Itagaki, K., Kaneda, H., Jacques, C., Pimentel, E., Maehara, H., & Bolt, G. 2008, *Cent. Bur. Electron. Telegrams*, 1463
- Yecheistov, V., et al. 2013, *Astron. Telegram*, 5536
- Yecheistov, V., et al. 2014, *Astron. Telegram*, 5905
- Zengin Çamurdan, D., Ibañoğlu, C., & M., Çamurdan C. 2010, *New Astron.*, 15, 476
- Zwitter, T., & Munari, U. 1996, *A&AS*, 117, 449